The Dissertation/Thesis/Capstone Committee for Inaia Rochelle Phoenix Certifies that this is the approved version of the following Dissertation/Thesis/Capstone:

MANIPULATION OF THE RIFT VALLEY FEVER VIRUS M-SEGMENT FOR VACCINE DEVELOPMENT

Committee:

Tetsuro Ikegami, Ph.D., Supervisor

Alexander Freiberg, Ph.D.

John Morrill, Ph.D., D.V.M

Robert Tesh, M.D.

Hideki Ebihara, Ph.D.

Dean, Graduate School of Biomedical Sciences

MANIPULATION OF THE RIFT VALLEY FEVER VIRUS M-SEGMENT

FOR VACCINE DEVELOPEMENT

by

Inaia Rochelle Phoenix, B.S.

Dissertation

Presented to the Faculty of the Graduate School of

The University of Texas Medical Branch

in Partial Fulfillment

of the Requirements

for the Degree of

Doctor of Philosophy

The University of Texas Medical Branch

June 2016

Dedication:

This work is dedicated to my loved ones. You make me laugh. You make me cry – mostly from laughing. You challenge me to be the best version of myself, even when I fight you kicking and screaming. You have saved me from myself and from the darkness more times than I can count. You bring such immense joy to my life. Without you I would have never made it through. You are my foundation. You are my inspiration. You are my strength.

Acknowledgements

First and foremost, I need to thank Nanda Lokugamage and Shoko Nishiyama. Without the two of you, I would never have completed, published, and defended the work presented here.

To my former labmates, Olga Slack and Sabarish Indran, thank you for training me and being patient with me.

To Jenny Head, thank you for being my lab "big sister" and writing buddy. I could not have gotten through those early steps without you.

Thank you to Matt Huante, Terence Hill, Victor Carpio, and Mark Griffin for your help with the first Aim.

Thank you, Kumari Lokugamage for always being available to help and to answer questions.

Thank you, Doug Watts for your insight on the early days of MP-12.

To my undergrad mentor, Doug Wood, thank you for always believing in me and pushing me to succeed.

Alan Barrett, thank you for being a co-mentor in so many ways and helping me get through graduate school better prepared for what lies next.

John Morrill and Hideki Ebihara, your kind words and support really got me through a very difficult time and really brought me back into the lab, when I didn't want to be there and didn't think I could do it.

Finally, to my mentor, Tetsuro Ikegami, it has been a rough road. We have not made it easy on each other, but I think that was for the best. This was an excellent learning experience for the both of us. While it has been frustrating, I can say, for my part, there is a tremendous amount of respect.

Manipulation of the Rift Valley fever virus M-segment for Vaccine Development

Publication No._____

Inaia Rochelle Phoenix, Ph. D.

The University of Texas Medical Branch, 2016

Supervisor: Tetsuro Ikegami

Rift Valley fever virus (RVFV) is a phlebovirus of the virus family, *Bunyaviridae*. Since the early 1900s, RVFV has continually caused economically devastating outbreaks in livestock and severe disease in humans. In pregnant ewes, RVFV infection can cause abortions in up to 100% of animals and high mortality rates (up to 60%), and it can cause fetal abnormalities and a high rate of mortality in newborn lambs. Originally, endemic to sub-Saharan Africa, RVF outbreaks have been documented in Egypt, Madagascar, the Arabian Peninsula, and, most recently, the island of Mayotte in the Indian Ocean. The proven potential for RVFV to cause outbreaks in "virgin soils" is of grave concern for the European Union and the United States of America, where competent vectors and susceptible host species are located. Vaccination of livestock is paramount in the prevention of outbreaks. Unfortunately, inactivated vaccines that are safe for both young and pregnant animals require boosters, and live-attenuated vaccines are not considered safe in pregnant animals. Thus, the development of a live-attenuated vaccine that is safe in pregnant animals is invaluable to the prevention of future RVF outbreaks and ultimately, the eradication of RVFV.

The first aim of this work was to determine the N-glycosylation status of the RVFV glycoproteins, Gn and Gc, and determine the roles of the N-glycans in DC-SIGN-mediated

infection. The results determined that the single N-glycan site within Gn, at nt. 438, was N-glycosylated and three sites within Gc, at nt. 794, 1035, and 1077; are N-glycosylated. We also noted that the doublet band of Gc is generated by two distinct glycoforms, Gc-large and Gc-small, which are due to heterogeneous N-glycosylation at N1077. Enhanced infection of RVFV by DC-SIGN occurs by the Gn/Gc N-glycans in a redundant manner, and the N-glycans present at N438 (Gn) and N1077 (Gc) play an important role in DC-SIGN mediated infection. This work will aid in the development of vaccines that target the DC-SIGN receptor towards the facilitation of dendritic cells acting in their antigen-presenting capacity instead of viral dissemination.

The second aim of the work presented was to create rMP-12 vaccine candidates that expressed increased levels of Gn and Gc. Neutralizing antibodies to Gn and Gc have been demonstrated to be important for protection against lethal RVFV challenge. Thus, we sought to optimize the translation efficiency of the preglycoprotein region of the M-segment. Within the preglycoprotein regions, there are five initiation codons, and the first initiation codon generates the 78 kDa-Gc precursor, while the second initiation codon generates the NSm-Gn-Gc precursor. We generated rMP-12 mutants with altered levels of Gn expression due to point mutations and truncation of the initiation codons. Truncation of the preglycoprotein region up to the 2nd initiation codon resulted in relative Gn expression levels that were almost 3-fold greater than the parental plasmid. However, this increase in relative Gn expression did not result in an increase in viral titer. We also investigated the Gn expression strategy of other phleboviruses, Sandfly fever Sicilian virus (SFSV) and Toscana virus (TOSV). Interestingly, relative Gn expression from the preglycoprotein regions of these viruses was 3-fold and 1.5 fold higher than RVFV. The knowledge gained from this aim will aid in the development of subunit vaccines based on the RVFV Gn and Gc proteins.

TABLE OF CONTENTS

LIST OF TABLES

LIST OF FIGURES

LIST OF ABBREVIATIONS

Ala: Alanine
ALT: Alanine aminotransferase
arMP12-ΔNSm: recombinant MP-12 that lacks NSm
Asp: Aspartate
AST: Aspartate aminotransferase
APTT: activated partial thromboplastin time
AUG: initiation codon
BHK: Baby Hamster Kidney cells
BSL Biosafety level
C13: Clone-13, naturally attenuated live vaccine
C3d: Complement component-3
CAG promoter: The cytomegalovirus early enhancer/chicken β actin promoter
CAK: cyclin-dependent kinase (CDK)-activating kinase
CBP: Creb-binding protein
cLuc: *Cypridia* luciferase
CRD: carbohydrate recognition region
cRNA: exact, complementary copy of the viral genome
CTD: carboxyl-terminal domain
C-type: calcium-dependent
CUC: leucine
DC: dendritic cells
DC-SIGN: Dendritic Cell- Specific Intercellular Adhesion Molecule 3-Grabbing Nonintegrin
DC-SIGNR: alternative name for L-SIGN
DIC: intravascular coagulation
DIVA: differentiation of infected from vaccinated animals
Dol-P: Dolichol-phosphate
E: envelope proteins
EEEV: Eastern Equine Encephalitis virus
EDEM: ER degradation-*e*nhancing α-*m*annosidase I–like protein
EDTA: Ethylenediaminetetraacetic acid
EGTA: Ethylene glycol-bis(β-aminoethyl ether)
eIF2α: eukaryotic initiation factor 2
eIF2-GDP: eukaryotic initiation factor 2 bound to guanoside diphosphate
eIF2-GTP: eukaryotic initiation factor 2 bound to guanoside triphosphate
Endo F: endoglycosidase F
Endo H: Endoglycosidase H
ENSO: El Nino Southern Oscillation
ER: Endoplasmic Reticulum
ERAD: ER associated degradation
ERGIC: ER-Golgi intermediate compartment
E.U.: European Union
FACS: Fluorescence-activating cell sorting
FBS: Fetal bovine serum
FBXO3: F-box Protein-3
FRhL-2: cell line derived from Rhesus macaque lung tissue
G: Glycine

Gal:	galactose
GFP:	Green fluorescent protein
Glc:	glucose
GlcNAc:	*N*-acetylglucosamine
gLuc:	*Gaussia* luciferase
Gly-null:	lacking N-glycan sequons
Gn-e:	ectodomain of Gn
Gtfs:	glycosyltransferases
HDAC-3:	Histone deacetylase-3
HHS:	U.S. Department of Health and Human Services
hSIGN:	transgenic mouse strain that expresses DC-SIGN under the CD11c promoter
I:	Isoleucine
IFN:	interferon
i.p.:	intraperitoneal
IRF-3:	Interferon Regulatory Factor-3
ISG:	an interferon-stimulated gene
ISRE:	IFN-stimulated response elements
L:	Leucine
LacNAc:	N-acetyl-D-lactosamine
LL:	dileucine motif
LDH:	Lactate dehydrogenase
L-segment:	Large-segment
L-SIGN:	Liver/Lymph node Specific Intercellular Adhesion Molecule 3-Grabbing Nonintegrin
Man:	mannose
MDA-5:	melanoma differentiation-associated protein 5
Met:	methionine
M-segment:	Medium-segment
MOI:	Multiplicity of infection
MRC-5:	cell line derived from 14-week old fetal lung tissue
MxA:	IFN-inducible cytoplasmic dynamin-like GTPase
N:	Asparagine
NANA:	sialic acid
NCoR:	Nuclear receptor corepressor-1
NDFL:	Modified La Sota NDV strain used for production of viral proteins
NDV:	New Castle disease virus
NF-KB:	Nuclear factor-KB
NIAID:	National Institute of Allergy and Infectious Diseases
NIH:	National Institutes of Health
nt:	nucleotide
NSm'	truncated NSm protein, synthesis begins at the 3rd initiation codon (nt 174)
OAS:	2'-5'-oligoadenylate synthetase
ORFs:	open reading frames
OST:	oligosaccharyltransferase
P:	Proline
PBMC:	human peripheral blood mononuclear cells
PBS:	Phosphate buffered saline
Phe:	phenylalanine
PIC:	pre-initiation complex

PKR: dsRNA-dependent protein kinase
PNGaseF: peptide-N-glycosidase F
Poly (ICLC): Polyinosinic-Polycytidylic Acid Stabilized with Polylysine and Carboxymethylcellulose
Pol II: polymerase II
PRNT: Plaque reduction neutralization test
PRR: Pathogen recognition receptor
PTV: Punta Toro virus
Q: Glutamine
r2segMP-12: 2-segment recombinant MP-12 encoding the L-segment and Gn/Gc
R-ΔNSm-ZH501: Recombinant ZH501 lacking expression of 78 kDa and NSm
Rbx1: Ring box-1
RIG-I: retinoic acid-inducible gene 1
RIPA: Radioimmunoprecipitation assay buffer
rMP-12: Recombinant MP-12
rMP12-ΔNSm21/384: Recombinant MP-12 encoding an in-frame deletion of 78 kDa/NSm
rMP12-C13 type: Recombinant strain of RVFV, has the backbone of MP-12 and resembles the naturally attenuated strain Clone 13
RNP: viral ribonucleocapsid
RPMI: Roswell Park Memorial Institute Medium
RVF: Rift Valley fever
rRVF-ΔNSm: Recombinant ZH501 lacking NSm
rRVF-wt: Recombinant ZH501
RVFV: Rift Valley fever virus
rRVFV: Recombinant RVFV
rRVFV-ΔNSs-EGFP: Recombinant RVFV expressing GFP in the place of NSs
S: Serine
S2: Stable Schneider 2 cell line, *Drosophila melagaster*
SAP30: Sin3A-associated protein 30
SDS-PAGE: Sodium dodecyl sulfate-polyacrylamide gel electrophoresis
SIGNR: mouse orthologs of DC-SIGN and L-SIGN
SIN: Sindbis virus
Skp1: S-phase kinase-associated Protein-1
S-segment: Small-segment
SFSV: Sandfly fever Sicilian virus
SFTSV: Severe Fever with Thrombocytopenia Syndrome virus
STT: Subunit of the oligosaccharyltransferase complex
STT: Subunit of the oligosaccharyltransferase complex
T: Threonine
TFIIH: transcription factor II H
TLR: toll-like receptor
tRNA: transfer RNA
TOSV: Toscana virus
UDP: Uridine diphosphate
UTMB: University of Texas Medical Branch
UTP: Uridine triphosphate
USAMRIID: U. S. Medical Research Institute for Infectious Diseases
USDA: U.S. Department of Agriculture
UTR: Untranslated region

UUKV:	Uukuniemi virus
Val:	Valine
VEEV:	Venezuelan Equine Encephalitis virus
VLPS:	Virus-like particles
vRNA:	viral RNA
WEEV:	Western Equine Encephalitis virus
ZH501:	Wild-type strain of Rift Valley fever virus
ZH548:	Wild-type strain of Rift Valley fever virus

CHAPTER 1: INTRODUCTION[1]

HISTORY

The area surrounding Lake Naivasha in Kenya experienced an unusually, heavy rainy season in 1930 (1). Over 31 inches of rain fell between February and May of that year, where usually about 4 inches is the norm. Starting in late June and continuing throughout the summer, a large number of abortions occurred in sheep flocks of the neighboring areas. In Kenya, many diseases can infect sheep, including bluetongue virus (a reovirus), heartwater disease (rickettsia), Nairobi sheep disease virus (a bunyavirus in the *Nairovirus* genus), and sheeppox (a poxvirus). However, the pathology of the pathogens listed did not match the pathology seen in the sheep in the Lake Naivasha area. About 1,200 ewes and lambs had succumbed to the unknown disease by mid-August, and it was determined, then, that both the ewes and lambs had suffered from the same disease. Within 24 hours after the onset of clinical signs (lethargy, lack of desire to move or eat), the newborn lambs, around 3 days old, died (1). The lambs had extensive liver necrosis. After a filtration experiment, the causative pathogen was determined to be a virus, and the pathogen was, subsequently, named Rift Valley fever virus (RVFV) after the region where it was identified.

Humans were also infected during the outbreak, including the local population that was in charge of sheep herding. Also, during the investigation of the disease, four of the European investigators developed the disease. Illness included fever, shivering, and a severe headache (similar to Dengue fever), which was followed by pain in or around the joints. A recurrence of symptoms occurred in one researcher about 3 days post recovery from the initial onset, and foor weeks, that researcher experienced headaches and vision problems.

In the late 1940s, after the first RVF outbreak in Kenya, RVFV was first isolated from a pool of mosquitoes that were harvested from a forest in Uganda (Entebbe strain) (2). This was

[1] Portions of this Chapter were previously published. Phoenix, I, Ikegami T. Pathogenesis of Rift Valley fever in humans. 2015. In Emerging and re-emerging human infections. John Wiley & Sons/Wiley Blackwell Press.

the first indication that mosquitoes serve as a vector for the transmission of RVFV, and because the forest was uninhabited, it demonstrated that in African forests, circulation of RVFV in mosquitoes occurs without human involvement. Later, it was found that persistence of RVFV, in Kenya at least, is due to the transovarial transmission of the virus from floodwater *Aedes* spp. mosquitoes to their offspring (3).

In South Africa in 1950, another prominent RVFV outbreak occurred, though RVFV was not identified as the causative agent until human cases started to occur in 1951. As the virus had not been documented in the country prior to this time, it was thought that RVFV was introduced from other African countries (4). Roughly, 100,000 sheep died during the course of the enzootic, and around 500,000 ewes aborted (4). During this outbreak, mortality and disease was also identified in cattle, though to a lesser extent than in sheep.

During another outbreak in South Africa in 1975, the first cases of hemorrhagic fever were reported. The origin of the RVFV strain that caused this outbreak is unknown. However, Grobbelaar et al. identified 15 distinct genetic lineages using partial M-segment sequences from over 200 viruses isolated from 1944 – 2010 (5). Isolates from South Africa (1971, 1974, and 1975) clustered with isolates from Kenya (1963 and 1965) and Zimbabwe (1969 and 1970) (5). Thus, a weak genetic link between the East African strains of RVFV and the 1951 South African strain exists (5-7).

In Egypt, in the summer of 1977, another RVF outbreak started and made its way up the Nile River Valley (8). Continuing through 1978, the outbreak produced an estimated 20,000-200,000 human infections and around 600 deaths (8). The responsible source of RVFV is thought to be either infected sheep imported from Sudan (9) or wind-blown infected mosquitoes(10), but the true source is unknown. This outbreak was the first outbreak north of the Saharan desert and highlighted the ingenuity of RVFV in spreading to regions outside its traditional boundaries.

Since the first introduction of RVFV to Egypt, more outbreaks have occurred in 1993, 1994, 1997, and 2003 (7). The use of vaccines in humans and livestock would have been useful in preventing human deaths and economic losses due to animal abortions/deaths. Repeated importation of animals from Sudan and the horn of Africa, with a disregard of proper quarantine procedures might be involved in the recurrence of RVF outbreaks in Egypt (9, 11).

The first RVF outbreak occurring outside of Africa, in the Arabian Peninsula, took place at the turn of the century (12). A close genetic tie between isolates from the Arabian Peninsula 2000 outbreak and from Kenya 1997 outbreak have been determined (6). The RVFV strain from Madagascar has also shown to be genetically linked to that from east Africa (13).

The ability of RVFV to spread unexpectedly and across vast areas is a cause for great concern, especially for non-endemic areas like the European Union (E.U.) and North America, which have susceptible human and animal populations. Veterinary vaccination is the most effective way to prevent RVF outbreaks. In endemic countries, veterinary vaccines, such as the Smithburn vaccine, that are available have concerns with efficacy and safety (14, 15). In the U.S., which is not endemic for RVFV, the MP-12 vaccine has been conditionally licensed for use in livestock for emergency use in the case of RVFV introduction (APHIS, 2013). Legal mportation of RVFV infected livestock is not a concern for the U.S. since importation of livestock from countries endemic for foot-and-mouth disease and/or rinderpest is prohibited (16), and countries endemic for foot-and-mouth disease and/or rinderpest are also endemic for RVFV (16). However, illegal importation of animals is a concern. Other ways to prevent the introduction of RVFV include the stringent regulation of shipping and possession of viral strains used in research. The U. S. government classifies RVFV a Category A priority pathogen (National Institute of Health), and an overlap select agent by the HHS (United States Department of Health and Human Services) and USDA (U.S. Department of Agriculture) (17). Select agents are pathogens that have been determined to be dangerous to public health, animal or plant health, or to products derived from plants and animals (18). Enhanced biosafety

level (BSL)-3, with exit shower, or BSL-4 is required for safe handling of RVFV in the U.S. Such biosafety measures are to prevent infection of laboratory staff and the possibility of RVFV escape from the research laboratory into the local population (19).

PATHOGENESIS IN HUMANS

Febrile illness

During early RVFV studies, there were a number of laboratory-acquired infections caused by the use of inappropriate safety measures (20-24). For the majority of patients, RVF is a non-fatal and self-limited, febrile illness (1, 20, 21, 24-28). Clinical signs and symptoms typically, develop four to six days post-infection (incubation period). The onset of symptoms is abrupt and include nausea with or without a sensation of fullness over the liver, rigors, fatigue, severe headaches, discomfort, and dizziness, (20, 21, 25). Tenderness and redness of the eyes, low blood pressure, elevation of body temperature (38.8ºC to 39.5ºC), continuous dull pain in the shoulders, back, neck or legs, and inability to sleep or have bowel movements follows the initial symptoms (1, 21, 24, 27-29). Sensitivity to light, loss of taste, nosebleeds, and diarrhea and/or vomiting can also occur (1, 21, 24, 27-29). Remission of symptoms can occur about hree days after symptom with some improvement and abatement of fever, typically, occurs around the fourth day. After the initial recovery, however, in some patients severe headaches and body temperature elevation recrudesces within one to three days post initial recovery (1, 24, 25, 28). Lasting up to ten days, this secondary phase contributes to the biphasic component of RVF. Even during the convalescent period, pain in the lower extremities can occur, up to 2 weeks (1, 21), and in one case, a massive blood clot in the coronary artery in a RVF patient (28). Also, long lasting discomfort in the abdominal area is experienced by some patients despise an obvious lack of spleen or liver enlargement (1). RVF patients may also still experience fatigue, eye pain, headaches, malaise, frequent headaches, weakness, and a sense of disequilibrium. During the initial febrile period (i.e. 3-4 days), RVFV is present in the blood.

On the fourth day post infection, neutralizing RVFV antibodies start appearing in the blood and begin to clear the infection (1, 21, 22, 24-26).

Hemorrhagic fever

In most RVF fatal cases, hemorrhagic disease is a leading cause of death, though the time from infection to death can vary (30-32). Hemorrhagic symptoms start abruptly and include a myriad of symptoms: fever, exhaustion, head and body aches, nausea, vomiting, infection of or bruising of the eyelid; bloody diarrhea; and bleeding in the mouth and/or gastrointestinal tract (31, 32). Enlargement of the spleen and liver, jaundice, throat pain, and a raised rash on the upper body are also symptoms (31, 32). Aspartate aminotransferase (AST), Lactate dehydrogenase (LDH), Alanine aminotransferase (ALT) are liver tissue damage indicators that, typically, are found to be elevated in RVF hemorrhagic disease, whereas platelets and hemoglobin amounts are reduced (31, 33). Patients, usually, die within 3 to 6 days post onset of symptoms. However, it can take up to 17 days in some cases for patients to succumb to RVF, and due to the widespread liver necrosis seen in autopsies, acute hepatic injury is considered a primary cause of death (30, 31). When hemorrhage or jaundice is not seen in patients, disseminated intravascular coagulation (DIC) with an increase in ALT/AST/LDH or D-Dimer, which is generated by the degradation of blood clots; or renal failure are considered the main causes of death (34, 35).

Neurological disorders

Usually, occurring one to two weeks post-onset of initial symptoms, (36), encephalitis due to RVFV infection is another severe manifestation that occurs in some cases. Encephalitis has also been seen in autopsies of RVF patients, who died of acute liver disease (37). Even without obvious viral damage to the eye, temporary blindness can still occur along with confusion, fever, and even paralysis (37-39). Lasting anywhere from 4 months (39) up to a year (36), paralysis can manifest as locked-in syndrome (all voluntary muscles are affected) (37); quadriplegia (all four limbs affected) (36); or hemiparesis (where only 1 side is affected) (39).

An increase in the white blood cell count found in the cerebral spinal fluid (CSF), indicates meningoencephalitis or inflammation of the meninges (36, 38). Hyperreflexia or over-reactive reflexes; stupor and coma; fever; stiffness in the neck; increased salivation; visual hallucinations; teeth-grinding; and convulsions are other symptoms (36-38). RVF-induced encephalitis can also cause inflammation and hemorrhage in both eyes (36). Histopathological examinations of the brain reveal perivascular cuffing and focal necrosis associated with macrophage and lymphocyte infiltration (37).

Ocular diseases

Maculopathy (the center region of the retina is damaged), or retinopathy (the whole retina is damaged) has been documented with RVFV infection. These pathologies can result in the loss of highly sensitive central vision and/or in blurry vision and can affect one or both eyes. These symptoms can manifest immediately after onset of initial symptoms to several weeks or months later (40-42). Detachment of the retina (40, 43), arterial occlusion or blockage of the retina arteries (40, 43-46); and irritation and swelling of the uvea or middle layer of the eye, which supplies the most blood to the retina (42, 44) can occur in some cases. Though partial improvement in vision can been seen in some patients after several months (41-43, 46); permanent blindness or impaired vision due to scarring of the central retina is still a concern (40-42, 44-47).

Thrombosis

Starting during the RVF febrile period and, possibly, lasting for weeks, another RVF complication is thrombosis. The mechanism of the formation of large thrombi caused by RVFV infection is unknown; however, DIC is thought to be involved. In one reported fatal case, a large thrombus formed in the vena cava after persistent thrombophlebitis in one of the legs. The thrombus, then traveled to the pulmonary artery and caused a embolus (23).

TRANSMISSION

In endemic areas in Africa, RVFV persists due to transmission between animals and mosquitoes (horizontal) and vertical transmission in mosquitoes **(Figure 1-1)** (48). RVFV

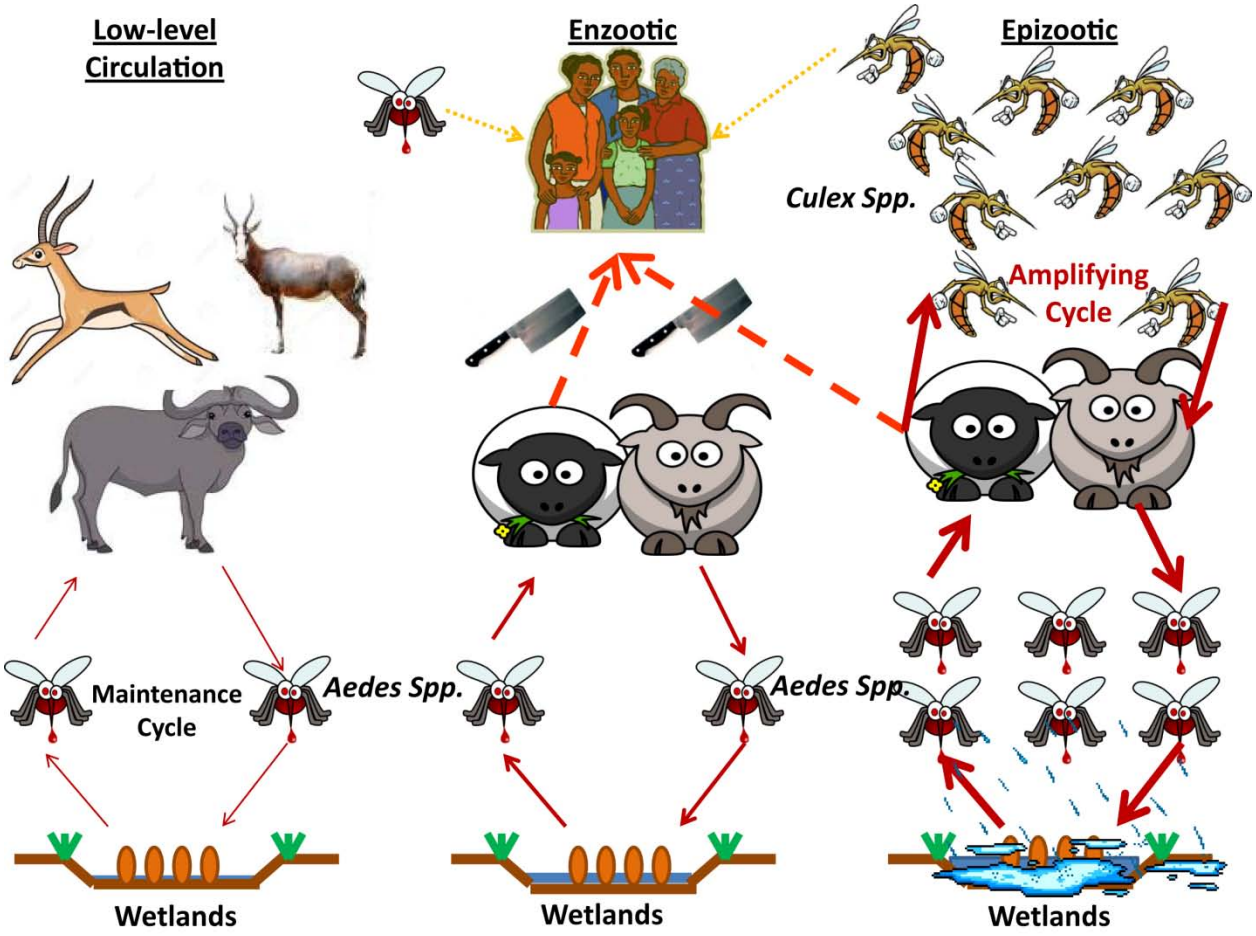

Figure 1-1: Transmission Cycle of Rift Valley fever virus. In endemic areas, low-level circulation of RVFV occurs between *Aedes spp*. of mosquitoes, which can transovarially transmit RVFV to their eggs, and indigenous wildlife, such as African buffalo, Springbok, and Blesbok. During enzootics, RVFV spillover into domesticated animals, such as sheep, goats, and cattle, can occur leading to potential human infections via slaughtering of livestock or via bites from infected mosquitoes. During epizootics, high rates of rainfall causes increased flooding of wetland areas, called dambos, most often due to the weather anomaly known as the El Nino Southern Oscillation (ENSO). This increased flooding leads to increased breeding grounds for *Aedes* and *Culex* spp. Culicine mosquitoes are thought to be involved in the amplifying cycle that leads to increased infections of livestock and of humans. Veneral transmission from infected male F1 *Aedes* mosquitoes to uninfected female mosquitoes might also occur.

survives severe drought conditions in east Africa via drought-resistant *Aedes* mosquito eggs (3). *Aedes* spp are capable of the transovarial transmission of RVFV to their offspring (3). During periods of drought, the shallow wetlands, where the infected female mosquitoes lay their

infected eggs, dry up, but the infected eggs are capable of surviving from season to season (49). Heavy rainfall, due to the weather phenomenon known as the El Niño Southern Oscillation (3, 50, 51), floods these shallow wetlands, known locally as dambos, and the infected *Aedes* mosquito eggs hatch. The infected larvae turn into infected adults, which then feed on local livestock allowing RVFV to be amplified and spread to other mosquitoes, animals, or humans (49). Epizootics occur when there is enough rain to form breeding sites for *Culex* mosquitoes, which feed on larger numbers of livestock and humans, thus amplifying RVFV spread (49, 52). In other endemic areas, such as Egypt, Madagascar, South Africa, Sudan, West Africa; RVFV persistence and transmission mechanisms are unclear. Independent introductions from other endemic areas, in the production of outbreaks, have been supported by genetic lineage analyses (13, 53, 54). While the principal hosts in the sylvatic cycle have yet to be identified, native ungulates, such as the blesbok, springbok, African Buffalo, dorcas gazelle, and rodents could be involved (48, 55).

RVFV infection of humans occurs via aerosolization, due to handling of infected tissue or blood during the slaughtering of livestock, assisted parturition, and necropsies; or the bite of an infected mosquito (49, 56). In the RVF outbreak in Egypt in 1977-78, infected patients did develop transient viremia (16), but no cases of horizontal (human-to-human) transmission were reported (52). However, there was a possible case of vertical transmission, where a pregnant mother may have transmitted RVFV to her fetus *in utero*, reported during the RVF outbreak in 2000 in Saudi Arabia. (57). Four days before giving birth, the pregnant mother had symptoms similar to RVF. RVFV IgG antibodies were detected in the mother, and the newborn had detectable RVFV-specific IgM antibodies. Elevated levels of ALT/AST, extension of activated partial thromboplastin time (APTT: a test for deficiency of intrinsic pathway factors) and prothrombin time, and jaundice were seen in the neonate, who died at 6 days old (57). There is no direct evidence to support a role for RVFV in human abortions, and the exact cause of the

infant's death is unknown. Before and after the RVF outbreak in Egypt (1977), the serological conversion rate of mothers who aborted their fetuses were 31.1% and 27.5%, respectively (58).

VIRAL LIFE CYCLE AND GENOME STRUCTURE

The first step in the RVFV life cycle begins with attachment to an attachment factor or receptor **(Figure 1-2)**. In the case of RVFV, two attachment factors, heparin sulfate (247) and L-SIGN (59), and one true receptor, DC-SIGN (60) have been identified. A

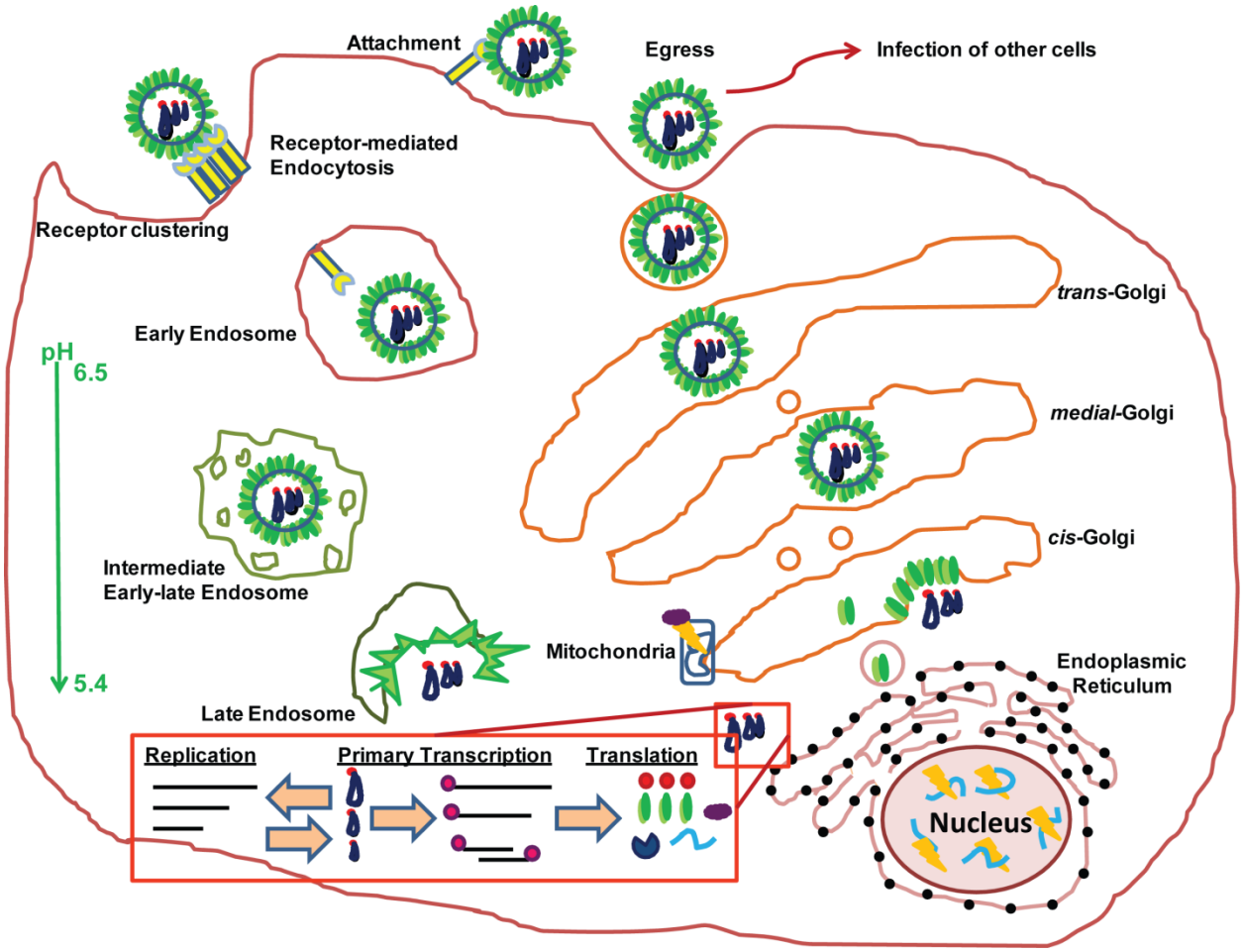

Figure 1-2: Rift Valley fever Life Cycle. The first step in the viral life cycle is viral Attachment to a receptor or attachment factor. In some cases, such as attachment to DC-SIGN, attachment to the receptor leads to Receptor Clustering, which can trigger Receptor-mediated Endocytosis. After endocytosis, the virion disassociates from the receptor in the Early Endosome, and as the pH of the endosome decreases, it becomes an Intermediate, Early-late Endosome and the membrane starts to disintegrate. At pH 5.4, a conformational change in Gc allows exposure of the fusion loop, which fuses the viral membrane with the Late endosomal membrane, releasing the viral contents into the cytoplasm. As antigenomic (positive-sense) strands of S-segment are packaged into the virion, NSs protein is rapidly synthesized from NSs mRNA, and NSs enters the nucleus, where it forms filamentous structures that prevent an anti-viral state. The L protein that is associated with the negative-sense genomic RNA strands, transcribes the viral mRNA, using capped 5' fragment of host-mRNA as a primer. After primary

transcription, the viral mRNA are translated into the viral proteins. The glycoproteins, Gn and Gc, form heterodimers in the Endoplasmic reticulum, where they are N-glycosylated. Then, they proceed through the Golgi apparatus secretory pathway, where the N-glycans can be further processed. NSm, on the other hand, colocalizes with the mitochondrial outer membrane, anchored through the C-terminal transmembrane domain, and inhibits apoptosis of the cell. Once Gn and Gc and the ribonucleoprotein complex accumulate in the *cis*-Golgi, viral assembly and subsequent Egress occurs. Trafficking of vesicles containing virions from the Golgi to plasma membrane is not well characterized. Once secreted out of the cell, the newly formed virions can spread into neighboring cells.

true, or authentic, receptor is defined as one that is necessary for both binding and internalization (59). After RVFV binds to DC-SIGN, receptor clustering occurs increasing the avidity of the interaction and inducing signals within the cytoplasmic tail, specifically the dileucine motif (LL), of DC-SIGN to allow receptor-mediated endocytosis (60). In the early endosomes, RVFV begins to disassociate from DC-SIGN, and as the pH of the endosome decreases, the membrane begins to disintegrate (intermediate early late endosomes). Virus penetration occurs 20-40 minutes after entry (60), when the low pH (5.4 for RVFV) allows a conformational change in Gc facilitating exposure of the fusion loop, which allows viral membrane-lysosomal membrane fusion (61). After being injected into the cytoplasm, primary transcription can begin by the L-protein that is attached to in the viral ribonucleocapsid (RNP), followed by translation of the viral proteins.

Three negative-strand RNA segments compose the RVFV genome, which consists of the Large (L: 6,404 nt)-, Medium (M: 3,885 nt), and Small (S: 1,690 nt)-segments **(Figure 1-3)**. In an ambi-sense manner, the nucleocapsid protein (N: 245 amino acids) and the nonstructural S protein (NSs: 265 amino acids), are encoded by the S-segment. The N protein is encoded in the viral-sense (negative-sense), whereas the NSs protein is encoded in the anti-viral-sense (positive-sense). Between the N and NSs open reading frames (ORFs), termination sites of transcription exist in both the anti-viral and viral-sense RNA. The RNP is formed when the N proteins encapsidate the viral genome RNA, which is used for transcription of viral RNA and genome RNA replication. Unlike the N protein, the NSs protein is not necessary for viral

replication or the life cycle, but instead, the NSs protein is a major virulence factor and is known to suppress the antiviral responses of the host.

Two overlapping ORFs are encoded by the M-segment, which produce four proteins: Gn (nt. 480-2,090); Gc (nt. 2,091-3,614); a nonstructural protein, NSm (nt. 135-479); and the less characterized 78 kDa protein (nt. 21-2,090). The envelope glycoproteins, Gn and Gc, are responsible for the formation of the viral particle and are involved in RVFV attachment and entry (62). Though the NSm has been shown to demonstrate anti-apoptotic functions in RVFV infected cells (63), it has been shown to be dispensable for viral replication in mammalian cells, along with the 78 kDa protein (64, 65), which plays a role in viral dissemination in mosquitoes.

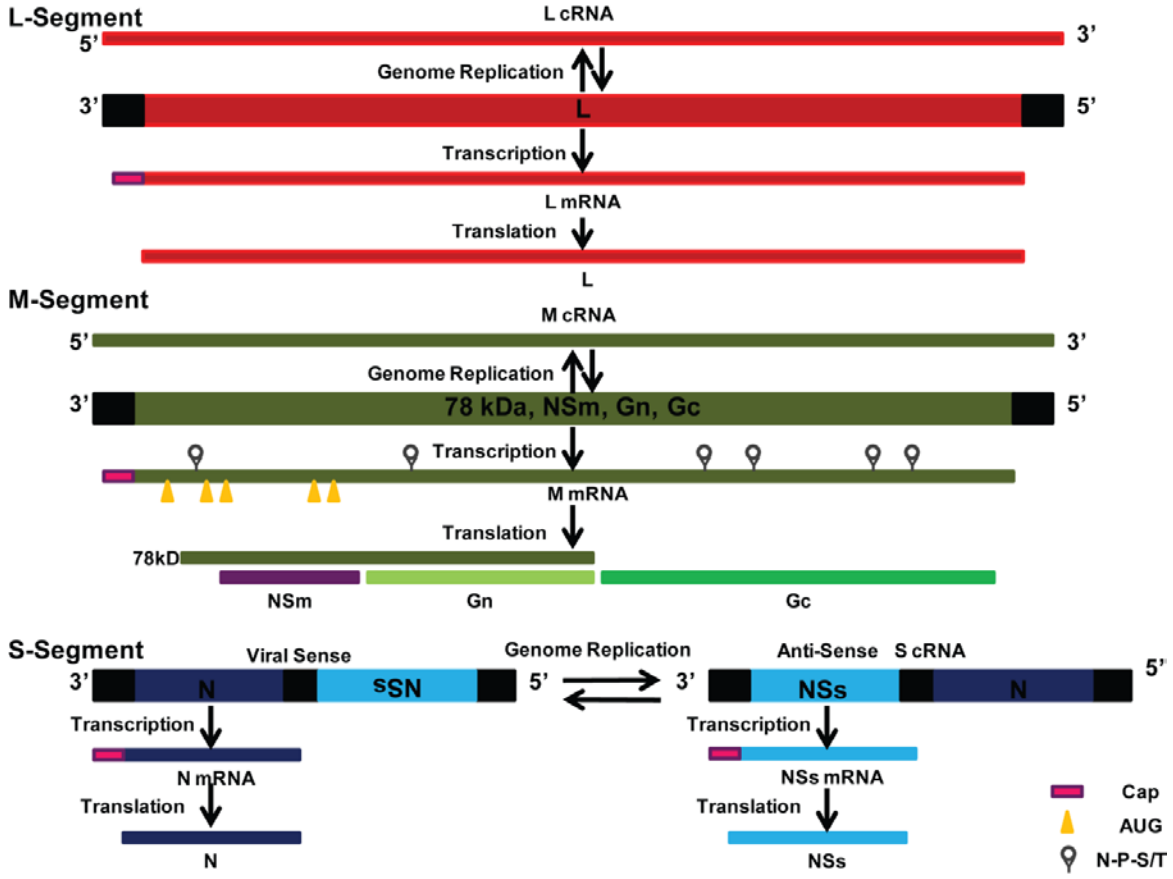

Figure 1-3: Schematic Representation of Rift Valley fever virus Gene and Protein Expression. Primary transcription of the negative sense, viral genomic RNA, into mRNA, begins with the L-protein removing the 10-18 nucleotides from capped 5' host mRNA, which is used as a primer for viral mRNA synthesis. From the viral mRNA, viral proteins are produced: L protein (RNA-dependent RNA polymerase), M-segment proteins (78 kDa, NSm, Gn, Gc), and S-segment proteins (N, NSs). M-segment proteins are produced from two open reading frames (ORF), and two polypeptides are produced: 78 kDa-

Gc, and NSm-Gn-Gc. These polyproteins are cleaved by signal peptidase to produce their individual proteins. NSs mRNA can be produced from the anti-genomic (positive sense) S-segment RNA that is incorporated into the virions, while N mRNA is produced from viral sense S-segment RNA in an ambisense coding strategy. Subsequently, viral RNA replication occurs due to the accumulation of N and L proteins. The RNP is formed when the N protein encapsidates the viral RNA, and this association, along the L protein, is essential for both viral RNA replication and transcription.

Five, in-frame initiation codons (AUGs) **(Table 1-1)** are located in the preglycoprotein region of the M-Segment, and each is involved in the biogenesis of precursors, which are then co-translationally cleaved, to produce the 78 kDa protein, the NSm protein, and the envelope glycoproteins, Gn and Gc (66). The first AUG encodes the 78 kDa, which has a carboxyl-terminal region identical to that of Gn. The 2nd initiation codon is the translation start of the NSm protein, and it generates the NSm-Gn-Gc polyprotein, which is then cleaved at the amino-terminus of Gn by signal peptidase. The 4th or 5th initiation codons may be used to translate the precursor(s) to Gn and Gc, but the exact codon or mechanism used is currently unknown.

Position	-6	-3	-2	-1	+1	+2	+3	+4	Strength
Kozak	G	A/G	C	C	A	U	G	G	Strong
AUG 1	C	U	A	A	A	U	G	U	Weak
AUG2	C	G	A	G	A	U	G	A	Adequate
AUG 3	G	G	A	G	A	U	G	C	Adequate(+)
AUG 4	G	A	C	C	A	U	G	G	Strong
AUG 5	A	G	C	A	A	U	G	A	Adequate(+)

Table 1-1: Kozak Consensus Sequence and RVFV Initiation Codon Sequences.
Presence of an A or G at the -3 within the sequence surrounding the initiation codon (where the A of AUG is +1), and a G at +4 confers a "Strong" Kozak sequence. The presence of one of these signals confers an "adequate" sequence. The presence of a G at -6 and a C at -2 and -1 are considered to be important and "strengthen" the sequence. "Adequate +" denotes the presence of either an A/G at -3 or G at + 4, and the presence of a G at -6 or a C at -2 and -1.

Lastly, the viral RNA-dependent RNA polymerase, or L-protein, is the only protein encoded by the L-segment. The L-protein is required for primary transcription of viral mRNA, which can then be translated into viral proteins. Through its endonuclease activity, the L protein "snatches" the 5' cap from host mRNAs along with 10-18 nucleotides and uses this capped RNA fragment as a primer for viral mRNA synthesis (67). The L-protein is also responsible for genomic replication, which begins with the synthesis of an exact complementary copy of the

genome (cRNA), which is then copied into viral RNA (vRNA) (68). Unlike viral mRNA synthesis, neither cRNA nor vRNA synthesis requires an oligonucleotide cap primer (68). N encapsidation of vRNA, however, is required for transcription and genome replication (68).

VIRAL VIRULENCE FACTORS: NSs and NSm

The NSs protein, encoded by the S-Segment of RVFV, is considered to be the major virulence factor of RVFV. Though dispensable for the viral life cycle, the NSs counteracts host antiviral responses and is necessary for proper replication. NSs is able to shut off host general transcription via interactions with TFIIH, an essential transcription factor necessary for host RNA polymerase I and II (69, 70). Degradation of dsRNA-dependent protein kinase (PKR) has also been shown to be a major function of NSs (71). Lastly, NSs inhibits the upregulation of interferon (IFN)-β via binding to SAP30 (Sin3A-associated protein 30) (72).

RVFV NSs shuts down general host protein transcription by inhibiting TFIIH. TFIIH is a major component of the pre-initiation complex (PIC), and it promotes transcription by opening the promoter site and activating Pol II through phosphorylation of its carboxyl-terminal domain (CTD) (73). Ten different subunits comprise TFIIH, which is composed of two subcomplexes: the CAK (cyclin-dependent kinase (CDK)-activating kinase) complex, and the core complex (73). The CAK complex contains cdk7, MAT1, cyclin H, and the core complex is made up of a helicase, XPB, and p8, p34, p44, p52, p62 (73). Another helicase, XPD, bridges the two subcomplexes through interactions with MAT1 and p44 (73). RVFV NSs binds to p44, and sequesters p44 from TFIIH assembly. RVFV serves as an adaptor protein bridging E3 ligase consisting of FBXO3, Skp1, Cullin 1, Rbx1, and E2, to p62 protein, for ubiquitination. Though ubiquitination of p62 via NSs has not been demonstrated, posttranslational degradation of p62 through proteasome has been demonstrated (74-76).

The degradation of PKR is another major function of RVFV NSs (77, 78). As an interferon-stimulated gene (ISG), PKR can inhibit both host and viral translation initiation via the phosphorylation of its substrate protein, eukaryotic initiation factor 2 (eIF2α). Translation of host

cell mRNA begins when the transfer RNA carrying methionine, which is delivered as a ternary complex with eIF2α bound to GTP, is located at the initiation codon. PKR is expressed constitutively. When PKR binds to dsRNA or 5' triphosphated ssRNA at the N-terminal domain, PKR causes structural change exposing the fusion domain and the C-terminus kinase-active domain and dimerizes to function as an activated kinase (79). The phosphorylated eIF2α forms a stable complex with eIF2B, which is required for the conversion of eIF2-GDP to eIF2-GTP, and thus, the sequestration of eIF2B leads to translational initiation shutoff. During RVFV RNA synthesis, RVFV NSs promotes the degradation of PKR through formation of viral E3 ligase complex (76, 80), which maximizes viral protein synthesis without triggering translational suppression.

While host general transcription shut off usually occurs at late time points in RVFV infection, IFN-β mRNA induction can occur as early as 3 hours post infection (81). Pathogen recognition receptors (PRR), including RIG-I (retinoic acid-inducible gene 1), TLR (toll-like receptor)-3, and MDA-5 (melanoma differentiation-associated protein 5); can recognize viral RNA and induce IFN-β gene expression through the activation of transcription factors, such as Interferon Regulatory Factor-3 (IRF-3) and Nuclear factor-KB (NF-KB). The induced IFN-β protein then upregulates IFN-α and ISGs via promoters known as IFN-stimulated response elements (ISRE), which include 2'-5'-oligoadenylate synthetase (OAS), IFN-inducible cytoplasmic dynamin-like GTPase (MxA), PKR, and RNase L. IFN-α induction can further increase the induction of ISGs. NSs inhibits IFN-β production via binding to SAP30 (72). SAP30 binds to the YY1 transcription factor on the IFN-β promoter along with the SAP30 associated repressor proteins, Sin3A, NCoR, and HDAC-3 (72). Recruitment of IRF-3 and the CREB-binding protein, CBP, along with subsequent acetylation of K8H4 and K14H3 are required for IFN-β promoter activation (72). CBP recruitment requires the binding of YY1 to the IFN-β promoter at -90 and -122 (72). After translation, NSs proteins are found both in the nucleus and the cytoplasm, and in the nucleus, the NSs proteins form filaments (82). These

unique NSs structures are detected in infected animals and are formed by the 17 amino acids located in the carboxyl terminus (83-85). RVFV NSs associates with the SAP30 repressor complex and inhibits YY1 binding at the -122 site thus preventing CBP recruitment to the IFN-β promoter activation (72).

RVFV NSm has also been demonstrated to be a virulence factor, though it is dispensable for viral replication. A previous study demonstrated that apoptosis of infected cells occurs earlier when infected with MP-12 mutants that lack NSm (64, 65, 86), which colocalizes with the mitochondria and is thought to suppress apoptosis via that interaction (63). The last 45 aa in the C-terminal region of the NSm protein targets it to the outer membrane of the mitochondria, where it prevents an apoptotic cascade via regulation of the p38 mitogen-activated protein kinase response (87-89). RVFV can retain virulence in the Wistar-furth inbred rat strain, even while lacking the 78 kDa and NSm proteins (90). Clearly, an indication of pathogenesis alteration, the infected rats did not die of acute hepatitis as expected, but instead died of delayed neurological diseases (90). However, Nishiyama el al. recently demonstrated CD1 mice inoculated with $1x10^3$ pfu of ZH501-ΔNSm21/384 succumbed to infection, and liver damage was noted (91). NSm' is a 13 kDa protein, which is produced from the 3rd AUG when the 2nd AUG is lacking, that like NSm, localizes to the mitochondria, though it is unknown whether NSm' has the same or similar anti-apoptotic activities as NSm (92). Viruses lacking both NSm and NSm' have been shown to be attenuated in murine macrophages and in mice (92). One or both proteins may play a synergistic role with the 78 kDa protein in viral dissemination in mosquitoes (92-94).

VIRAL DISSEMINATION IN MOSQUITOES: 78 kDa and NSm/NSm'

In a study using recombinant ZH501 RVFV, a wild type isolate from Egypt, the entire coding region of NSm was deleted producing rRVF-ΔNSm (93). The infection, dissemination and transmission rates in *Aedes aegypti* and *Culex quinquefasciatus* were determined and compared to the wild-type parental virus, rRVF-wt (93). In *Ae. aegypti,* the infection-,

dissemination-, and transmission-rates were all significantly lower with the rRVF-ΔNSm mutant compared to the wild-type (93). Only five of the 129 *Ae*. mosquitoes used in the experiments, were infected, and of those five, only one was positive for dissemination, and subsequently, transmission (93). In *Cx quinquefasciatus*, on the other hand, infection and dissemination rates of the rRVF-ΔNSm mutant were significantly lower, but the transmission rate was similar to that of the wild-type virus (93).

Kreher et al found that a recombinant (ZH548) virus lacking the first initiation codon (AUG S1 KO), the first through third initiation codons (AUG S1+2+3 KO), and that lacking the second and third initiation codons (AUG 2+3 KO) grew to lower titers than the parental virus in the *Aedes albopictus* C6/36 cell line (92). The AUG S1+2+3 KO virus displayed the most reduced viral titer in the C6/36 cells compared to the other mutants (92). Infection and dissemination rates of these mutants in *Ae. aegypti* mosquitoes were also determined (92). At 14 days post infection, the AUG 2+3 KO had similar infection rates compared to the parental virus, and the dissemination rate was similar at day 14, but it did not rise by day 21, as did the parental virus (92). The infection rate of the AUG S1 KO mutant was similar to the parental virus at day 14 but was reduced at day 21 (92). However, the ability of this virus to disseminate in mosquitoes was severely reduced, as only one mosquito displayed dissemination (92). Because the infection rate of the AUG S1+2+3 KO was so low, the consequences of the abolishment of 78 kDa, NSm, and NSm' on infection and dissemination in *Ae. aegypti* mosquitoes could not fully be elucidated (92). Overall, this study demonstrated that infection of C6/36 cell is modulated by NSm/NSm' activity, while 78 kDa plays the major role in viral dissemination in *Ae. aegypti* mosquitoes (92).

ANTIVIRAL THERAPIES

Though many antiviral therapies have been studied, no licensed therapeutics for Rift Valley fever are currently available. Ribavirin, a broad spectrum antiviral that has been used to treat several other viruses that cause hemorrhagic fever, has been investigated for its anti-

RVFV properties. As a synthetic analog of guanosine, ribavirin is thought to act in an antiviral capacity in several ways. The proposed mechanisms of antiviral activity of ribavirin include polymerase inhibition (as a nucleoside analog of guanosine), RNA mutagenesis (incorporation into viral genomes), and competitive inhibition of inosine monophosphate dehydrogenase (necessary for guanosine biosynthesis) (95). However the exact mechanism by which it works is not fully understood and it can produce adverse side effects (96, 97). Its large size also prevents it from being able to pass the meningeal barrier, and because of this, ribavirin was unable to prevent meningeal-encephalitis in a group of RVF patients in Saudi Arabia (96).

Protection from RVFV infection involves innate immune responses and type I IFN induction (98-100). Swiss-Webster mice were completely protected from RVFV challenge when given Poly (ICLC) daily starting at 24 hours post infection (100). Four doses of 20 μg poly (ICLC) given intraperitoneally (i.p) was required to prevent mortality (100). Viremia was reduced in rhesus monkeys that received five, daily doses of recombinant leukocyte A IFN-α or human leukocyte IFN (98). Adverse side effects and a lack of safety and efficacy studies in RVF patients have limited the potential for ribavirin and poly (ICLC) and ribavirin as RVF treatments (101).

Several compounds have demonstrated anti-viral properties against members of the *Bunyaviridae* family. Curcumin is has been shown to have anti-viral, anti-inflammatory, and anti-arthritic properties (102). This compound can inhibit the IKK complex and, subsequently, RVFV replication. Another antiviral molecule in the early stages of development for RVF treatment is FGI-106 (103). In cell culture, wt RVFV was inhibited by FGI-106, and in a lethal RVFV challenge in mice, onset of disease was delayed with FGI-106 treatment (103). Further study will be required to understand the antiviral mechanism of FGI-106 to determine its anti-RVFV therapeutic potential.

Broad spectrum inhibitors of RNA or enveloped viruses that are being investigated as potential treatment of RVF include Favipiravir, Favipiravir relatives, and LJ001. Favipiravir, or T-

705, inhibits the RNA-dependent RNA polymerase of RNA viruses, and it is currently in Phase III clinical trials for treatment of influenza (104-107). Early research on T-705, as a prospect for RVFV treatment, involved surrogate studies using Punta Toro virus (PTV), a new world phlebovirus transmitted by sandflies, which causes self-limited febrile illness in humans and can be handled in BSL-2 conditions making it more useful for preliminary studies than pathogenic RVFV (103). When given two times a day (30 mg/kg/day) starting 24 hours post lethal-challenge, T-705 was able to protect 90% of PTV (5000 PFU) infected C57BL/6 mice (108). Due to theses promising results, further investigation into the anti-RVFV properties of RVFV were undertaken using the pathogenic RVFV strain, ZH501 in both golden Syrian hamsters (107) and Wistar-Furth rats (Caroline 2014). Hamsters infected with RVFV usually die of infection within 48 hpi (107, 108). Sixty percent of hamsters given T-705 (200 mg/kg/day), twice daily starting at 24 hpi, survived lethal RVFV infection, and T-705 treatment ameliorated acute disease and protected against late-stage encephalitis better than ribavirin (107). However, in the WF rat study, the 6 rats (out of 72 total) that succumbed to aerosol infection, died of late-stage encephalitis, despite treatment with T-705 at various doges (20, 50, 100 mg/kg) (109). These results were due to lower doses of T-705 (2 rats given 20 mg/kg; 1 given 50 mg/kg) or delayed treatment with 100 mg/kg (2 in the 12 hpi group and 1 in the 48 hpi group) (109). Overall, 90% of WF rats that were treated with 100 mg/kg started at 48 hpi survived infection with highly lethal RVFV aerosol infection (109). These results suggest T-705 may be a viable resource in RVF treatment, and since it is in Phase III clinical trials, its safety profile in humans has been well-established.

T-1106, a pyrazine derivative similar to T-705, was more efficacious than T-705 in a PTV hamster model of infection but not in a mouse model (110). Unlike T-705, T-1106 is able to target the liver, which is greatly affected in the PTV hamster model, which may explain the differences in efficacy between the two animal models. A number of enveloped viruses are inhibited by the aryl rhodanine derivative, LJ001, which is able to prevent viral-host membrane

fusion, via insertion in the viral membrane (111). LJ001 works at non-cytotoxic levels, and with wt-RVFV was pretreated with LJ001, mortality is mice was completely prevented (111). Efficacy and safety studies are required fully evaluate the potential of LJ001 as an antiviral treatment for RVFV.

Another interesting antiviral strategy is to use peptides structurally similar to viral components that inhibit fusion (112). A fusion-inhibiting peptide, RVFV-6, demonstrated to be effective at inhibiting fusion of RVFV-ZH501, which uses a Class II type fusion mechanism (112). Class II type fusion proteins are distinguished from Class I and Class III type by the location and structure of the "fusion peptide" or "fusion loop" (113). The Class II fusion loops are anti-parallel β-sheets composed of aromatic and hydrophobic amino acids, and they are internally located (113). The putative fusion loop of RVFV is located within Gc, and several peptides were designed based on the sequences of the Gc protein (112). The RVFV-6 peptide, which is based on the Gc stem region (N450-468), demonstrated the ability to not only inhibit RVFV infection, but was also able to inhibit Andes virus (Class II), Ebola virus (Class I), and Vesicular Stomatitis virus (Class III) (112). Interestingly, other viruses that have Class II type fusion proteins, such as Venezuelan Equine Encephalitis virus (VEEV), Eastern Equine Encephalitis virus (EEEV), and Western Equine Encephalitis virus (WEEV) were not inhibited; even at the highest concentration used (50 μM) (112). The proposed mechanism of fusion-inhibition by RVFV-6 involves two steps: 1) association with RVFV, independent of Gc; followed by 2) Conformational changes in Gc due to the low pH environment of the late endosome allow specific binding of RVFV-6 to Gc (112). Binding of RVFV-6 to Gc prevents fusion of the viral membrane with the host membrane and release of the viral contents into the cytoplasm (112). Future studies that identify where RVFV-6 binds to the Gc, if binding is reversible, and *in vivo* efficacy studies will be invaluable in determining if the true antiviral potential of this fusion-inhibiting peptide and others (112).

VACCINE CANDIDATES

Due to the sporadic nature of RVF epidemics, vaccination is paramount to preventing further spread of the virus. Symptomatic RVF can be prevented by the antibodies to the virus induced by vaccination (114). Currently, no fully licensed RVF vaccines exist outside endemic countries. Factors that are of concern when producing a RVF vaccine include the rapid induction of protective immunity and low manufacturing cost. As ruminants are the most susceptible to RVFV disease, the prioritization of veterinary vaccines is the most important factor in RVF prevention. Also, since farmers, veterinarians, and anyone that works closely with animals are also at high risk during an RVF outbreak, an efficacious and highly safe vaccine should be available for human use, as well. It is thought that a single RVFV strain could be used to develop a vaccine due to the high genetic homology seen among RVFV isolates and cross-reactivity among divergent strains (7).

Live-attenuated vaccines

Wild-caught mosquitoes from the Semliki Forest region of Uganda were used to derive the first live-attenuated vaccine for RVF (115). The Entebbe RVFV strain was isolated from the mosquitoes, then was passaged 82 times in the brains of suckling mice (4). After being further passaged in embryonated eggs and then mice, the first experimental vaccine was released in 1951 in South Africa (4). Since 1971, the vaccine has been amplified in BHK-21 cells, and it is used as a veterinary vaccine in endemic areas (4, 116). With a single dose, the vaccine produces life-long immunity and within 5-7 days, and it is inexpensive **(Table 1-2)** (4). However, fetal malformations and abortions have been reported when pregnant animals are vaccinated with the Smithburn vaccine (14). Reversion to a virulent phenotype and ability to spread via local, competent vectors prevents the vaccine from being recommended in non-RVFV endemic countries (4). Because the vaccine is a live vaccine, there have been reports of the creation of reassortments with wild-type RVFV, including reassortant 95EG Cow-2509 strain isolated in

Egypt from the aborted fetus of a vaccinated cow and the SA184/10 strain that was isolated from a South African who was vaccinating sheep and suffered a needle injury (5)

Type	Commercially Available	Industry Involved	Safe in Pregnant Animals	Single Dose	Genome Structure	Reference
Inactivated	**YES**	OBP	**YES**	**NO**	Formalin-inactivated	Kamal 2011; FAO 2015
Smithburn	**YES**	OBP & others	**NO**	**YES**	Live, attenuated	Smithburn, 1949
MP-12	**NO**	Zoetis (PFIZER)	**?**	**YES**	Mutagenized, attenuations in S, M, & L	Morrill *et al.,* 1987, 1991, 1997.
arMP-12-Δ-NSm	**NO**	**MCI, Sante Animale**	**?**	**YES**	78 kDa/NSm region deleted from M segment	Morrill *et al.,* 2013; Weingartl *et al.,* 2014; Morrill *et al.,* 2013.
Clone-13	**YES**	**OBP (S.Africa)**	**NO**	**YES**	NSs region deleted from S segment	Muller *et al.,* 1995; Dungu *et al.,* 2010; von Teichman *et al.,* 2011. Makoschey *et al*., 2016
R566	**NO**	**Merck Animal Health**	**?**	**YES**	Clone 13 S & MP-12 M & L segments	Kortekaas *et al.,* 2014.
DDVax	**NO**	**Merial/ Deltamune**	**YES**	**YES**	Deleted NS region of S & M segments of ZH501	Bird *et al.,* 2008, 2011.
NDV-GnGc	**NO**	**Deltamune**	**?**	**YES**	NDV expressing RVFV Gn/Gc	Kortekaas, de Boer *et al.,* 2010; Kortekaas, Dekker *et al.,* 2010.
NSR-Gn	**NO**	**Merck Animal Health**	**?**	**YES**	Non-spreading RVFV expressing Gn	Oreshkova *et al.,* 2013.

Table 1-2: Commercially Available and Vaccine Candidates for RVFV. Modified from a presentation by Dr. Doug Watts (ASTMH 2014) and The FAO Report 2015: *The last hurdles towards RVFV control*.

.

Clone-13 (C13) is another live-attenuated vaccine for RVF and was plaque-cloned from the 74HB59 RVFV strain, which was isolated in the Central African Republic from a nonfatal

RVF case (117). After purification, it was determined that C13 lacks a large portion of the NSs open reading frame (ORF) (117). Both the M- and L-segments are wild-type, but due to the missing ORF, C13 lacks the expression of a functional NSs (118). Studies have demonstrated the efficacy and safety of C13, even in young animals (calves/lambs) and in pregnant ewes (119, 120). Also, C13 has an inherent DIVA marker (differentiation of infected from vaccinated animals): anti-NSs antibodies present in livestock would indicate wild-type RVFV infection, as C13 would not induce antibodies to NSs (121). Though there have been some concerns of efficacy in the production of C13, it has been licensed in South Africa, Zimbabwe, Botswana, and Namibia (122). In addition, a recently published study has demonstrated that the Clone-13 RVFV strain can be vertically transmitted from pregnant ewes to their fetuses and cause stillbirths and malformations (123).

Other live attenuated vaccine candidates have been produced using the reverse genetic system for RVFV (65, 124-126). Gene deletion involving the other RVFV virulence factor, NSm, has also been investigated (127). Both the NSm and NSs genes were removed from the wild-type ZH501 strain, and this vaccine strain was demonstrated to be safe in newborn and pregnant animals and very efficacious (128, 129). These gene deletions can be used as DIVA markers. It should be noted that in another study, that intranasal inoculation of rZH501-ΔNSs, resulted in 100% mortality in C57BL/6 mice, whereas subcutaneous footpad inoculation resulted in 100% survival and no signs of clinical infection (130).

The MP-12 live-attenuated vaccine, on the other hand, encodes a functional NSs protein. It was developed by the United States Army Medical Research Institute of Infectious Diseases (USAMRIID) for human use to replace the TSI-GSD-200 vaccine (149). Subsequently, it demonstrated efficacy in animals (135, 136, 138, 139, 140). MP-12 was derived from the serial passage of the wild-type ZH548 strain in human diploid MRC-5 cells that were exposed to 5-fluorouracil, a chemical mutagen for viral RNA (131). Twelve passages generated 23 mutations within all three segments of MP-12 (132, 133). When the NSs of ZH548 was replaced

with that of MP-12, virulence was not affected indicating the S-segment of MP-12 is partially attenuated (126). The other two segments are attenuated, and it is thought that, in combination, the M- and L-segment mutations produce the attenuated phenotype of MP-12 (134). Though there have been reports of abortions in pregnant animals (135, 136), MP-12 has repeatedly been shown to be safe and efficacious in animals (137-140). However, MP-12 lacks a DIVA marker.

Since the MP-12 strain has potential as a vaccine candidate, various modifications have been investigated. The arMP-12 ΔNSs16/198 vaccine strain was developed using reverse genetics and encodes an in-frame truncation of the NSs gene (Δ16-198), identical to the C13 strain, but the N- and C-terminal peptides are linked with additional Asp-Val (141). While this vaccine strain produced a lower neutralizing antibody titer in mice than parental MP-12, no viremia was detected in any of the mice inoculated (141). Also, as no anti-NSs antibodies were produced, this vaccine strain contains a DIVA marker (141). The R566 strain is a reassortant MP-12 strain that encodes the M-and L-segments of MP-12 and the S-segment of C13 (142). However, when compared to that of C13, the immunogenicity of R566 was decreased (142). Both R566 and arMP-12 ΔNSs16/198 are attenuated in all three segments reducing the potential creation of virulent RVFV reassortments with wild-type viruses (15). A novel 2-segmented MP-12 vaccine candidate, encoding the replacement of the NSs protein with that of Gn and Gc coupled with the L-segment, has been developed by Brennan et al. (2011). The r2segMP-12 strain produced lower amounts of Gn and grew to lower titers in both mammalian and insect cell culture compared to a three segmented rMP-12, which included the two r2segMP-12 segments and an M-like segment that encoded GFP in between the UTRs of the M-segment (143). An MP-12 strain that lacks NSm, arMP12-ΔNSm, has also been investigated for vaccine potential (136). The vaccine strain demonstrated high immunogenicity in ruminants, but reassortment risk with wild-type virus strains would need to be evaluated as the virus retains the NSs gene.

Formalin-inactivated vaccines

A formalin-inactivated vaccine for RVFV was derived from the Entebbe strain. The wild-type strain was passaged 184 times in mice, grown in African green monkey kidney cells, and finally, was formalin-inactivated (144, 145). The vaccine was named NDBR 103 and starting in 1977, more than 500 laboratory personnel and various volunteers (145, 146) and 963 United Nation soldiers (147, 148) were vaccinated with NDBR103. The TSI-GSD-200 vaccine was subsequently produced in diploid FRhL-2 cells following more rigorous regulations of safety (142),(147). USAMRIID and the Salk Institute worked together to produce the TSI-GSD-200 vaccine, and a 12-year long study demonstrated long-lasting protection in humans that received three vaccinations (149). Beyond 6 months, additional booster vaccinations are required to maintain immunity, which is considered to be a neutralizing titer of 1:40 (149). Minor events and one report of Guillian-Barre syndrome were noted, but there have not been any reports of any other severe adverse events, such as anaphylaxis or death, reported with either to NBDR 103 or TSI-GSD-200 (146, 150). The only RVFV vaccine for humans is TSI-GSD-200, but it is exceptionally expensive is not available for public use.

There are also formalin-inactivated RVFV veterinary vaccines available. These vaccines are based on highly virulent wild type strains, such as Menya/Sheep/258 or ZH501 (4, 14, 151). Full protection depends on boosters, recommended every 6 months, which can be costly in resource poor-settings.

Subunit vaccines

Due to the lack of infectious virus particles, subunit vaccines are considered a safe alternative to traditional vaccines. *Drosophila melanogaster* cells, the Stable Schneider 2 (S2) cell line, have been used to develop RVFV subunit vaccines. This cells line can produce proteins that are secreted into the supernatant and can be kept in serum-free medium (152). The ectodomain of Gn (Gn-e) was purified from S2 cells and was used to immunize mice (152). When the adjuvant, Stimune, was added, two immunizations of Gn-e were adequate to protect

mice from a lethal challenge of RVFV (152). In another study, Gn-e was produced with Flag and Strep-tags, and lambs were protected from RVFV lethal challenge with one immunization when formulated with Stimune (153).

Using a recombinant baculovirus system, Faburay et al. generated a Gn-Gc subunit vaccine candidate and vaccinated six sheep (154). After a primary dose of 50 µg adjuvanted with montanide ISA125, three sheep had antibody reactivity to Gne (the Gn ectodomain) at 7 days post vaccination (154). All six sheep seroconverted by day 14 post vaccination, and five of the six sheep had protective neutralizing antibodies ($PRNT_{80} \geq$1:40) (154). A booster dose was given at day 21 post vaccination, and all six sheep had increased neutralizing antibody titers ($PRNT_{80} \geq$1:1280) (154). At day 328 post vaccination, neutralizing antibody titers were analyzed and still demonstrated to be protective ($PRNT_{80} \geq$1:80) (154). Because this subunit vaccine candidate only encodes the glycoproteins, it has an intrinistic negative DIVA marker, the N protein (154). Indeed, none of the sheep vaccinated produced an antibody response to RVFV N (154).

Virus-like particles (VLP)

Virus-like particles (VLP) are another option for RVFV vaccine candidates because they can mimic wild-type virus but are exceptionally safe because they lack a viral genome (155). As such, inactivation or attenuation is not required, and they have the potential to produce a more potent immune response, with a lower dose, than inactivated vaccines because they retain the same size and epitopes of wild-type virus (155). Insect cells (152, 156-158) or mammalian cells (159-162) can be used to produce VLPs, but insect cells are preferred due to cost concerns by a variety of methods, including a Drosophila insect expression system (33), a recombinant baculovirus expression system (107) or via expression systems utilizing the gag protein of the Moloney murine leukemia virus (112, 113).

Other vaccines

Replicon RVFV vaccines based on Sindbis virus (SIN) or Venezuelan equine encephalitis have also been investigated (163, 164). After vaccination, IgG_1, IgG_{2a} and IgG_{2b} were induced by a VEEV replicon that encoded the ectodomain of Gn. In mice, the CAdVax vector system, Gn and Gc proteins that are expressed by an adenovirus vector, was shown to be efficacious an safe (165, 166). In mammals, New Castle disease virus (NDV) does not inhibit type-I IFN responses making it an attractive viral vector (167). As such, the RVFV Gn gene was inserted into the La Sota NDV strain (NDFL platform), which is attenuated, and when cattle were vaccinated twice, neutralizing antibodies were produced (168-171). When both Gn and Gc were expressed by the NDFL platform, mice were protected from challenge and had sterile immunity (153).

The stability of DNA plasmids makes them practical vaccine options for diseases that occur in tropical areas, where high temperatures can be a concern. Plasmids encoding the glycoproteins (Gn/Gc) of RVFV were shown to produce neutralizing antibodies and protection from RVFV challenge (172, 173). In another study, the ectodomain of Gn was fused the three, tandem repeats of the C3d mouse homolog, which binds to the complement receptor 2, which can be found on T cells or B cells, or follicular dendritic cells. Antibody production may result from the activation of these cells. Mice injected with the plasmid encoding Gn-C3d were protected from wild-type challenge and displayed Th2-type immune responses (174). The RVFV N protein has been demonstrated to also induce cellular immunity (175, 176), and a plasmid construct that had ubiquitin fused to the N protein protected mice from wild-type RVFV challenge (177).

Non-spreading RVFV replicons, those that lack an M-segment, are also being developed with the idea that cells can be infected, but cannot produce viable viral particles due to the lack of glycoproteins (178, 179). For example, plasmids that encode both the S- and L- segments (full-length) and a plasmid that encodes the Gn/Gc glycoproteins are transfected into BHK cells

that stably express T7 RNA polymerase (178). Alternatively, the replicon could be recovered by transfection of cells stably expressing S- and L-segments by T7 RNA polymerase with a plasmid expressing Gn/Gc proteins (179). The replicons could be also obtained by infection of different type of cells with replicon and co-expression of Gn/Gc proteins (179). The replicon is then injected into mice or ruminants and completes a single round of infection. Studies have demonstrated this approach to be safe and produce immunity to RVFV (153, 178, 179).

In laboratories that study RVFV, cases of accidental exposure will need to be properly addressed, and, as such, post-exposure vaccination studies have been performed (180). Mice that were challenged with a lethal dose of RVFV were protected by post-exposure vaccination with MP-12 that lacked NSs but not MP-12 with a fully functional NSs (180). Though protection waned after 20 mins post-exposure, strong protection was conferred when mice were vaccinated 20 minutes post challenge (180). Early induction of type-IFNs most likely play a role since the MP-12 with a functioning NSs, which prevents IFN induction, failed to protect, but further studies will be necessary to confirm.

N-GLYCOSYLATION AND RVFV N-GLYCOSYLATION

Proteins are highly diverse not simply due to their amino acid sequences, but due to post-translational modification. Glycosylation is the most common post-translational modification of proteins, and it is estimated that over half of all expressed cellular proteins are glycosylated (181). There are five types of glycosylation: N-linked, O-linked, glypiation, c-linked, and phosphoglycosylation (181). N-linked, where an *N*-acetylglucosamine (GlcNAc) is attached to the amino group of an asparagine (N), is the most common (at least 90% of glycoproteins are N-glycosylated) and well described (181). N-linked glycosylation takes place in the Endoplasmic Reticulum (ER) and Golgi apparatus and proceeds in a step-wise fashion, and it is divided into four main events: precursor production, attachment of N-glycan to nascent protein, trimming of the N-glycan, and maturation of N-glycans (181). N-glycosylation produces three types of N-glycans: oligomannose or high mannose, hybrid, and complex type **(Figure 1-4)** (181).

Experimentally, high mannose and hybrid N-glycans are identified by their susceptibility to digestion endoglycosidase H (endo H), whereas peptide-N-glycosidase F (PNGaseF) will cleave all three N-glycans at the GlcNAc-asparagine bond **(Figure 1-4)** (181). Each type is determined by the terminal sugars, but all three types contain a common core ($Man_3GlcNAc_2$), which is produced by a common precursor ($Glc_3Man_9GlcNAc_2$-P-P-Dol).

Before translation of glycoproteins, an N-linked glycan starts as a precursor on the cytoplasmic side of the ER **(Figure 1-5)** (181). Dolichol-P, a polyisoprenol lipid in the membrane of the ER, receives a GlcNAc-1-P from UDP-GlcNAc via the enzymatic activities of GlcNAc-1-phosphotransferase producing the first necessary product of N-glycan production: Dol-P-P-GlcNAc (181). Tunicamycin, an antibiotic that is used in N-glycosylation studies, is an analog of UDP-GlcNAc and prevents the GlcNAc-1-phosphotransferase from attaching the GlcNAc to Dol-P, thus preventing N-glycosylation (181). Once Dol-P-P-GlcNAc is produced,

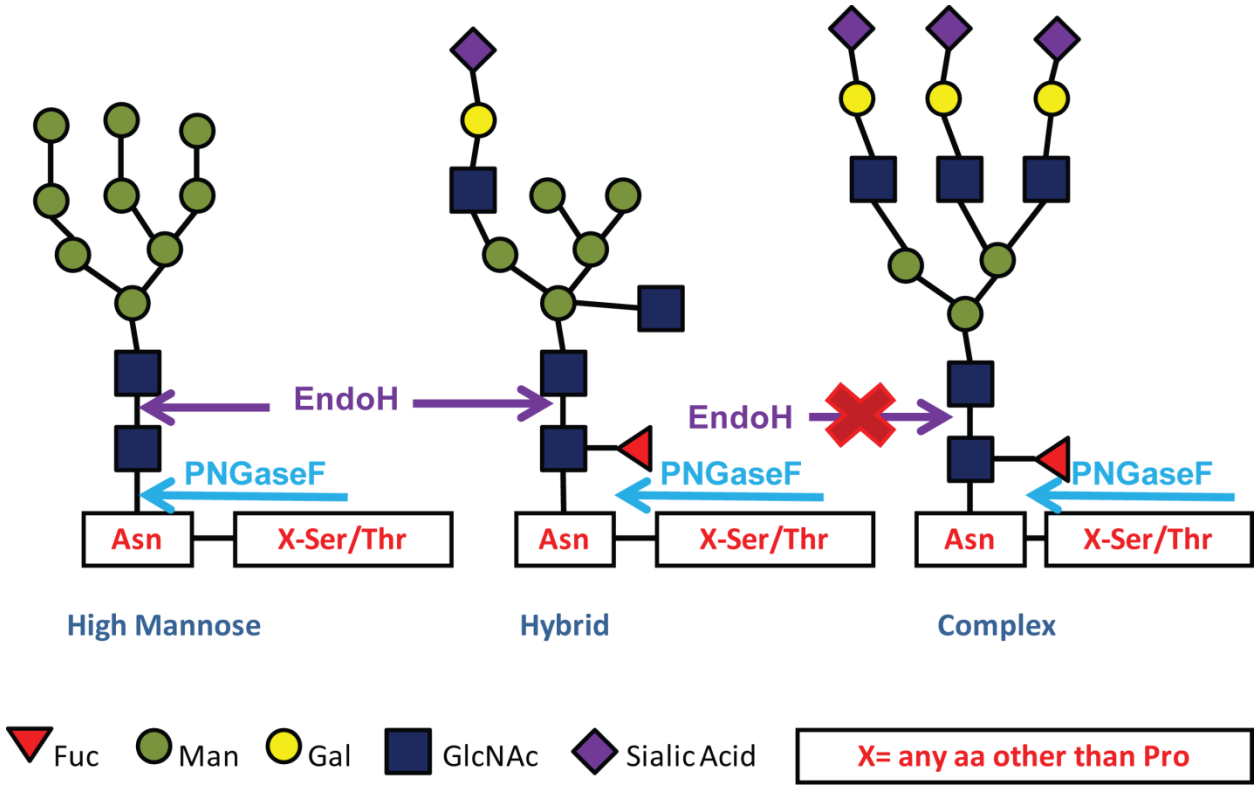

Figure 1-4: Types of N-linked Glycans. There are three types of asparagine (N)- linked Glycans: High mannose, Hybrid, and Complex. Branches of high mannose type N-glycans terminate in Mannose sugars, designated by green filled circles. For hybrid-type, one branch terminates in mannose sugars,

while the other branch can terminate in a wide variety of sugars. The branches of Complex type N-glycans can terminate in a wide variety of sugars, the most common type is a NANA complex, which are long strings of repeating Galactose (Gal- yellow-filled circles) followed by Sialic Acid (purple-filled diamonds). The GlcNAc of each Glycan is linked to the N found in a common motif encoded by the genome: N-X-Serine (S)/Threonine (T). Experimentally, high mannose and hybrid N-glycans are identified by their susceptibility to digestion endoglycosidase H (endo H), whereas peptide-N-glycosidase F (PNGaseF) will cleave all three N-glycans at the GlcNAc-asparagine bond.

another GlcNAc is transferred from UDP-GlcNAc; then five mannoses are added in a stepwise fashion from GDP-Man, all via distinct glycosyltransferases (Gtfs) (181). A proposed enzyme, "flippase", transfers the $Man_5GlcNAc_2$-P-P-Dol precursor across the ER membrane into the ER lumen, along with Dol-P-Man and Dol-P-Glc (181). On the lumen side, Dol-P-Man and Dol-P-Glc add four mannose residues and three glucose residues, respectively to complete the precursor ($Glc_3Man_9GlcNAc_2$-P-P-Dol), which can be transferred to the peptide (181).

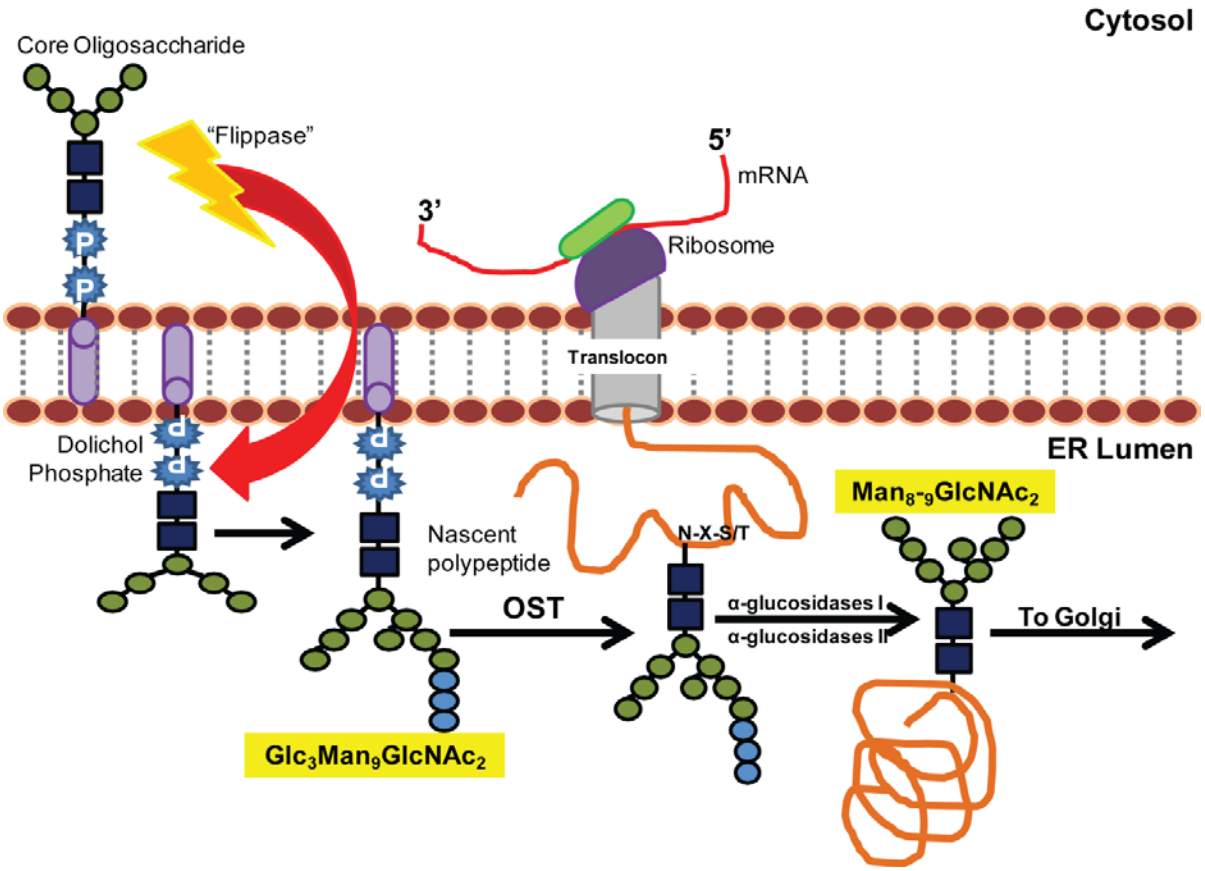

Figure 1-5: Addition of N-glycan Precursor to Nascent Polypeptide. The core precursor of the N-glycan is produced on the cytosol side of the endoplasmic reticulum. An enzyme, "flippase", flips the core precursor into the ER lumen, where it is further modified to $Glc_3Man_9GlcNAc_2$. Then, the precursor is added to the nascent polypeptide by the oligosaccharide transferase (OST). The precursor is further

modified to $Man_{8-9}GlcNAc_2$, and once proper folding of the peptide has occurred, the peptide is sent to the Golgi apparatus (*cis*-Golgi), where further modification of the N-glycan can occur. Proteins that are not properly folded either bind to chaperones in the ER for refolding or are marked for the ER associated degradation (ERAD) pathway by EDEM (*E*R *d*egradation-*e*nhancing α-*m*annosidase I–like protein *Modified from http://mol-biol4masters.masters. grkraj.org/html/ Co_and_Post_Translational_Events4-Glycosylation_of_Proteins.htm

For the precursor to be added to the peptide, a signal motif must be present in the amino acid sequence (181). The signal motif is asparagine (N) followed by any amino acid, other than proline, followed by serine (S) or threonine (T): N-X-S/T (181). Occasionally, N-X-Cysteine (C) can be glycosylated when the C is in a reduced form (181). The presence of an N-X-T/S/C motif in the amino acid sequence is necessary but not sufficient for N-glycosylation due to many factors, including presence in the ER lumen and how quickly the protein folds after translation (181). In addition, when the amino acid in the X position is acidic [aspartate (D); glutamate (E)], the efficiency of N-glycosylation is reduced (181).

The “en bloc” transfer of the N-glycan occurs via the membrane-bound, oligosaccharyltransferase (OST) (181). In mammals, there are three OST complexes that have been identified (Mammalian OST-I, OST-II, and OST-III) (181), and they are comprised of seven to eight nonidentical subunits (182). The active site is in the STT3 subunit (183), and there are two isoforms STT3A and STT3B, which have different kinetic properties and act can in concert or sequentially (184). In addition to the standard N-glycan precursor ($Glc_3Man_9GlcNAc_2$-P-P-Dol), STT3B can also mediate the transfer of intermediate precursors found in the ER lumen ($Glc_3Man_{5-9}GlcNAc_2$-P-P-Dol) (182, 184). The STT3A unit is involved in the co-translational addition of the N-glycan precursor to the peptide (184). As the growing peptide is passed through the protein translocation channel into the ER lumen, the STT3A subunit, which is associated with the channel (185), adds the N-glycan precursor ($Glc_3Man_9GlcAc_2$-P-P-Dol), to the growing peptide. Translation occurs very rapidly, and activity of the OST is highly dependent on protein conformation in its ability to add the precursor (181). Thus, the most N-glycans are located on the N-terminal region of the protein (181). However, in some cases N-

glycosylation can occur post-translationally via the STT3B isoform (184). It has been demonstrated that extreme C-terminal N-glycan sites (usually within the last 50 residues) tend to be skipped by the STT3A OST but are acted on by the STT3B OST (184). Also, the presence of internal N-glycosylation sites (located between 65-75 residues from the N-terminal region and >50 residues from the C-terminal end) increases the likelihood of C-terminal N-glycosylation by the STT3B OST (184). Lastly, C-terminal N-glycosylation is affected by the amino acids in the T/S/C sites of the sequon, where T>S>C (184).

After the N-glycan precursor ($Glc_3Man_9GlcNAc_2$-P-P-Dol) is added to the growing peptide by the OST, sequential trimming of the glucose residues occurs by α-glucosidases I and II **(Figure 1-5)** (181). This event, along with the addition of an innermost glucose, occurs during the folding of the protein and increases the amount of time the protein spends in the ER (181). Many proteins also have an additional mannose residue trimmed by ER α-mannosidase I, which leaves the final precursor as $Man_8GlcNAc_2$ (181). The trimming process provides an avenue for the ER chaperones, calnexin and calreticulin, to help properly fold the glycoproteins (181). Proteins that do not fold or are misfolded are marked for the ER associated degradation (ERAD) pathway by EDEM (ER degradation-enhancing α-*m*annosidase I–like protein), which is α-mannosidase I–like protein without enzymatic activity (181). EDEM binding to a misfolded protein results in poly-ubiquitination and exportation from the ER into the cytoplasm, where the protein is degraded by proteasomes. Also, N-glycosylation by STT3B of cryptic N-glycan sites (sites only glycosylated when the C-terminal region is destabilized) can also mark the protein for ERAD (184). Upon leaving the ER, the N-glycans of many glycoproteins terminate in eight or nine mannose residues (181). Sometimes incomplete processing can occur leaving a glucose residue, which will be cleaved along with the attached mannose by Golgi-resident endo-α-mannosidase (181). This cleavage creates a different $Man_8GlcNAc_2$ isomer than the one produced the ER (181).

In the *cis*-Golgi, further trimming takes place by α1–2 mannosidases IA, IB, and 1C, which produce $Man_5GlcNAc_2$ **(Figure 1-6)** (181). Hybrid and complex N-glycans cannot be formed without this key intermediate as they cannot be further processed in the *medial*- and *trans*-Golgi (181). Proteins not processed in the *cis*-Golgi have oligomannose or high mannose type N-glycans (181).

In the *medial*-Golgi, the generation of hybrid and complex N-glycans begins with the addition of a GlcNAc to the $Man_5GlcNAc_2$ by the N-acetylglucosaminyltransferase, GlcNAcT-I **(Figure 1-6)** (181). This step is necessary for the N-glycans to be further trimmed by α-

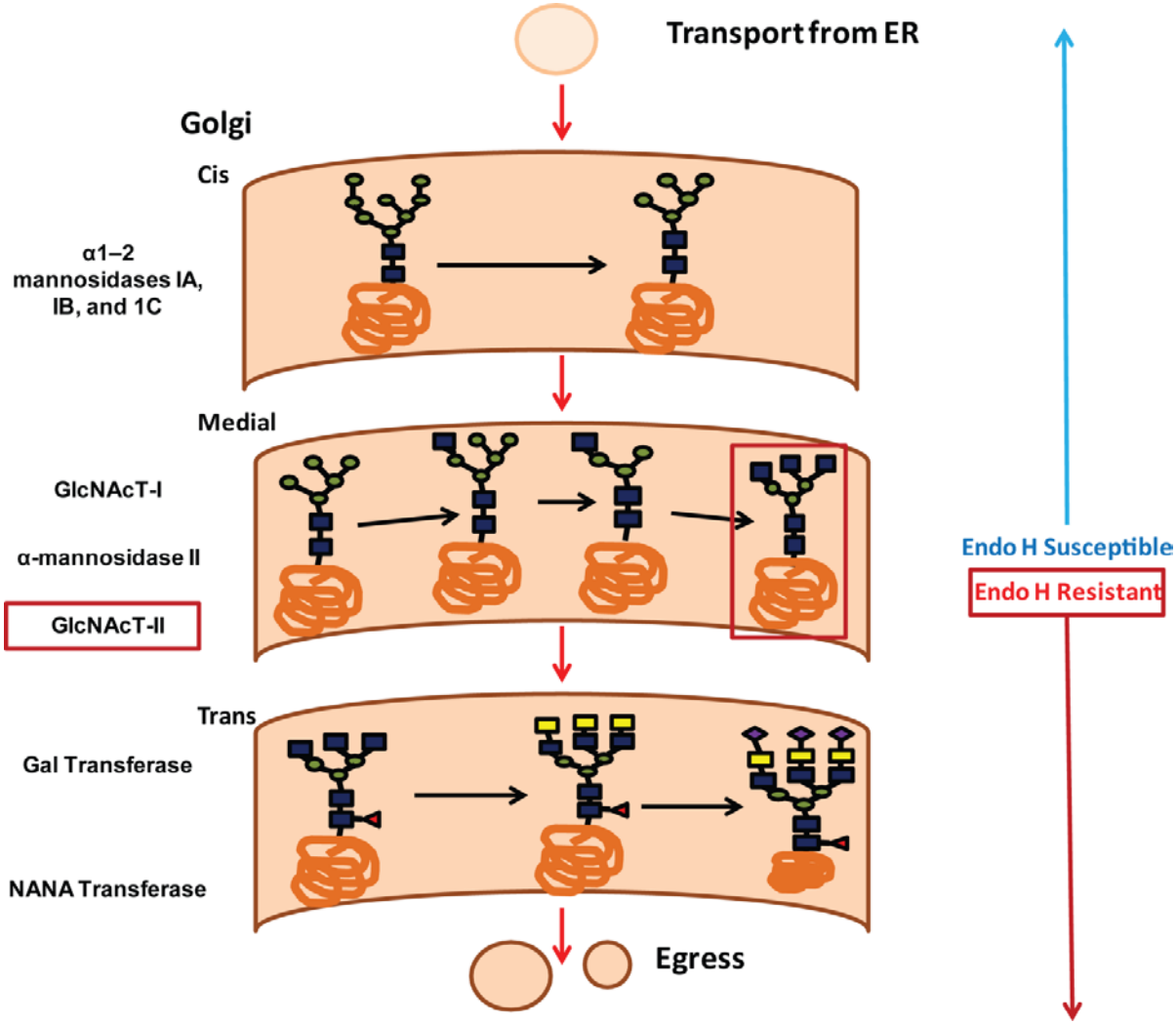

Figure 1-6: Trimming and Addition of Sugar Moieties to N-glycans in the Golgi Apparatus. In the *cis-Golgi*, the N-glycan is trimmed by α1–2 mannosidases IA, IB, and 1C. This step is required for the production of hybrid and complex type N-glycans. In the *medial*-Golgi, the N-glycan is further acted upon

by GlcNAcT-I, which adds a GlcNAc to the mannose α1-3 in the core, followed by trimming of mannose residues in another branch in the core by α-mannosidase II (hybrid type). Trimming of mannose residues by α-mannosidase II allows an addition of GlcNAc to the mannose α1-6 in the core by GlcNAcT-II (complex type). Trimming of mannose by mannosidase II is required for the production of complex type N-glycans. Addition of two GlcNAcs by GlcNAcT-II, confers Endo H resistance to the N-glycan. Each step in the entire process is sequential and requires the previous step and interaction of N-glycan with the enzymes.

mannosidase II, which removes two mannose residues to produce $GlcNAcMan_3GlcNAc_2$ (181). If α-mannosidase II fails to trim the mannose residues, hybrid glycans ($GlcNAcMan_5$-4GlcNAc2) are formed (181). The precursor for complex glycans are produced when GlcNAcT-II adds a second GlcNAc to the other branch of the mannose core creating a biantennary precursor (181). After this step, the N-glycans are resistant to digestion by endoglycosidase H (endo H) (181). Tri- and tetra-antennary N-glycans can be created via addition of GlcNAcs to the other carbons of the core mannose by GlcNAcT-IV, and bisecting GlcNAcs can be added to either hybrid or complex N-glycans to the β-mannose of the core by GlcNAcT-III (181).

So-called maturation of N-glycans occurs in the *trans*-Golgi (181). Here, sugars are added to the core, the GlcNAc branches are elongated by further sugar additions, and the elongated branches are then "decorated" with terminal sugars (181). The core GlcNAc, attached to the asparagine, receives a fucose residue in many vertebrates, and in mammals, few other sugar additions to the N-glycan core occur (181). In many hybrid and complex glycans, a β-linked galactose residue is added to the GlcNAc on the main branch(es), creating a building block, Galβ1-4GlcNAc or the "LacNAc"sequence (181). While other sugar variations can occur, the most common additions are tandem repeats of LacNAc creating poly-LacNAc branches (181). Lastly, the addition of sialic acid (NANA), fucose, galactose (Gal), *N*-acetylgalactosamine (GalNAc), and sulfate to the branches denotes the "capping" or "decorating" step of hybrid and complex N-glycan production (181). Antibodies and lectins interact with the terminal sugars of N-glycans, and as such, many terminal sugars are α-linked so that they extend away from the β-linked ribbon-like poly LacNAc branches (181).

Glycoproteins can exist as homogeneous or heterogeneous glycoforms (181). Many glycoproteins display “microheterogeneity”, meaning that one particular N-glycan site may have no N-glycan present or different types of N-glycans present, depending on the cell type, cell cycle, availability of glycosidases and Gtfs, rate of transport through the translocon, rate of transport through the ER and Golgi, and localization of glycosidases and glycosyltransferases (Gtfs) in the lumens of the ER and Golgi (181). If a particular glycosidase or Gtf encounters an N-glycan at one site before another, the remodeling of that site may interfere with the remodeling of the other (181).

RVFV encodes six putative N-glycosylation sites: one in the preglycoprotein region (N88), which is an upstream of Gn coding region, and five within the Gn/Gc region that are found at: N438 (Gn); N794 (Gc); N829 (Gc); N1035 (Gc); and N1077 (Gc) **(Figure 2-1)**. Two studies regarding the N-glycosylation status of RVFV Gn and Gc, have been reported (186, 187). In the first study, BSC40 cells (African green monkey kidney cells) were infected with a recombinant vaccinia virus expressing the entire ORF of the M segment and extending beyond the termination codon of the authentic RVFV M segment, which produced the 78 kDa protein from the 1st AUG, NSm from the 2nd AUG (186). It was determined that the 78 kDa protein’s electric mobility was increased when incubated with Endo H and Endo F, whereas the 14 kDa (NSm) protein’s mobility did not change (186). There are two putative N-glycosylation sites located within the 78 kDa protein: one in the preglycoprotein region (N88), which is shared with the NSm protein, and one (N438) shared with Gn. These data indicate that at least one of the two putative N-glycosylation sites is utilized by the 78 kDa protein, but the one putative site of the NSm is not utilized. These results are reasonable because the 78 kDa protein is probably a structural protein expressed with a putative signal peptide, while NSm is a nonstructural protein expressed without a signal sequence (187). Also, as both Endo F and Endo H are only able to digest high mannose or hybrid-type glycans, the N-glycan(s) on the 78 kDa protein appear(s) to be high mannose- or hybrid-type. In this study, the mobility of the Gn and Gc proteins was also

increased when incubated with Endo H and Endo F indicating site usage and the presence of high-mannose or hybrid-type glycans. In a follow-up study, immunoprecipitated 78 kDa proteins were incubated with Endo F for various times, and two distinct shifts in mobility were seen, indicating that both N-glycosylation sites within the 78 kDa protein are utilized (187). The mobility of the Gn protein was also increased indicating that the shared N-glycosylation site, N438, is utilized by both the 78 kDa protein and the Gn protein (187). Three species of Gc proteins were seen, when treated with Endo F over time, indicating that three of the four putative sites are utilized (187). However, the N-glycosylation status was inconclusive as Gc exists as a doublet in infected cells (61, 186-188).

DENDRITIC CELL-SPECIFIC INTERCELLULAR ADHESION MOLECULE 3-GRABBING NONINTEGRIN (DC-SIGN), LIVER/LYMPH NODE SPECIFIC INTERCELLULAR ADHESION MOLECULE 3-GRABBING NONINTEGRIN (L-SIGN), AND THEIR MOUSE ORTHOLOGS

DC-SIGN (CD209) is a calcium-dependent (C-type), type II transmembrane protein (189). Other members of the C-type Lectin family include L-SIGN, the mannose receptor, and langerin (DEC-205). This lectin family is characterized by their ability to recognize carbohydrate structures of cellular and viral proteins (190-192). The expression sites of DC-SIGN include DCs found in the dermis, though not Langerhans cells, and those found in lymphoid tissues or near mucosal surfaces (193-195). DC-SIGN has also been identified on macrophage cells in the placenta, called Hofbauer cells; alveolar macrophages, and in the liver sinusoids on Kupffer cells (193, 194)

DC-SIGN binds ligands via its carbohydrate recognition region (CRD) **(Figure 1-7)** (196, 197). Attached to the CRD is the neck region, which is made up of eight tandem repeats consisting of 23 amino acids and is responsible for the tetramerization of the lectin (198-200). This tetramerization is necessary for proper biological functions of DC-SIGN. The lectin spans the plasma membrane via the transmembrane region, and it has a cytoplasmic tail, which consists of a tyrosine residue, followed by a tri-acidic region and a dileucine motif. The tail

region is involved in internalization (194), and removing the dileucine motif via site-directed mutagenesis has been demonstrated to abolish DC-SIGN internalization (59, 60, 198).

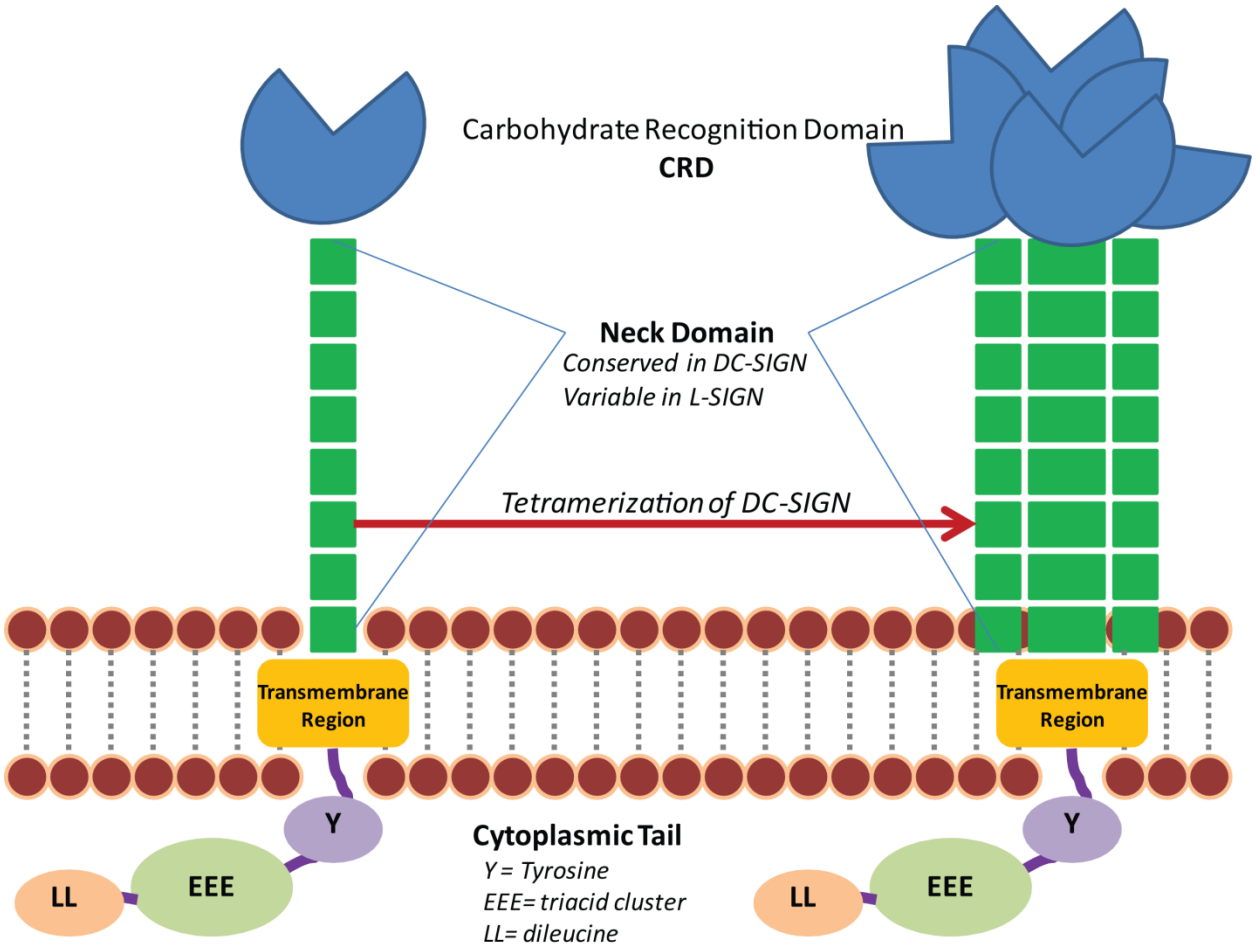

Figure 1-7: Schematic of DC-SIGN showing Tetramerization of DC-SIGN. DC-SIGN binds ligands via its carbohydrate recognition region (CRD). The Neck domain is made up of eight tandem repeats consisting of 23 amino acids and is responsible for the tetramerization of the lectin. In L-SIGN, the neck region contains many polymorphisms and can range from 3 up to 9 repeat regions, while it is conserved in DC-SIGN. The lectin spans the plasma membrane via the transmembrane region, and it has a cytoplasmic tail, which consists of a tyrosine residue, followed by a tri-acidic region and a dileucine motif. The tail region is involved in internalization via the dileucine motif (LL). Tetramerization is required for antigen (or virus) interaction and internalization.

In its antigen presenting capacity, DC-SIGN has been demonstrated to internalize ligands (201). Identification of self and pathogen ligands for DC-SIGN has been made possible via determination of carbohydrate specificity of the lectin. DC-SIGN preferentially binds to non-sialylated fucose-containing Lewis antigens and high-mannose N-glycans (200, 202). Viral pathogens can use DC-SIGN in a *cis*-fashion, where it facilitates entry and infection of the cell

expressing DC-SIGN (60), or in a *trans*-fashion (203), where it binds to viral particles and transfers them to other cells, which the virus then infects.

Originally, identified as a receptor for human immunodeficiency virus-1 (HIV-1), DC-SIGN has been identified as a either an attachment factor or authentic entry receptor for other viruses, including members of the filovirus (204), alphavirus (205), arenavirus (206), and flavivirus families (198, 207). DC-SIGN was also recently identified as an authentic entry receptor for bunyaviruses, including members of the *phlebovirus* (60), and *nairovirus* genus (208). In the study of phlebovirus entry, human peripheral blood mononuclear cells (PBMCs) were used to generate immature DCs (60). These DCs were then exposed to RVFV for 7 h(60). Antibodies against the N protein were used to immunostain the viruses, and FACS analysis determined the number of infected cells(60). The fraction of infected cells increased over time, between 0-25 hours post infection (hpi), and at the highest multiplicity of infection (MOI), more than 70% of DCs were infected(60). These results confirm DCs can be infected with RVFV. Raji cells, a B-lymphocyte cell line, are generally not infected by phleboviruses or are infected at very low levels. Thus, when parental Raji cells were infected with 1 MOI of RVFV and analyzed by FACS at 18 hpi, less than 10% of cells were infected with RVFV, whereas when DC-SIGN was expressed, around 60% of cells were infected (60). When inhibitors of DC-SIGN, such as EDTA (5 mM) and anti-DC-SIGN mAb 1621 (25 $\mu g*ml^{-1}$) were present during infection, the number of infected cells decreased to less than 10% and less than 30%, respectively(60). These results confirm DC-SIGN mediates RVFV infection in Raji-DC-SIGN cells. In a follow-up experiment, UUKV was produced in BHK-21 cells and then treated with Endo H or PNGase F under reducing or non-reducing conditions. Under reducing conditions, both the Gn (1 N-glycosylation site) and the Gc (4 N-glycosylation sites) glycoproteins were sensitive to Endo H digestion indicating presence of high mannose- or hybrid-type glycans (60). Under non-reducing conditions, infectivity determined by plaque assay was not significantly affected (60). However, when binding was determined by FACS, less than 30% of PNGase treated viral particles could

bind and less than 10% of Endo H treated viral particles could bind to Raji-DC-SIGN cells (60). These results also suggest an important role for high mannose or hybrid-type glycans in UUKV binding to DC-SIGN.

L-SIGN (DC-SIGNR; CD209L) shares 77% amino acid identity to DC-SIGN and is structurally very similar (190, 193, 194). However, unlike DC-SIGN, the neck region of L-SIGN contains many polymorphisms and can range from 3 up to 9 repeat regions (203). Expression of L-SIGN also differs as L-SIGN has been identified on the endothelial cells (LSECs) of lymph node and liver sinusoids, and on the endothelial cells of the placenta (209, 210).

Similar to DC-SIGN, L-SIGN binds to high mannose type N-glycans(203, 207), but unlike DC-SIGN, L-SIGN does not bind to fucose-containing Lewis antigens (197). L-SIGN is unable to bind to Lewis antigens due to the serine residue at N363, which prevents the creation of a hydrophobic pocket that allows stabile binding of the Lewis antigen in the CRD (197, 199). It has been demonstrated that L-SIGN only binds to high mannose type N-glycans and not hybrid or complex type (211). The inability of L-SIGN to bind to hydrid type N-glycans is due to the steric hinderance of a core GlcNAc (β1-4 linked), found in hybrid type N-glycans, with the phenylalanine (Phe^{325}) residue with the CRD of L-SIGN (211).

A recent study has shown that L-SIGN is an attachment factor for phleboviruses and not an authentic receptor like DC-SIGN (59). The authors used rRVFV that expresses GFP in the place of NSs, and lab strains of Toscana virus and Uukuniemi virus for comparison. HeLa cells and Raji-cells that stably express L-SIGN were exposed to the viruses for 20 hours, then flow cytometry was used to analyze viral replication. The parental Raji cells, which did not express L-SIGN, had low infection (<5%) even at higher moi: rRVFV-ΔNSs-EGFP (10moi), TOSV (5 moi) , and UUKV (10 moi) (59). On the other hand, the viruses could infect cells even at the lower moi of 1, when L-SIGN was expressed: rRVFV-ΔNSs-EGFP (~5%), TOSV (~18%) , and UUKV (~5%). The same trend occurred when L-SIGN was expressed by HeLa cells with higher

infection rates compared to the Raji cells at an moi of 1-1.25: rRVFV-ΔNSs-EGFP (~85%), TOSV (~85%), and UUKV (~30%).

For the rest of the study, the authors used UUKV as a surrogate for bunyaviruses. Inhibitors of L-SIGN (EGTA, an antibody to L-SIGN, and mannan) limited binding of UUKV to the Raji-cells that expressed L-SIGN, confirming that the lectin was involved in viral binding (59). However, when the Raji cells expressed L-SIGN that lacks the dileucine motif (unable to be endocytosed), at mois of 0.2, 1, and 5 the percentage of infected cells were similar to cells that expressed L-SIGN with the dileucine motif (59). These results indicated that while L-SIGN is important for binding UUKV, it is not necessary for viral infection of the cell (59).

This study is in contrast to another study that used rhabdovirus particles pseudotyped with RVFV Gn/Gc, Severe Fever with Thrombocytopenia virus Gn/Gc, or La Cross Virus Gn/Gc (212). Twenty-four hours post infection of Raji cells that express L-SIGN (listed as DC-SIGNR in the paper), viral infection was analyzed by luciferase activity and only the SFTSV Gn/Gc pseudotype appeared to have enhanced infection by L-SIGN. The RVFV Gn/Gc and LACV Gn/Gc pseudotypes showed similar luciferase activity to that of Raji Cells that did not express L-SIGN (212). These contradictory results may be due to the differences in viral N-glycosylation and assembly of rhabdoviruses and bunyaviruses. It has been documented that differential N-glycosylation can affect viral binding to L-SIGN or DC-SIGN (198, 205, 207).

The functions of human DC-SIGN and L-SIGN have only been investigated *in vitro* mostly due to a lack of a functional ortholog in mice. Sequencing analyses have demonstrated that the mouse genome encodes eight DC-SIGN-like genes that are dubbed SIGNR. One of the genes was determined to be a pseudogene, SIGNR6, while the other seven produce distinct proteins (213). In terms of carbohydrate binding, SIGNR1, -3, and -7 are similar to DC-SIGN, with SIGNR-1 being the only one capable of binding to Lewis antigens (213). As far as L-SIGN, SIGNR-5 and-8 are the most similar in terms of binding (213).

However, in terms of structure there are few similarities between human DC-SIGN and L-SIGN with the mouse SIGNRs. SIGNR-2 does not have a membrane anchor and the other SIGNRs have much shorter neck regions than the human lectins (213). The longest neck region is that of SIGNR-1, which contains four repeat regions, while the neck of SIGNR-2 has only two and the rest have no repeated neck sequences (213). Due to the short neck regions, the mouse SIGNs cannot form stable oligomers, which may affect binding avidity to their respective ligands. Only SIGNR-3 contains a tyrosine-based internalization motif, but both SIGNR-3 and SIGNR-1 are able to release ligands at low pH values similar to that of DC-SIGN (213). Human DC-SIGN are expressed by similar cell types, but SIGNR-5 does not mediate receptor internalization like DC-SIGN (214). Thus, due to these structural, expression, and binding differences, it is not possible to use mouse SIGNs as surrogates for human DC-SIGN/L-SIGN studies.

For this reason, hSIGN mice were created via the introduction of a transgene encoding DC-SIGN into C57/Bl6 mice (215). The CD11c promoter controls expression of DC-SIGN in these mice in an effort to reproduce part of its expression pattern (216). When hSIGN mice were infected with M. tuberculosis, they survived longer than the wild-type mice, possibly due to DC-SIGN limiting inflammatory responses (215). However, because the other mouse SIGNs and the mannose receptor were not knocked out, they may have also contributed to this effect (216). Though, hSIGN mice may not be able to fully elucidate human DC-SIGN functions *in vivo*, they may be valuable in CD4+ and CD8+ induction studies, which will be paramount in evaluating DC-vaccines (216).

JUSTIFICATION OF STUDIES

Since first being described in 1931, RVFV has continued to cause sporadic outbreaks throughout Africa and more recently, the Arabian Peninsula (217). These outbreaks cause devastating losses of livestock, particularly sheep, goats, and cattle; and death in humans can occur (217). RVFV is transmitted via contact with infected tissues or via mosquitoes, and two

genera (*Aedes* and *Culex*) are primarily involved in the maintenance and amplification of RVFV (218). The outbreak of RVFV in Saudi Arabia and Yemen, in 2000, increased the concern of the spread of RVFV to other naïve geographical regions, where susceptible livestock and competent vectors are present. A more recent outbreak in South Africa (2010-2011), had an approximate case fatality rate of 11% (219). The following year in Mauritania, there were 17 human deaths reported out of 34 cases (220). RVFV has continually demonstrated to invade "virgin soils", and studies indicate that competent mosquito vectors, such *Aedes* and *Culex* spp., are present in the United States (221, 222). Also, as both livestock and humans produce enough viremia to transmit RVFV to mosquitoes (223), RVFV introduction into the United States, and the ease with which it can become endemic is a serious concern.

Recently, the C-type lectin, DC-SIGN, was identified as a receptor for RVFV (224). Like other studies involving DC-SIGN, high mannose-type glycans were demonstrated to be important for UUKV binding to DC-SIGN, but other phleboviruses were not investigated in this regard (224). However, there have been very few studies investigating the type and usage of N-glycans of RVFV and their role in infectivity. Kakach et al. (1989) performed a time-course digestion of Gn and Gc with endoglycosidase F (Endo F), which does not cleave all types of N-glycans, nor did they investigate the individual N-glycosylation sites of these proteins. By determining the usage and type of N-glycans present, we can better determine their roles in receptor binding, such as their interactions with DC-SIGN. This work will aid in the development of vaccines that target the DC-SIGN receptor, which is found on immature dendritic cells that patrol tissues in search for viral pathogens. DC-SIGN, in its antigen-presenting capacity, can allow the induction of both humoral and cellular responses (225), which are important in the immunogenicity of vaccines.

Among 33 RVFV isolates tested, all five initiation codon sites encoded within the preglycoprotein region of the RVFV M-segment were conserved suggesting functional roles (226). The first and second start codons initiate translation of the 78 kDa-Gc and NSm-Gn-Gc

precursor proteins, respectively; whereas the fourth and fifth codons initiate translation of the Gn-Gc protein precursor, when the upstream initiation codons are abolished (227). A fundamental understanding of the RVFV Gn/Gc expression mechanism will lead to the rational design of highly safe and immunogenic vaccine candidates.

SPECIFIC AIMS

Specific Aim 1: Determine the role of Gn/Gc N-glycosylation in RVFV MP-12 infection via DC-SIGN. Hypothesis: No single N-glycan plays a dominant role in MP-12 infection via DC-SIGN. Rationale: Five putative N-glycosylation sites are found in Gn/Gc at N438 (Gn), N794 (Gc), N829 (Gc); N1035 (Gc) and N1077 (Gc). DC-SIGN has been identified as a receptor for RVFV, and high-mannose-type glycans are DC-SIGN ligands. It is unknown which asparagines within the N-X-S/T sequons are N-glycosylated, and which N-glycans support DC-SIGN binding in RVFV infection. I aim to identify N-glycosylation sites in RVFV Gn and Gc, and characterize their roles in viral infection mediated by DC-SIGN and L-SIGN. The results will be important for the rational design of next generation RVF vaccines, which retain DC-SIGN carbohydrate ligands. Reverse genetics for the RVFV MP-12 strain and Jurkat cells stably expressing human DC-SIGN or L-SIGN will be used for this study.

Specific Aim 2: Characterize the mechanism of Gn/Gc expression via ribosomal leaky scanning of the 5 initiation codons in the RVFV M-Segment. Hypothesis: RVFV Gn/Gc expression is regulated in the context of the leaky five AUGs upstream of Gn/Gc. Rationale: The RVFV M-segment encodes at least two glycoprotein precursor proteins (78 kDa-Gc and NSm-Gn-Gc), and 78 kDa, NSm, Gn, and Gc proteins are produced by the co-translational cleavage of these precursors. The two precursor proteins are made through leaky scanning of ribosome at the 1st initiation codon. Reverse genetics allowed us to generate RVFV MP-12 M-segment mutants, which lack the 78 kDa and/or NSm proteins. Abolishment of the 1st or the 2nd AUGs will lead to the generation of surrogate precursor protein(s) for Gn and Gc production. However, it is unknown how the alteration of precursor proteins affects the cleavage efficiency

to produce Gn or Gc proteins or viral replication. Since rMP12-ΔNSm21/384, which encodes an in-frame deletion in 78 kDa/NSm region, is considered a next generation MP-12 vaccine, further characterization of M-segment preglycoprotein coding region is important for the proper evaluation and production of next generation vaccines. I aim to quantitatively characterize the expression of the Gn protein from precursor proteins produced from the RVFV M-segment lacking selected initiation codon(s) in preglycoprotein region, using a reporter assay. Furthermore, I will also characterize the virological phenotype of RVFV MP-12 mutants encoding initiation codon mutation(s) within the preglycoprotein region.

CHAPTER 2: N-glycans on the Rift Valley fever virus envelope glycoproteins, Gn and Gc, redundantly support viral infection via DC-SIGN[2]

INTRODUCTION

Within the RVFV M-segment, there are six, potential N-glycan sites (sequon) predicted by the presence of an asparagine (N), followed by any amino acid (X), followed by serine or threonine (S/T) **(Figure 2-1A)** (181). The locations for these N-glycan sequons are the following: N88 (78 kDa), N438 (78 kDa and Gn), N794 (Gc), N829 (Gc), N1035 (Gc), and N1077 (Gc). NSm is not N-glycosylated at N88 because the NSm polypeptide is anchored to the membrane at the C-terminus, while the N-terminus is exposed to cytoplasm. The N88 site is N-glycosylated in the 78 kDa protein (186). The N438 site, shared by the 78 kDa protein and Gn, are N-glycosylated in both proteins (66, 232). According to a previous study, three of the four sites within Gc are N-glycosylated (66). Gc is a class II fusion protein and has a similar structure to the envelope E proteins of alphaviruses and flaviviruses according to the crystal structure (233). The three domains that comprise RVFV Gc are domain I (aa.691-759, 852-901 and 981-1024), domain II (759-852, 901-981), and domain III (1024-1120), and the putative fusion loop, (aa. 820-830), resides within domain II (61). The N829 sequon is located within the fusion loop.

Human DC-SIGN is a C-type lectin that has been identified as a receptor for RVFV (60)**.** DC-SIGN shares 77% amino acid identity with L-SIGN, or DC-SIGNR, but they are expressed on different cell types and have different sugar-binding affinities (234). L-SIGN is expressed on the endothelial cells of liver and lymph node sinuses, as well as the endothelial cells lining capillaries of the placenta, whereas DC-SIGN is expressed on dendritic cells and some macrophages (234). Unlike DC-SIGN, L-SIGN has been demonstrated to not support RVFV

[2] Portions of this chapter have been previously published. Phoenix I, Nishiyama S, Lokugamage N, Hill TE, Huante M, Slack O, Carpio V, Freiberg AN, Ikegami T. **2016.** N-glycans on the Rift Valley fever virus Envelope Glycoproteins Gn and Gc Redundantly Support Viral Infection via DC-SIGN. ***Viruses*****.** 8, 149. doi: 10.3390/v8050149

infection (235). As DC-SIGN interacts with N-glycans on glycoproteins, the N-glycans of RVFV Gn and Gc are expected to be involved in infection mediated by DC-SIGN. Gc N-glycosylation at each sequon has not been resolved. Moreover, the roles of the RVFV N-glycans in DC-SIGN mediated infection are not known. In the present study, we sought to analyze RVFV Gc N-glycosylation and pinpoint its role in DC-SIGN mediated infection using reverse genetics and mutagenesis.

MATERIALS AND METHODS

Media, Cells, Viruses. Baby hamster kidney cells that express the T7 RNA polymerase (BHK/T7-9 cells) were cultured in Minimum Essential Medium (MEM)-alpha media supplemented with 10% fetal bovine serum (FBS) (Invitrogen), penicillin (100 U/ml), streptomycin (100 µg/ml), and Hygromycin (600 µg/ml) (236). Dulbecco's Modified Eagle's Medium (DMEM) supplemented with 10% FBS, penicillin (100 U/ml), and streptomycin (100 µg/ml) was used to culture Vero E6 cells (ATCC C1008). Dr. Rafael Delgado (Molecular Microbiology Laboratory, Hospital Universitario 12 de Octubre, Madrid, Spain) kindly provided a parental Jurkat cell line along with Jurkat cells stably expressing human DC-SIGN (Jurkat-DC-SIGN) or L-SIGN (Jurkat-L-SIGN) (237). These Jurkat cells were maintained in Roswell Park Memorial Institute Medium (RPMI) – 1640 supplemented with 10% FBS, penicillin (100 U/ml), and streptomycin (100 µg/ml). The RVFV MP-12 lot 7 vaccine (238) was passaged twice in Vero cells to produce the MP-12 strain used in this study. Reverse genetics (124) was used to rescue recombinant RVFV MP-12 (rMP-12) and the various N-glycosylation mutants (N438Q, N794Q, N1035Q, N1077Q, N438Q/N794Q, N438Q/N1035Q, N438Q/N1077Q). Viral titers were determined by plaque assay in Vero E6 cells (239).

Plasmids. We constructed 7 plasmids: pProT7-vM(+)N438Q, pProT7-vM(+)N794Q, pProT7-vM(+)N1035Q, pProT7-vM(+)N1077Q, pProT7-vM(+)N438Q/N794Q, pProT7-vM(+)N438Q/N1035Q or pProT7-vM(+)N438Q/N1077Q; following the manufacturer's instructions using Pfu Ultra High-Fidelity DNA polymerase (Agilent Technology) for site-directed

mutagenesis. A point non-synonymous mutation (N to Q) is encoded by each of the plasmids at the asparagine of each putative N-glycan sequon (where aa.1 represents the first methionine of M-segment open reading frame), and the mutations were confirmed by sequencing. We rescued seven rMP-12 N-glycan mutants using these plasmids: N438Q, N794Q, N1035Q, N1077Q, N438Q/N729Q, N438Q/N1035Q or N438Q/N1077Q. We also modified the pCAGGS-vG plasmid to analyze Gc N-glycosylation, and the modified plasmid, The pCAGGS-vG-Gly-null plasmid encodes all of the N-to-Q mutations: N438Q, N729Q, N829Q, N1035Q, and N1077Q. Using pCAGGS-vG-Gly-null plasmid, we then inserted each of the N-glycan sequons to produce single N-glycan plasmids: pCAGGS-vG-N438(+), pCAGGS-vG-N794(+), pCAGGS-vG-N829(+), pCAGGS-vG-N1035(+), and pCAGGS-vG-N1077(+).

Precipitation of Gn/Gc by Concavalin A beads. Using TransIT-293 (Mirus), we transfected Human Embryonic kidney 293 cells ($5x10^6$ cells) with pCAGGS-vG or the mutants (2 µg), according to the manufacturer's instructions. Cells were washed with PBS at 48 hours post transfection, and RIPA buffer (150mM NaCl, 50mM Tris-HCl, 1% NP-40, 0.5% sodium deoxycholate, 0.1% sodium dodecyl sulfate) containing 1mM of $CaCl_2$, $MgCl_2$, and $MnCl_2$; was used to harvest the cellular lysates. After mixing 20 µl of Agarose bound concanavalin A (Vector, AL-1003), the samples were incubated further at 4^oC for 16 hours. The samples were, then, washed with PBS with $CaCl_2$ and $MgCl_2$ three times, re-suspended in denaturing buffer, and heated for 5 mins at 95^oC.The samples were then digested with 1000 units of PNGase F or Endo H (New England BioLabs) for 24 hours at 37^oC. Non-treated samples served as a control. Sample buffer (2X) was added to the samples, which were then boiled for 10 mins, followed by separation in 12% SDS-PAGE gels.

Western Blotting. SDS-polyacrylamide gel electrophoresis (SDS-PAGE) under reducing conditions was performed followed by Western blot analysis (240). RVFV Gc and Gn were detected by anti-RVFV Gc rabbit polyclonal antibody (ProSci, Inc.; CAT#4521) or anti-RVFV Gn mouse monoclonal antibody (4D4), respectively.

Radiolabeling of Virus Particles. The rMP-12 or mutants were used to infect Vero E6 cells a MOI of 0.1 to 3 at 37^{o}C. Before the [^{35}S] labeling of polypeptides, the infected cells were incubated with MEM lacking methionine/cysteine and L-glutamine, and complemented with 1% dialyzed FBS, 20mM L-glutamine, penicillin (100 U/ml) and streptomycin (100 µg/ml) for 30 min at 37^{o}C. At 1 hpi or 4 hpi, Trans [^{35}S] label (MP Biomedicals), a metabolic labelling reagent, was added to infected cells of the single asparagine mutant experiment or double asparagine mutant experiment, respectively. Supernatant was harvested at 16 hpi followed by low-speed centrifugation (4800 rpm for 5 min) to remove any cellular debris. Using a polyclonal anti-RVFV antibody, virus particles were immunoprecipitated, followed by four wash steps using PBS. Sample buffer (2X) containing 5% mercaptoethanol was used to resuspend the sample, which were then boiled at 100°C for 10 mins. Lastly, SDS-PAGE followed by autoradiography was used to analyze Gn and Gc band mobility.

Infectivity of rMP-12 or the N-glycan mutants in Jurkat-DC-SIGN or Jurkat-L-SIGN cells. rMP-12 or the mutants (6.3x10^{6} RNA copies corresponding to an MOI of 3.6 in Vero E6 cells) were used to infect Jurkat, Jurkat-DC-SIGN, or Jurkat-L-SIGN cells (1x10^{6} cells). Cells were incubated for 6 hours at 37°C post-infection. Paraformaldehyde (4%) was used to fix cells at 4^{o}C for 30 mins. After a PBS wash, permeabilization buffer (Affimetrix eBioScience) was used to permeabilize the cells for 25 min at 4^{o}C. Alexa Fluor 488-conjugated anti-GFP rabbit antibody (Life Technologies) and anti-RVFV mouse ascite were diluted in permeabilization buffer, then incubated with the permeabilized cells at 4^{o}C for 40min. Alexa Fluor 488-conjugated normal rabbit IgG (EMD Millipore) was used as an isotype control for GFP detection. After two wash steps with permeabilization buffer, Alexa Fluor 647-conjugated goat anti-mouse IgG (Life Technologies) was incubated with the cells for 30 min at 4°C. Cells were washed three times with permeabilization buffer, then resuspended in FACS buffer. Cells were collected on the Canto or LSRII Fortessa (BD Biosciences, San Jose, CA, USA) in the UTMB Flow Cytometry

and Cell Sorting Core Facility using FACSDiva software (version 8.0.1, BD Biosciences) and analyzed in FlowJo version 9.7 (TreeStar, Ashland, OR, USA).

Statistical Analysis. GraphPad Prism version 6.05 for Windows (GraphPad Software Inc., La Jolla, CA, USA) was used for statistical analyses using an unpaired Student's *t* test for the comparison of two groups.

RESULTS

RVFV Gc N829 is a N-P-S Sequon and is located at the Fusion Loop

There are six N-X-S/T sequons encoded by the RVFV M-Segment: N88 (78 kDa: N-I-T), N438 (78 kDa/Gn: N-G-S), N794 (Gc: N-E-T), N829 (Gc: N-P-S), N1035 (Gc: N-L-T), and N1077 (Gc: N-G-T) **(Figure 2-1A).** Previous work has demonstrated that the OST cannot access the asparagine (N) when there is a proline (P) at the X-site; meaning that N-glycosylation does not occur at N-P-S/T sites (241-243). RVFV Gc N829, which is located within the putative fusion loop, is an N-P-S sequon, and it is most likely not N-glycosylated. When the RVFV Gc was aligned with related sandfly fever phleboviruses [Sandfly fever Sicilian virus (SFSV), Toscana virus (TOSV) and Punta Toro virus (PTV)], this N-P-S sequon was found in these viruses as well **(Figure. 2-1B).** The RVFV Gc N794 sequon corresponded to sequons found in the Gc of TOSV and Sandfly fever Sicilian virus (SFSV), but not in that of PTV. In SFSV, TOSV, and PTV, the RVFV Gc 1035 sequon could be aligned to N1180, N1180, and 1161, respectively. None of the three viruses analyzed contained a sequon corresponding to N1077. Our results indicate that while RVFV Gc N1077 is unique to RVFV, the Gc N794 and N1035 sequons are evolutionarily conserved across Naples, RVFV, and Sicilian serocomplexes.

RVFV Gc N794, N1035, and N1077, but not N829 are N-glycosylated

In an effort to analyze the N-glycosylation status of the RVFV Gc sequons, plasmids encoding the RVFV M-segment ORF with a single N-glycan or lacking all putative N-glycans (pCAGGS-vG-Gly-null) were constructed **(Figure 2-2A).** We transfected 293 cells with the

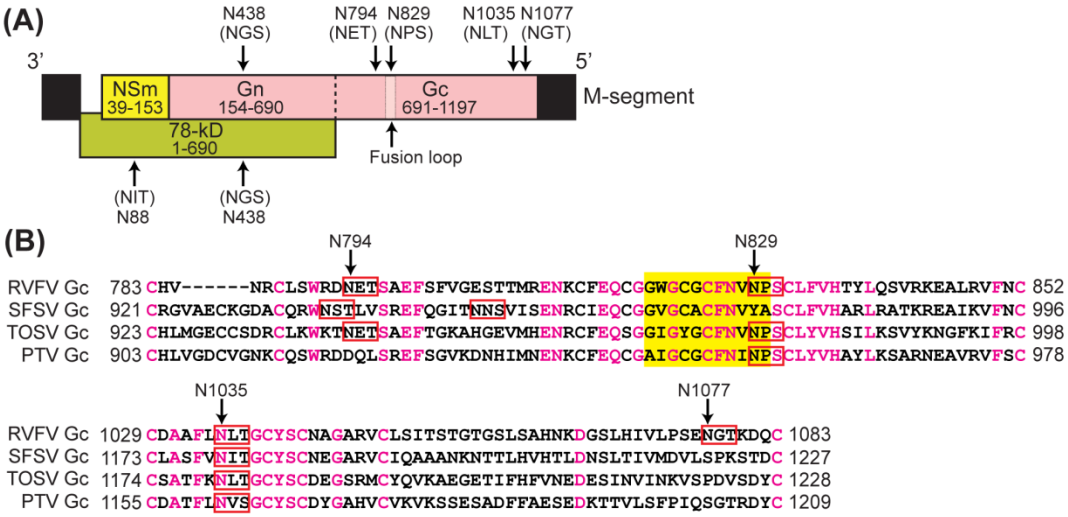

Figure 2-1: The Asparagine (N)-X-Serine (S)/Threonine (T) Sequons of Rift Valley fever virus and Other Related Phleboviruses. (A) Schematic diagram of the M-segment RNA and protein expression. The RVFV M-segment encodes a single M mRNA, and co-translational cleavage and leaky ribosomal scanning of the initiation codons produce at least 4 proteins: 78 kDa, NSm, Gn, and Gc. The 78 kDa, Gn, and Gc are structural proteins, while NSm is a nonstructural protein. There are 6 N-X-S/T sequons, which are potentially utilized for N-glycosylation: N88 (78 kDa), N438 (Gn and 78 kDa), N794 (Gc), N829 (Gc), N1035 (Gc), and N1077 (Gc). (B) Partial alignment of Gc amino acid sequences among RVFV, Sandfly fever Sicilian virus (SFSV: Genbank Accession No. U30500), Toscana virus (TOSV: Genbank Accession No. X89628), and Punta Toro virus (PTV: Genbank Accession No. DQ363407). Conserved amino acids are shown in pink, while the N-X-S/T sequons are shown in red squares. Positions of amino acids at the N- and C-termini of sequences are also shown. The fusion loop at aa.820 to 830 is shown in yellow.

mutant plasmids: pCAGGS-vG-Gly-null, pCAGGS-vG-N438(+), pCAGGS-vG-N794(+), pCAGGS-vG-N829(+), pCAGGS-vG-N1035(+), or pCAGGS-vG-N1077(+); and used the parental plasmid, pCAGGS-vG, as a control. Cell lysates were harvested at 48 hrs post transfection and then incubated with concanavalin A agarose beads. The samples were washed, and the precipitates were analyzed by Western blot with anti-Gc or anti-Gn antibody **(Figure 2-2B).** The presence of an N-glycan at each site was determined by paired, precipitated samples that were treated with either PNGase F [cleaves between the innermost N-acetyl-glucosamine (GlcNAc) and the asparagine of high mannose-type, hybrid-type, and complex-type N-glycans] or Endo H (cleaves the chitobiose core of high mannose-type and some hybrid-type N-glycans). Treatment with either PNGase F or Endo H lead to an increase in migration of the parental Gn and Gc, confirming the presence of N-glycans on these proteins. Enzymatic

digestion of the N-Gly null (Gn/Gc lacking all sequons), with either PNGase F or Endo H did not result in a migration change, as expected, as no sequons are present on Gn and Gc in this plasmid. The bands of N438(+) Gn displayed increased migration after digestion by either PNGase F or Endo H compared to non-treated samples. In addition, compared to the non-treated samples, the bands of Gc N794(+) and N1035(+) displayed increased migration after digestion with either PNGase F or Endo H. No migration change was seen in Gc N829(+) bands post-digestion with either PNGase F or Endo H, and the bands displayed a similar pattern of migration to that of the N-Gly null bands. Interestingly, only the bands of N1077(+) displayed as a doublet, and the slower migrating band was not present post- PNGase F or Endo H digestion. These results support previous work (187) that Gn is N-glycosylated, and they demonstrate the presence of N-glycans at 3 sites on Gc. This study identified that N794, N1035, and N1077, but not N829, are utilized for N-glycosylation (all high mannose or hybrid type).

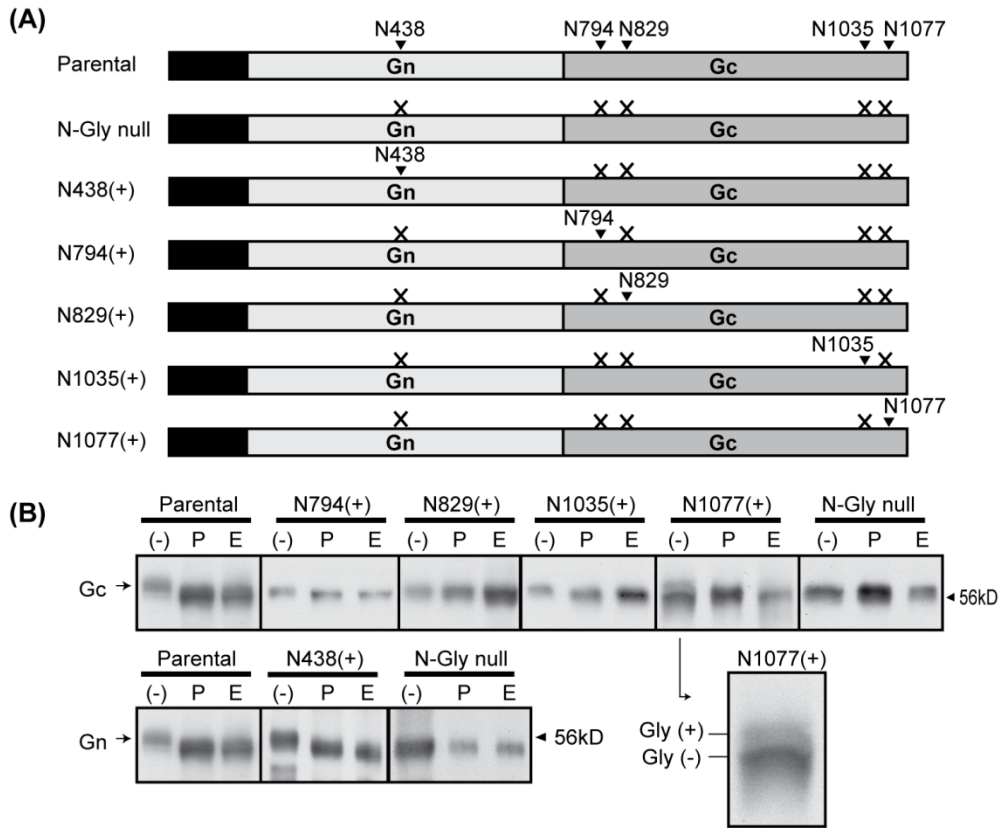

Figure 2-2: Rift Valley Fever Virus N-glycosylation and Enzymatic Digestion of N-glycans. (A) Schematics of the M-segment ORF encoded in the following plasmids: pCAGGS-vG (Parental),

pCAGGS-vG-Gly-null (N-Gly null), pCAGGS-vG-N438(+) [N438(+)], pCAGGS-vG-N794(+) [N794(+)], pCAGGS-vG-N829(+) [N829(+)], pCAGGS-vG-N1035(+) [N1035(+)], or pCAGGS-vG-N1077(+) [N1077(+)]. N-to-Q mutations were made in the X-sites, and the remaining single asparagine site is shown with an arrowhead. (B) 293 cells were transfected with plasmids shown in A. Then, Gn/Gc were precipitated with concanavalin agarose beads, and subsequently detected by anti-Gc antibody (top panels) or anti-Gn antibody (bottom panels). Samples were either not treated (-), or treated with PNGase F (P) or Endo H (E). An image of untreated N1077(+) lane is enlarged to show both glycosylated [Gly(+)] and unglycosylated [Gly(-)] bands.

Generation of Recombinant RVFV encoding N-to-Q Substitutions at one or more N-glycan sequons

To elucidate the roles of the individual RVFV Gn/Gc N-glycans, the asparagine (N) of each individual sequon was replaced with a glutamine (Q), and recombinant RVFV MP-12 strains were produced encoding N794Q, N1035Q, N1077Q, N438Q/N794Q, N438Q/N1035Q, or N438Q/N1077Q **(Figure 2-3A).** Glutamine was used because it is a neutral and polar acid similar to asparagine. After immunoprecipitation, radiolabeled virions were analyzed by Western blot. As expected, the Gn bands of the MP-12 mutants that encoded N438Q (e.g., N438Q, N438Q/N794Q, N438Q/N1035Q, and N438Q/N1077Q), migrated faster than the Gn band of the parental control **(Figure 2-3A and B).** The bands of Gc displayed as a doublet (Gc-large and Gc-small), but there was only the Gc-small band present in N1077Q, N438Q/N1035Q, or N438Q/N1077Q. Our results, **(Figure 2-2B)**, for pCAGGS-N1077(+) indicate heterogeneous N-glycosylation occurs at this site. Thus, the Gc-large band of the N794Q mutant may be due to N-glycosylation at N1035 and N1077, while the Gc-large band of the N1035Q mutant may be due to N-glycosylation at N794 and N1077. The lack of a Gc-large band for the N438Q/N1035Q was interesting since this mutant could be N-glycosylated at both N794 and N1077 like the single, N1035Q mutant **(Figure 2-3B).**

The replication kinetics in Vero cells of the single and double mutants were similar to parental rMP-12 (MOI=0.01) **(Figure 2-3C).** The rescue of rMP-12 encoding two or more mutations within Gc (i.e. N794Q/N1035Q, N794Q/N1077Q, N1035Q/N1077Q N438Q/N794Q/N829Q/N1035Q/N1077Q, or N794Q/N829Q/N1035Q/N1077Q) were attempted,

but after three independent attempts for each virus, no viable viruses were detected. In Vero cells, the rMP-12 encoding N829Q replicated efficiently (data not shown), but since N829 is not utilized for N-glycosylation **(Figure 2-3B),** it was not included in further experiments.

RVFV Gn and Gc N-glycans redundantly support viral infection via DC-SIGN

A previous study indicated that DC-SIGN (CD209), which is a C-type lectin expressed on macrophages and immature dendritic cells, is a receptor for RVFV (60). Another C-type lectin, L-SIGN, which has 77% amino acid identity to DC-SIGN has recently, been demonstrated to be an attachment factor for RVFV (59). To determine the function of the RVFV Gn/Gc N-glycans during the infection of cells that express these lectins, we used Jurkat cells stably expressing human DC-SIGN or L-SIGN (237) and co-express GFP in up to 17% of the population. The cells were mock infected or infected with rMP-12 (MOI of 3.6 – as determined by plaque assay in Vero E6 cells) to determine the infection efficiency. The cells were fixed at 6 hpi, permeabilized, and stained with anti-GFP and anti-RVFV antibodies. In our sample preparation, the GFP-positive population of Jurkat cells co-expressing GFP was not

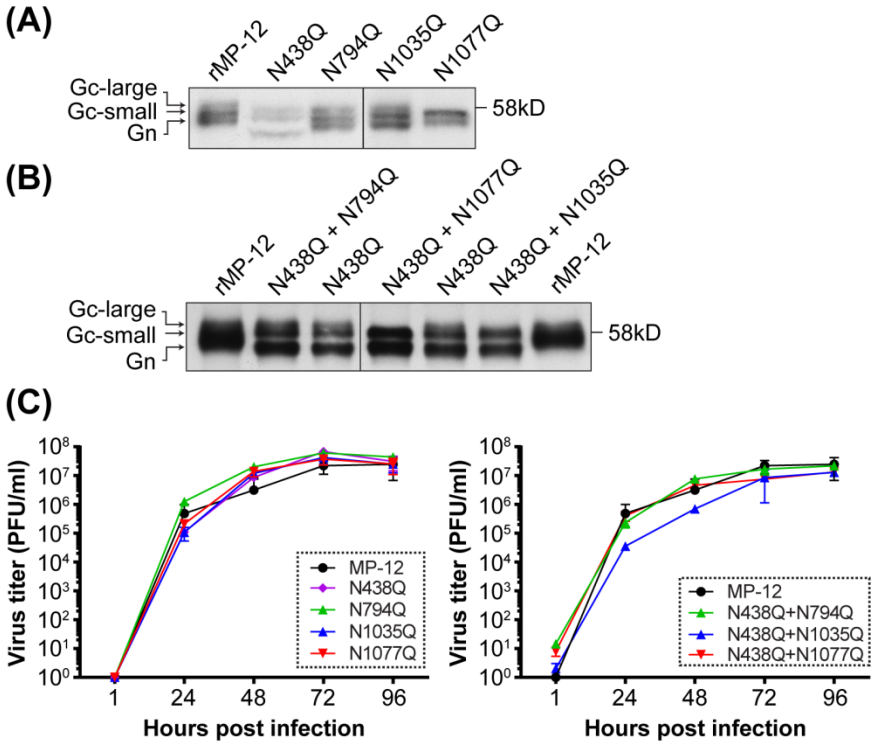

Figure 2-3: Gn/Gc of Recombinant MP-12 encoding N-to-Q mutation(s). The Gn/Gc migration patterns of rMP-12, N438Q, N794Q, N1035Q, and N1077Q mutants (A) or N438Q/N794Q, N438Q/N1035Q, and N438Q/N1077Q mutants (B). Vero E6 cells were infected with rMP-12 or the mutants at an MOI of 0.1 to 3, and metabolically labeled with [^{35}S] methionine/cysteine from 1 to 16 hpi. The cleared culture supernatants were subjected to immunoprecipitation using anti-RVFV antibody. Precipitated virions were analyzed by 7.5% SDS-PAGE and autoradiography. Gc-large: slow migrating Gc; Gc-small: fast migrating Gc. (C) Virus growth kinetics in Vero cells. Vero cells were infected with indicated rMP-12 mutants at an MOI of 0.01. Virus titers were determined at 1, 24, 48, 72 and 96 hours post infection. Means +/- standard deviations of three independent experiments are shown.

distinguishable from the GFP-negative population without the anti-GFP antibody. To analyze RVFV infection via DC-SIGN, relative number of RVFV-infected cells in the GFP-positive cell population [Q2/(Q2+Q3)] was normalized to that of RVFV-infected cells in the GFP-negative cell population [Q1/(Q1+Q4)] (background infectivity level in Jurkat cells: 100%) **(Figure 2-4A-C).** This value represents the infectivity of rMP-12 via DC-SIGN, over the nonspecific infectivity independent of DC-SIGN. In DC-SIGN positive cells, there was a 7.5 to 15-fold increase in rMP-12 positive cells compared to the GFP-negative cells **(Figure 2-4B).** In cells that express DC-SIGN, every one of the single N-glycan mutants (N438Q, N794Q, N1035Q, or N1077Q) displayed increased infection (N438Q: 4.4-fold, N794Q: 7.9-fold, N1035Q: 6.5-fold, and N1077Q: 6.1-fold) compared to the cells that did not express the lectin **(Figure 2-4B)**. Interestingly, the double mutants, N438Q/N794Q and N438Q/N1035Q still displayed increased infection of 3.3-fold and 6.2-fold, respectively, in DC-SIGN expressing cells **(Figure 2-4C)**. The N438Q/N1077Q mutant, on the other hand, only displayed a 1.5-fold increase of infection of DC-SIGN-positive cells compared to cells not expressing DC-SIGN **(Figure 2-4C)**. In L-SIGN positive cells, there was a 2.1-fold increase of rMP-12 infectivity, compared to GFP-negative (L-SIGN-negative) cells **(Figure 2-5A-C)**. The fold increase of each rMP-12 mutant infection was more moderate in Jurkat-L-SIGN cells: N438Q: 1.0-fold, N794Q: 1.1-fold, N1035Q: 1.2-fold, and N1077Q: 1.4-fold. In all, these data indicated that Gn N438 and Gc N794, N1035, and N1077 redundantly support virus infection via DC-SIGN.

DISCUSSION

In the rough endoplasmic reticulum (ER), N-glycosylation of nascent proteins begins with the “en bloc” transfer of an oligosaccharide N-glycan precursor by the OST complex (181). After addition of the precursor, the nascent protein continues through the ER and the Golgi, where the N-glycan precursor comes into contact with glycosidases and glycosyltransferases (181). These enzymes further process (trimming or addition of sugar residues) the sugar moieties on the N-glycan (181). In the present study, it was determined that out of the four potential N-glycan sites of RVFV Gc, three (N794, N1035, and N1077) are N-glycosylated. N-glycosylation does not occur when a proline is present at the X-site (N-X-S/T) of the sequon (241-243), and as expected, RVFV Gc N829, which is an N-P-S sequon, was not N-glycosylated. The results also showed that RVFV Gn and Gc are susceptible to Endo H treatment indicating the presence of high mannose or hybrid type N-glycans.

There are two subunits, STT3A or STT3B, of the OST which catalyze N-glycosylation in mammalian cells (244). Generally, the STT3A-OST adds N-glycans as the polypeptide is translocated into the ER lumen through the translocon (245). When N-X-S/T sequons are skipped by the STT3A-OST complex, the STT3B-OST can add N-glycans to the nascent peptide, post-translationally (244). While rare, N-glycosylation by the STT3B-OST complex is usually of the N-X-S/T sequons located near the C-terminus that were skipped by the STT3A-OST complex (244). In this study, the heterogeneous N-glycosylation of RVFV Gc N1077 was observed leading to the appearance of two differently sized Gc bands (Gc-large and Gc-small). N1077 is located 121 amino acids upstream of the C-terminus, while the “cut-off” for STT3B-mediated OST N-glycosylation is 65-75 amino acids (246). Thus, further study is required to confirm that N1077 is post-translationally N-glycosylated by STT3B-OST.

DC-SIGN-mediated viral infection was analyzed using Jurkat-DC-SIGN cells. These cells co-expressed DC-SIGN and GFP in up to 17% of cell population **(Figure 2-6)**, and overall GFP-positive cells were coexpressed with DC-SIGN **(Figure 2-7)**. In the samples prepared at an

early stage of infection (6 hpi), we compared the relative number of infected cells in the DC-SIGN/GFP-positive population to those in the DC-SIGN/GFP-negative population. This relative number represents viral infectivity via DC-SIGN (or L-SIGN) over the background infectivity in Jurkat cells. The background infectivity is most likely due to the presence of heparin sulfate, which has been demonstrated to be an attachment factor for RVFV (247). RVFV infection of CHO K1 cells was shown to be reduced in a dose-dependent manner when preincubated with soluble heparin (247). However, even in cells that were defective in producing heparin sulfate (CHO pgsD-677 cells), residual infection by RVFV still occurred (247). These results coupled with the results from this study indicate that RVFV most likely uses a number of attachment factors and receptors to bind to and infect a multitude of permissive cells. MP-12 infection occurred preferably in DC-SIGN/GFP-positive population, indicating that DC-SIGN acts as a receptor for RVFV (60). The N438Q/N1077Q mutant no longer retained enhanced infectivity via DC-SIGN, while the N438Q, N794Q, N1035Q, N1077Q, N438Q/N794Q, and N438Q/N1035Q mutants showed an increased viral infection via DC-SIGN compared to cells not expressing the lectin. Thus, our result indicated that Gn N438 or Gc N1077 play an important role in viral infection via DC-SIGN, and that Gn and Gc N-glycans redundantly support virus infection via DC-SIGN.

It should be noted that recombinant RVFV lacking one or more sequons may have unpredictable effects on the usage of other sequons. We observed reduced infectivity of the N438Q or N1035Q mutants in Jurkat-DC-SIGN cells, while the N438Q/N1035Q double mutation had little impact on viral infection in those cells. In addition, the N438Q/N1035Q mutant did not show a distinct Gc-large band unlike the N438Q/N794Q mutant. Since the Gc-large for the N438Q/N1035Q mutant could be N-glycosylated at N794 and N1077, the N-glycosylation status either at N794 or N1077 may be altered in the N438Q/N1035Q mutant. Effects of N-terminal N-glycosylation on C-terminal sites have been studied in the rabies virus glycoprotein (G) (248). The rabies virus G is type I membrane glycoprotein and encodes three sequons: N37, N247,

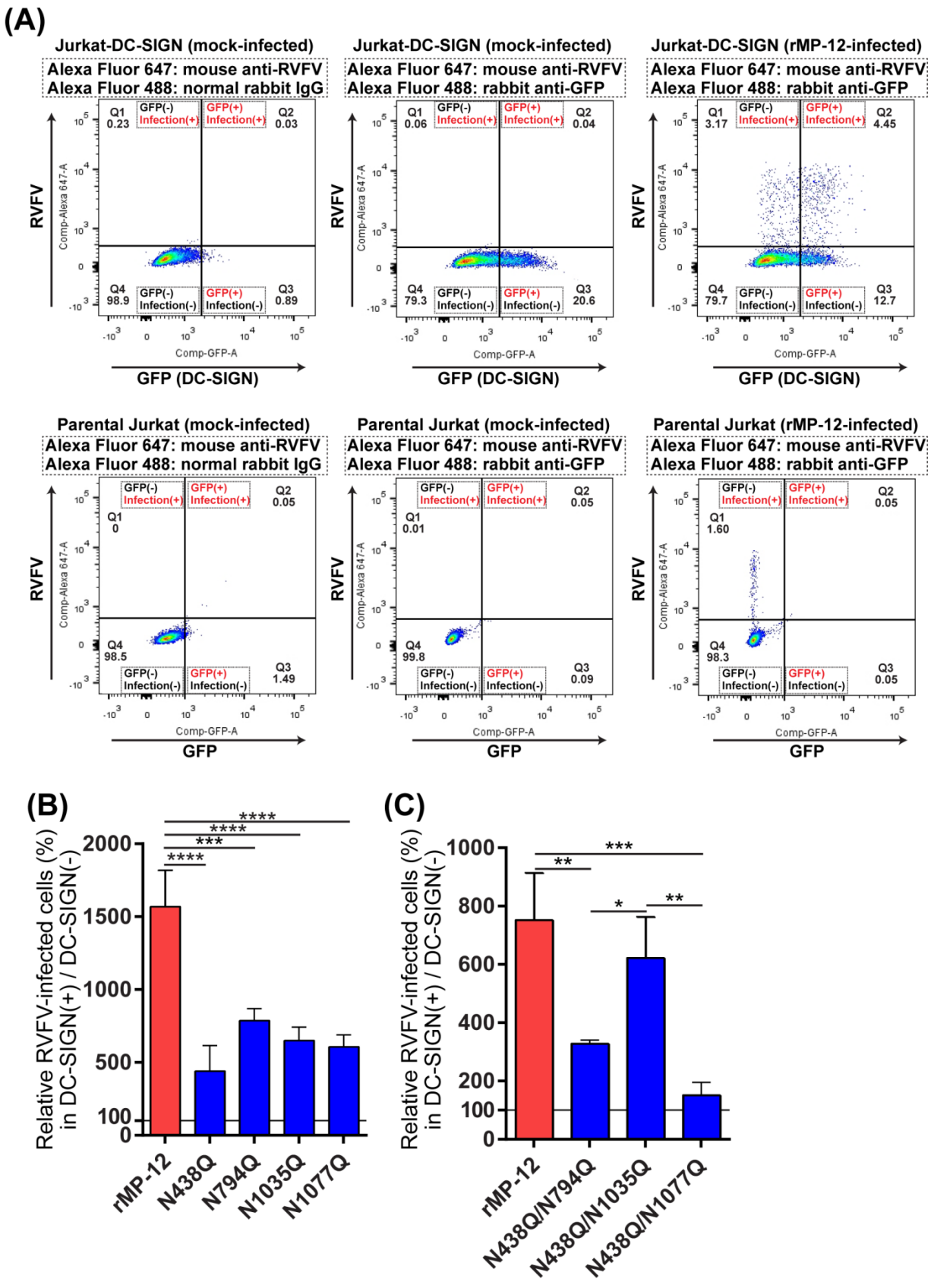
(A)
Jurkat-DC-SIGN (mock-infected)
Alexa Fluor 647: mouse anti-RVFV
Alexa Fluor 488: normal rabbit IgG
Q1 0.23
Q2 0.03
Q4 98.9
Q3 0.89
Jurkat-DC-SIGN (mock-infected)
Alexa Fluor 647: mouse anti-RVFV
Alexa Fluor 488: rabbit anti-GFP
Q1 0.06
Q2 0.04
Q4 79.3
Q3 20.6
Jurkat-DC-SIGN (rMP-12-infected)
Alexa Fluor 647: mouse anti-RVFV
Alexa Fluor 488: rabbit anti-GFP
Q1 3.17
Q2 4.45
Q4 79.7
Q3 12.7
Parental Jurkat (mock-infected)
Alexa Fluor 647: mouse anti-RVFV
Alexa Fluor 488: normal rabbit IgG
Q1 0
Q2 0.05
Q4 98.5
Q3 1.49
Parental Jurkat (mock-infected)
Alexa Fluor 647: mouse anti-RVFV
Alexa Fluor 488: rabbit anti-GFP
Q1 0.01
Q2 0.05
Q4 99.8
Q3 0.09
Parental Jurkat (rMP-12-infected)
Alexa Fluor 647: mouse anti-RVFV
Alexa Fluor 488: rabbit anti-GFP
Q1 1.60
Q2 0.05
Q4 98.3
Q3 0.05
GFP(-) Infection(+)
GFP(+) Infection(+)
GFP(-) Infection(-)
GFP(+) Infection(-)
RVFV
Comp-Alexa 647-A
Comp-GFP-A
GFP (DC-SIGN)
GFP
(B)
Relative RVFV-infected cells (%) in DC-SIGN(+) / DC-SIGN(-)
rMP-12
N438Q
N794Q
N1035Q
N1077Q
(C)
Relative RVFV-infected cells (%) in DC-SIGN(+) / DC-SIGN(-)
rMP-12
N438Q/N794Q
N438Q/N1035Q
N438Q/N1077Q

Figure 2-4: Infectivity of Recombinant MP-12 encoding a Glutamine (Q) in place of a Asparagine (N) at N-X-S/T sequon(s) in Gn or Gc in Jurkat-DC-SIGN cells. (**A**) Jurkat-DC-SIGN cells stably co-expressing green fluorescent protein (GFP) and human DC-SIGN (~17% in cell population) (top panels), or parental Jurkat cells, which express neither DC-SIGN nor GFP (bottom panels), were mock-infected (left and center panels) or infected with rMP-12 (right panels) at a multiplicity of infection (MOI) of 3.6. At 6 hpi, cells were fixed, permeabilized, and then stained with a cocktail of mouse anti-RVFV antibody and Alexa Fluor 488-conjugated rabbit anti-GFP antibody, or a cocktail of mouse anti-RVFV antibody and Alexa Fluor 488-conjugated normal rabbit IgG. Subsequently, cells were stained with Alexa Fluor 647-conjugated goat anti-mouse IgG, and analyzed by flow cytometry. Since permeabilized Jurkat-DC-SIGN cells showed poor intrinsic GFP signals, as shown with Alexa Fluor 488-conjugated normal rabbit IgG (left top panel), rabbit anti-GFP antibody (center and right top panels) was used to detect GFP signals of permeabilized Jurkat-DC-SIGN cells. Q1, GFP-negative (DC-SIGN-negative) and RVFV-infected cell population; Q2, GFP-positive (DC-SIGN-positive) and RVFV-infected cell population; Q3, GFP-positive (DC-SIGN-positive) and uninfected cell population; Q4, GFP-negative (DC-SIGN-negative) and uninfected cell population; (**B**,**C**) Jurkat-DC-SIGN cells were infected with rMP-12 or that lacking one (**B**) or two sequons (**C**). Relative number of RVFV-infected cells in the GFP-positive cell population. (Q2/(Q2+Q3) normalized to that of RVFV-infected cells in the GFP-negative cell population (Q1/(Q1+Q4) are shown. Graphs represent mean + standard deviations for three independent experiments.

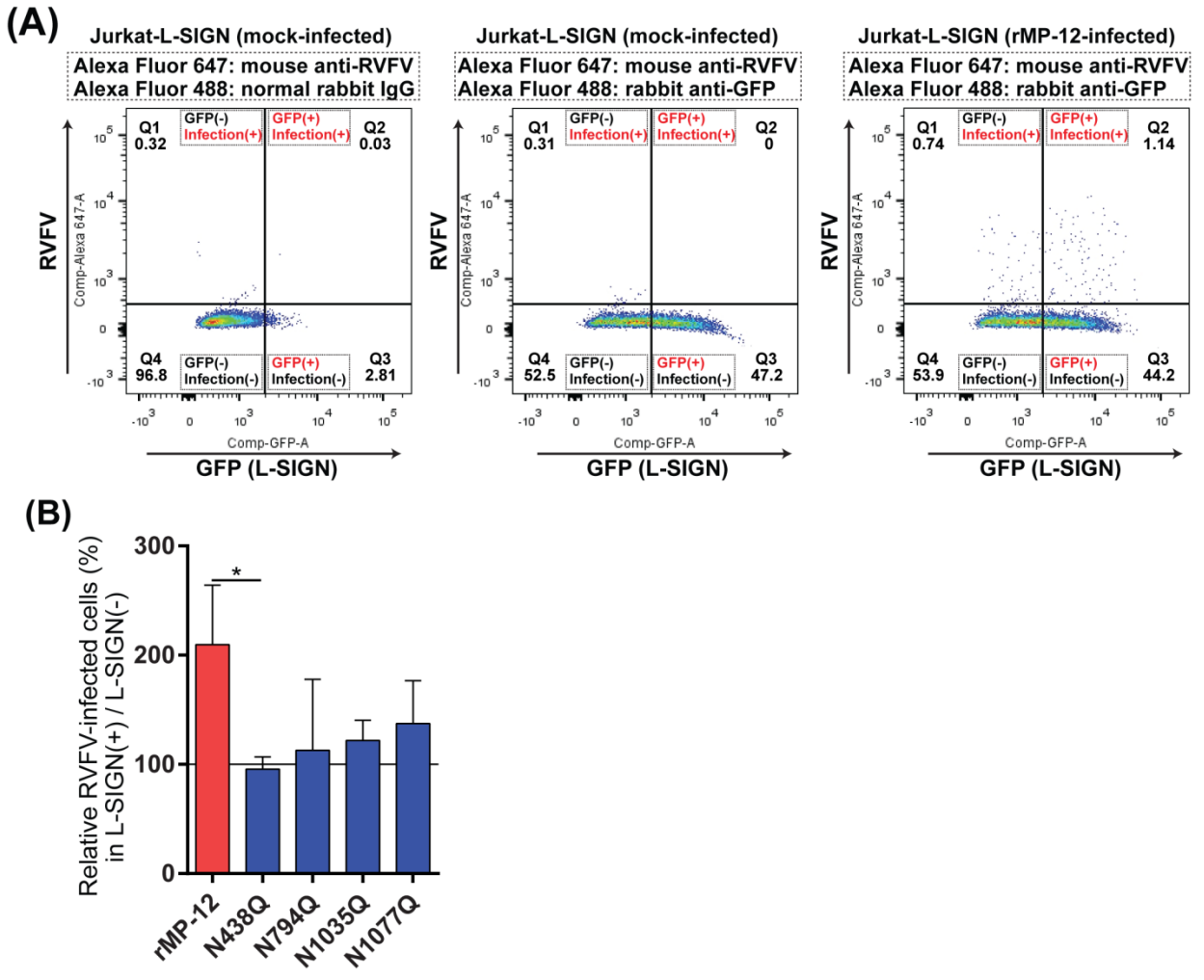

Figure 2-5. Infectivity of Recombinant MP-12 encoding a Glutamine (Q) in place of an Asparagine (N) at N-X-S/T sequon(s) in Gn or Gc in Jurkat-L-SIGN cells. (A) Jurkat-L-SIGN cells were mock-infected (left and center panels) or infected with rMP-12 at an MOI of 3.6 (right panel). At 6 hpi, cells were

fixed, permeabilized, and then stained with a cocktail of mouse anti-RVFV antibody and Alexa Fluor 488-conjugated rabbit anti-GFP antibody (center and right panels), or a cocktail of mouse anti-RVFV antibody and Alexa Fluor 488-conjugated normal rabbit IgG (left panel). Then, cells were stained with Alexa Fluor 647-conjugated goat anti-mouse IgG, and analyzed by flow cytometry. Intrinsic GFP signal was weak, and thus, anti-GFP antibody was used to detect GFP-positive cells. Q1, GFP-negative (L-SIGN-negative) and RVFV-infected cell population; Q2, GFP-positive (L-SIGN-positive) and RVFV-infected cell population; Q3, GFP-positive (L-SIGN-positive) and uninfected cell population; Q4, GFP-negative (L-SIGN-negative) and uninfected cell population. (B) Jurkat-L-SIGN cells were infected with rMP-12 or the mutants, as described. Relative number of RVFV-infected cells in the GFP-positive cell population [Q2/(Q2+Q3)] normalized to that of RVFV-infected cells in the GFP-negative cell population [Q1/(Q1+Q4)] are shown. Graphs represent mean + standard deviations for 3 independent experiments.

and N319. The G lacking N37 and N319 was largely susceptible to Endo H, while intact G or G lacking only N37 were resistant to Endo H. Thus, the presence of an N-glycan at one site can affect the processing of an N-glycan at another site. Another study showed that the insertion of a new sequon (N58) in human plasminogen activator influences the processing of the N-glycosylation at N117 (249). While this is beyond the scope of the current study, determination of carbohydrate chains at each asparagine residue will elucidate this mechanism of N-glycosylation modification during Gn/Gc maturation of each mutant.

We also analyzed the infectivity of MP-12 and the mutants in Jurkat-cells that coexpress L-SIGN and GFP **(Figure 2-5)**. We observed only a 1.2-fold augmentation of MP-12 infection via L-SIGN, in contrast to the 7.5-15-fold augmentation of infectivity via DC-SIGN. This result is consistent with the previous study by Hofmann et al. that demonstrated mosquito-borne RVFV or La Crosse virus (genus *Orthobunyavirus*) specifically utilize DC-SIGN, but not L-SIGN, while tick-borne Severe Fever with Thrombocytopenia Syndrome virus (SFTSV: genus *Phlebovirus*) uses both DC-SIGN and L-SIGN for entry (235). Both DC-SIGN and L-SIGN are homotetrameric type II membrane proteins and retain 77% amino acid identity (234). L-SIGN selectively binds to the trisaccharide Manα1-3(Manα1-6)Manα1 on high mannose glycans, while DC-SIGN binds to high mannose glycans (preferably with 8 or 9 mannoses) or fucose-containing structures including the Lewis-X trisaccharide: Galβ1-4(Fucα1-3) GlcNAc (250-252). Though both DC-SIGN and L-SIGN bind to high mannose-type N-glycans, the pH-dependent release of the oligosaccharide ligand by L-SIGN is not as efficient as DC-SIGN (252), which might explain the poor infectivity of RVFV via L-SIGN. Indeed, Leger et al. recently

demonstrated that an L-SIGN mutant that lacked the dileucine motif (required for endocytosis) did not reduce infectivity of UUKV in HeLa cells expressing the mutant L-SIGN compared to HeLa cells expressing the wild type L-SIGN, which indicates that L-SIGN does not act as an authentic receptor for UUKV entry (59).

We also noted that RVFV Gn/Gc lacking all N-glycans could be still expressed without showing unstable characteristics. The N-to-Q mutation of Bunyamwera virus (genus *Orthobunyavirus*) Gn N60 resulted in the loss of immunoreactivity with an anti-Gc monoclonal antibody (253). Further, the N-to-Q mutation of Hantaan virus (genus *Hantavirus*) Gn N134 resulted in poor accumulation of Gn and poor immunoreactivity to anti-Gn monoclonal antibodies (254). Thus, RVFV N-glycans might be dispensable for protein stability. On the other hand, rMP-12 encoding N1035Q/N1077Q, N438Q/N794Q/N829Q/N1035Q/N1077Q, or N794Q/N829Q/N1035Q/N1077Q were not rescued successfully. Thus, N-glycans may play a role in combination to form a functional Gn/Gc complex for viral assembly.

We demonstrated the presence of N-glycans in Gn (N438) and Gc (N794, N1035, and N1077). RVFV Gc consists of two distinct N-glycoforms (Gc-large and Gc-small), due to heterogeneous N-glycosylation at N1077. We found that an enhanced RVFV infection via DC-SIGN occurs in a redundant manner through Gn and Gc, and that N-glycans at Gn N438 and Gc N1077 play an important role in viral infection via DC-SIGN. Our study will support better understanding of the post-translational N-glycan modification of Gn/Gc and the role in progeny infection.

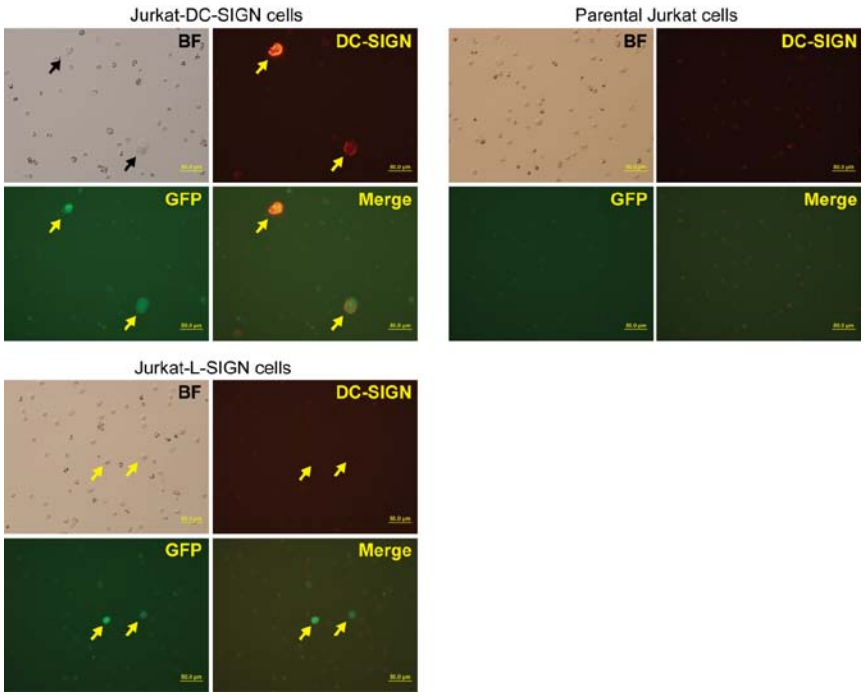

Figure 2-6: Co-expression of GFP and DC-SIGN in Jurkat-DC-SIGN cells. Jurkat (parental), Jurkat-DC-SIGN, Jurkat-L-SIGN cells were fixed with 4% paraformaldehyde for 15 min on ice, and then, incubated with anti-human DC-SIGN rabbit monoclonal antibody (Cell Signaling Tech: #13193) for 16 hours at 4oC. After washing with PBS, cells were stained with Alexa Fluor 594 goat anti-rabbit IgG (ThermoFisher: #A-11037) at 37oC for 1 hour. Washed cells were observed in a chamber slide under Olympus IX71 fluorescense microscope. Jurkat-DC-SIGN and Jurkat-L-SIGN cells, but not parental Jurkat cells, express GFP intrinsically. BF (top left): bright field image, DC-SIGN (top right): Alexa Fluor 594 signals (red) specific to DC-SIGN, GFP (bottom left): cells expressing GFP intrinsically, Merge, (bottom right): merged image of DC-SIGN and GFP. Arrows show the location of GFP-positive cells.

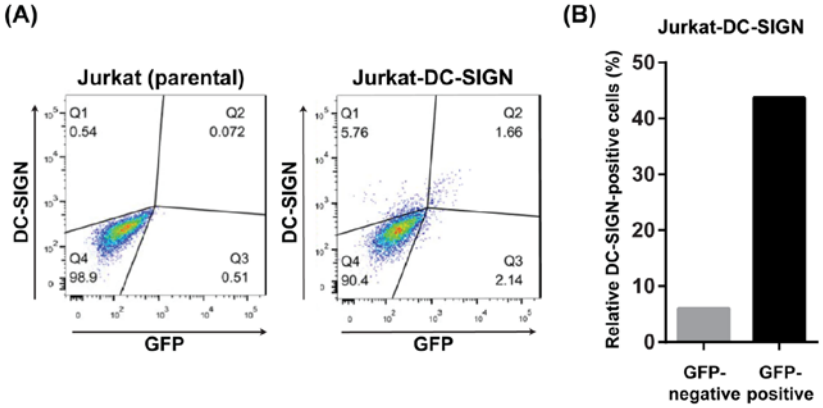

Figure 2-7: Populations of Cells co-expressing GFP and DC-SIGN in Jurkat-DC-SIGN cells. Populations of cells co-expressing GFP and DC-SIGN in Jurkat-DC-SIGN cells. Indirect staining of extracellular DC-SIGN using anti-human DC-SIGN rabbit monoclonal antibody (#13193: Cell Signaling Technology, Inc., Danvers, MA, USA) followed by staining with Alexa Fluor 647 goat anti-rabbit IgG (#A-121244: Thermo Fisher Scientific, Waltham, MA, USA) was performed on parental Jurkat cells and Jurkat-DC-SIGN cells. After extracellular staining, cells were fixed with 4% paraformaldehyde for 30 mins at 4 ^{o}C, and then permeabilized with permeabilization buffer (Affimetrix

eBioScience, San Diego, CA, USA) for 30 mins at 4 ^{o}C. After permeabilization, Alexa Fluor 488 anti-GFP mouse monoclonal antibody B-2 (Santa Cruz Biotechnology, Inc., Dallas, TX, USA) was used to stain cells for 30 mins at 4 ^{o}C. Though Jurkat-DC-SlGN cells intrinsically express GFP, the GFP-positive population was not detected separately from GFP-negative cells in permeabilized samples, due to weak signals (Fig. 2-6), without using anti-GFP antibody. Cells were washed three times with permeabilization buffer, resuspended in FACS buffer, and collected on a LSRII Fortessa (BD Biosciences, San Jose, CA, USA) in the UTMB Flow Cytometry and Cell Sorting Core Facility using FACSDiva software (version 8.0.1, BD Biosciences) and analyzed in FlowJo version 9.7 (TreeStar, Ashland, OR, USA). Fluorescence Minus One (FMO) controls for Alexa-647 and anti-GFP were done in parental Jurkat cells and Jurkat-DC-SlGN cells. (A) FACS images of parental Jurkat (left panel), and Jurkat-DC-SlGN cells (right panel). (B) Relative DC-SIGN-positive cells in GFP-negative cells or those in GFP-positive cells in Jurkat-DC-SlGN cells. It should be noted that GFP-positive cells (3.8%) and DC-SIGN-positive cells (7.42%) were detected in Jurkat-DC-SlGN cells, which was lower than those detected using Alexa Fluor 488-conjugated anti-GFP rabbit antibody, probably due to decreased sensitivity of mouse anti-GFP antibody and anti-DC-SIGN antibodies in the co-staining protocol.

CHAPTER 3: Mutational Analysis of the Rift Valley fever virus Glycoprotein Precursor proteins for Gn protein Expression[3]

INTRODUCTION

The Small (S) -, Medium (M)-, and Large (L)- segments comprise the negative-stranded RNA genome of RVFV. The L protein, the viral RNA polymerase, is the only protein encoded by the L-segment, whereas the S-segment encodes two proteins, NSs and the nucleocapsid (N), in an ambisense manner. The envelope glycoproteins, Gn and Gc, are encoded by the M-segment along with the 78 kDa protein and NSm, which are accessory proteins (66, 230, 255). The context of the Kozak sequence surrounding the initiation codon of the mRNA affects translation initiation efficiency (256). A strong Kozak consensus sequence contains a adenine (A) or guanosine (G) at position -3 (where the A of the AUG is +1 and there is no 0 position), and a G is at position +4 in vertebrate cells (256). An adequate sequence will contain only one of these parameters (256). Strong Kozak sequences are further enhanced by a G at -6 and C at positions -2 and -1 (256).

The Kozak context surrounding the 1st initiation codon is very weak in RVFV M mRNA **(Table 1-1)**. However, this RVFV M-segment sequence resembles the strong context in invertebrates (92). Though the 2nd AUG is surrounded by the G at the -3 position, the 3rd AUG, which was originally thought to not be involved in translation, contains a G at -6, in addition to the one at -3. Thus, both the 2nd and the 3rd AUG support the Kozak context in vertebrate cells. Similarly, the 4th and 5th AUGs are also surrounded by strong and adequate Kozak contexts for translation, respectively **(Table 1-1)**. Leaky scanning of ribosome at the 1st AUG allows for the production of, at least, two polypeptides generated from the 1st AUG (at nt. 21) and the 2nd AUG (nt. 136) **(Figure 3-1A).** The 78 kDa protein and Gc are produced from the polypeptide generated from the 1st AUG by cleavage upstream of Gc by signal peptidases. The precursor

[3] Portions of this chapter have been previously published. Phoenix I., Lokugamage N, Nishiyama S, Ikegami T. **2016.** Mutational Analysis fo the Rift Valley fever virus Glycoprotein Precursor Proteins for Gn Protein Expression. ***Viruses*****.** 8, 151. doi: 10.3390/v8060151.

produced from the 2nd AUG is also cleaved by signal peptidases, but generates NSm, Gn, and Gc. The first and second AUGs can be abolished without abolishing Gn and Gc expression because Gn-Gc precursor proteins can be generated from the 3rd, 4th, or 5th AUGs. A lack of the 2nd AUG abolishes the expression of NSm protein, however, the 3rd AUG can alternatively generate NSm', an N-terminally truncated form of NSm that can co-localize with the mitochondrial outer membrane like NSm (92).

Because viral replication is not dependent on the expression of the 78 kDa and NSm proteins (64, 65), studies have focused on removal of these proteins for vaccine development (64). Indeed, a recombinant MP-12 vaccine, rMP12-ΔNSm21/384, which encodes an in-frame truncation in the 78 kDa/NSm region induced apoptosis sooner than parental rMP-12 in 293, J774.1 and Vero E6cells. In one study, NSm and 78 kDa were deleted from the recombinant ZH501 strain, a pathogenic RVFV, strain, (R-ΔNSm-ZH501), and the dissemination rate in mosquitoes (*Aedes aegypti*) was less efficient than that of the parental rZH501 strain (93, 94). However, when this same R-ΔNSm-ZH501 strain was used to infect rats, it retained neurovirulence (90). Therefore, abolishment of the NSm and 78 kDa proteins, may reduce viral dissemination in mosquitoes, while also weakly attenuating pathogenic RVFV. A subsequent study using a recombinant ZH548 strain, the parental strain used to produce MP-12, showed that specific abolishment of the 78 kDa protein, produced a strain that also had reduced dissemination in mosquitoes (92). This study also demonstrated that abolishment of the 2nd and 3rd AUGs prevented the expression of NSm and NSm', respectively, which lead to reduced viral titers in mammalian cell culture (92). Thus, a rMP-12 strain lacking the 78 kDa and NSm proteins would be a viable candidate vaccine as it would have good immunogenicity and a DIVA marker.

The expression levels of Gn and Gc proteins may be changed by the alteration of glycoprotein precursor proteins by abolishment of the 1st and/or the 2nd AUGs. Using recombinant vaccinia viruses, Suzich et al. analyzed the impact of specific AUG abolishment

(AUG to CUC substitution) in the pre-Gn region, while Kakach et al. analyzed the effects of truncation of the pre-Gn region on Gn expression levels **(Table 3-1)** (186, 227). The abolishment of the 1st AUG (Δ1) slightly increased the Gn expression, whereas the abolishment of the 2nd AUG (Δ2), 2nd and 3rd AUGs (Δ2+3), the 2nd, 3rd, and 4th AUGs (Δ2+3+4), or the 2nd, 3rd, 4th and 5th AUGs (Δ2+3+4+5) decreased the synthesis of Gn, compared to that from the parental wild-type M-segment. Thus, the "default" NSm-Gn-Gc precursor protein from the 2nd AUG is apparently more efficient than the NSm'-Gn-Gc precursor (from the 3rd AUG) or the Gn-Gc precursors (from the 4th or 5th AUGs), for Gn expression. However, the relative expression levels were analyzed by autoradiography **(Table 3-1)**, and further, quantitative analysis of Gn expression levels by AUG alterations will be necessary to correctly understand the impact of mutagenesis in the M-segment start codons.

Mutant	Gn Expression (%)	Gc Expression (%)
No mutation	100	100
Δ 2	48	66
Δ 2+3	46	72
Δ 2+3+4	23	44
Δ 2+3+4+5	11	49
Truncation up to AUG 2 (Kakach 1988)	116.7	91.7
Truncation up to AUG 2 (Suzich 1990)	130	100
Truncation up to AUG 3	204.2	204.2
Truncation up to AUG 4	212.5	183.3
Truncation up to Gn	0.0	4.2

Table 3-1: Rift Valley fever virus Gn and Gc Expression Alteration due to Abolishment of Initiation Codons. Kakach et al used antigen-capture ELISA to determine the expression levels of Gn and Gc produced from the AUG mutants indicated. The AUG mutants were generated using truncated (up to AUG indicated) RVFV M-segments present in recombinant vaccinia viruses. Suzich et al. counted the amount of RVFV-specific proteins found in bands corresponding to Gn and Gc sizes. Cleared cellular lysates from infected cells were immunoprecipated with antibodies to Gn and Gc and separated by SDS-PAGE. Bands corresponding to Gn and Gc sizes were cut and protein counted. Protein amounts from the non-mutated virus was normalized to 1 (100%). *Modified from Kakach et. al. 1988. J-Virol. and Suzich et al. 1990 J-Virol.

Though the live-attenuated MP-12 vaccine has been demonstrated to be safe and efficacious in livestock and has been licensed, conditionally, for veterinary use in the United

States(137-139, 257-259); it lacks a DIVA, differentiation of infected from vaccinated animals, marker. Removal of either the 78 kDa protein or NSm or both would provide a negative DIVA marker for the MP-12 vaccine. The rationale underlying the development of rMP12-ΔNSm21/384 is the abolishment of the 78 kDa and NSm proteins from the MP-12 vaccine (136, 260). However, little is known about the impact of specific mutation or truncation in the preglycoprotein coding region on the virological phenotype, as well as on Gn and Gc expression levels. Our hypothesis is that optimization of the translation efficiency of the preglycoprotein region of the RVFV M-Segment will lead to an increase in Gn secretion and, subsequent, increase in viral titer. The aims of this study were to determine the effects on Gn secretion and viral phenotype due to the abolishment of the 1st, 2nd, 3rd, 4th, and/or 5th AUG by point-mutation or in-frame deletion to determine the potential of rMP-12 mutants for vaccine development.

To quantify the changes in Gn expression levels, due to mutagenesis of the pre-Gn region, we developed a reporter assay, where the N-terminal region of Gn was fused to *Gaussia* luciferase (gLuc). In this system, the 1st and 2nd AUGs produce Gn/gLuc precursor proteins (precursor-1 and -2, respectively), and the NSm and Gn/gLuc fusion proteins are cleaved from precursor-2, due to the signal sequence upstream of Gn. Since the precursor-1 mimics the 78 kDa-Gc precursor protein and encodes the signal peptide at the N terminus, in addition to that upstream of Gn, we assumed that the precursor-1 cannot be further cleaved into the Gn/gLuc protein. Surrogate Gn/gLuc precursors can be produced from the 3rd, 4th, or 5th AUG (precursor-3, -4, and -5, respectively) and generate cleaved Gn/gLuc proteins **(FIGURE 3-1B)**. Various AUG (Met) to CUC (Leu) mutants were analyzed for relative gLuc activity of secreted Gn/gLuc proteins in the culture supernatant. Subsequently, reverse genetics was used to rescue recombinant MP-12 (rMP-12) encoding various AUG mutations, and the effects of AUG abolishment on viral phenotypes was characterized. This work will support the understanding of

the effects of initiation codon knockout within the RVFV M-segment preglycoprotein region, and the development of NSm or 78 kDa knockout mutants for vaccine development.

MATERIALS AND METHODS

Media, Cells, Viruses. DMEM supplemented with 10% FBS, penicillin (100 U/ml), and streptomycin (100 µg/ml) was used to maintain human embryonic kidney (293) cells, Vero cells, (ATCC CCL-81), and Vero E6 cells (ATCC C1008). BHK/T7-9 cells that stably express T7 RNA polymerase (236) were cultured in MEM-alpha supplemented with 10% fetal bovine serum (FBS) (Invitrogen), penicillin (100 U/ml), streptomycin (100 µg/ml), and hygromycin (600 µg/ml). Reverse genetics was used to rescue the recombinant RVFV MP-12 (rMP-12) strains encoding mutation(s) in the preglycoprotein region of the RVFV M-segment as described previously (124). Viral titers were determined in Vero E6 cells by plaque assay (239).

Plasmids. DNA synthesis (gBlocks, Integrated DNA Technologies, Coralville, IA) made the chimeric DNA construct consisting of RVFV MP-12 M-segment (nt. 1-533: containing 18 amino acids of N-terminal Gn) fused with gLuc (lacking nt.1-51 to remove an intrinsic signal sequence for gLuc), followed by two tandem Strep-tags and a Flag tag to generate: pCAGGS-PreGn-gLuc-SF. Gibson assembly mastermix (New England BioLabs, Ipswich, MA) was used to clone the DNA fragment into the pCAGGS plasmid, which made the parental pCAGGS-PreGn-gLuc-SF plasmid. Site-directed mutagenesis of the pCAGGS plasmid was not feasible because of the long GC tract in the CAG promoter sequence. Thus, to create each AUG mutant, the DNA fragment encoding nt.1-830 of parental pCAGGS-PreGn-gLuc-SF insert sequence was first transferred into a pProT7 plasmid, which does not contain long GC tracts. Then, site-directed mutagenesis was performed and CUC (Leu) was introduced in the place of the AUG (Met); thus abolishing the initiation codons. The mutated insert sequences were re-transferred into the pCAGGS-PreGn-gLuc-SF plasmid.

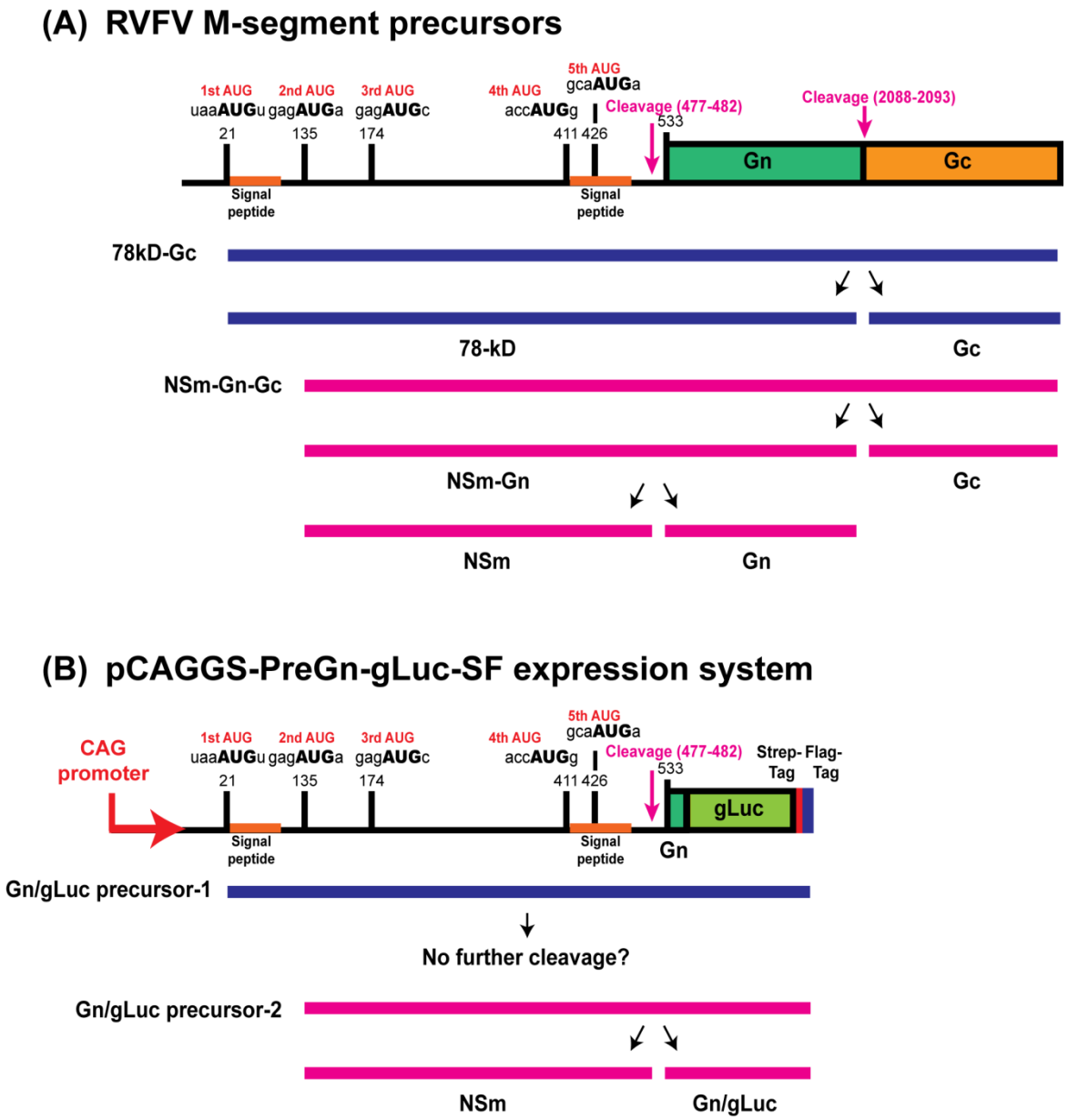

Figure 3-1: Gene Expression of the Rift Valley fever virus M-segment and pCAGGS-PreGn-gLuc-SF. (A) The polypeptides synthesized from the 1st AUG (78 kDa-Gc) or the 2nd AUG (NSm-Gn-Gc) are cleaved by signal peptidases [14, 16, 31]. The 78 kDa protein and Gc are generated from the 78 kDa-Gc precursor, while NSm, Gn, and Gc are made from the NSm-Gn-Gc precursor. (B) The pre-Gn region was fused to the gLuc ORF lacking the intrinsic signal peptide, which allows for secretion of Gn/gLuc fusion proteins from the cell via the Gn signal peptide. The Gn/gLuc precursor-1 makes a chimeric protein consisting of the pre-Gn region and gLuc, while the Gn/gLuc precursor-2 generates NSm and the Gn/gLuc fusion protein.

Western Blotting. Sample buffer (2X) was used to suspend cells followed by boiling for 10 mins. Under reducing conditions, SDS-polyacrylamide gel electrophoresis (SDS-PAGE) was

performed to separate samples, followed by Western blot analysis (240) using anti-actin antibody (I-19, Santa Cruz Biotech) and anti-Flag M2 antibody (Sigma-Aldrich) to detect the C-terminal Flag-tagged Gn/gLuc protein or precursor proteins.

***Gaussia* and *Cypridia* luciferase assays.** TransIT-293 transfection reagent was used, according to the manufacturer's instructions, to co-transfect 293 cells (subconfluent, $1x10^6$ cells in 6-well plate) with the pCAGGS-PreGn-gLuc-SF or the AUG mutant plasmids (2.0 µg) along with pSV40-CLuc (0.1 µg; encodes *Cypridia* luciferase, cLuc, downstream of the SV40 promoter). Culture supernatants were harvested at 36 hpi, and we performed gLuc assay (BioLuc Gaussia Luciferase Assay Kit, New England BioLabs) and cLuc assay (BioLuc Cypridina Luciferase Assay Kit, New England BioLabs), separately, according to the manufacturer's instructions.

Statistical Analysis. GraphPad Prism version 6.05 (Graphpad Software Inc.) was used for statistical analyses. For the gLuc/cLuc values normalized to parental construct value in Figures 3-2B and 3-3C, or virus titers in Figure 3-4A, arithmetic means of $\log_{10}$ values were analyzed by one-way ANOVA followed by Tukey's multiple comparisons test.

RESULTS

The Gn/gLuc Precursor-1 does not efficiently generate Gn/gLuc Fusion Proteins

The parental pCAGGs-PreGn-gLuc-SF plasmid and a transfection control plasmid (pSV40-Cluc) were cotransfected into 293 cells. A natural signal peptide is encoded by the expressed cLuc proteins, which get secreted into the secretory pathway. Thus, secreted cLuc can serve as a control for the measurement of secreted Gn/gLuc fusion proteins in transfected cells. At 36 hours post transfection, cell lysates and culture supernatants were collected for Western blot and luciferase analyses, respectively.

Western blot using an anti-Flag antibody demonstrated that precursor protein production **(Figure 3-2A)** was altered by AUG abolishment. The corresponding band for the precursor-1 was no longer visible when the first AUG was abolished, as expected. When the 2nd AUG was

abolished, the precursor-2 band disappeared. The band corresponding to precursor-3, produced from the 3rd AUG appeared when the 2nd AUG was abolished (i.e., Δ1+2 or Δ2). Based on the migrations of the bands, precursor-4 and -5, produced from the 4th and 5th AUGs, respectively; and the cleaved Gn/gLuc fusion proteins were indistinguishable. No Gn/gLuc fusion proteins were detected when all five of the AUGs were concomitantly abolished. However, the Gn/gLuc fusion protein band, while decreased, was detectable when the 2nd through 5th AUGs were abolished.

After measuring the activities of gLuc and cLuc in the culture supernatant, the ratio of gLuc to cLuc was normalized to that of parental pCAGGS-PreGn-gLuc-SF **(Figure 3-2B).** Little gLuc activity (0.79% compared to parental 100%) in the supernatant was measurable when all five the AUGs were simultaneously abolished. However, when the 1st AUG was present, but the other four (2nd-5th) were abolished, there was detectable, but decreased, gLuc activity (7.7% compared to parental 100%). Thus, precursor-1, which is produced from the 1st AUG, can also generate Gn, though at a decreased level.

Precursor-2 plays a major role in Gn/gLuc Expression

The relative secretion levels of the cleaved Gn/gLuc proteins of various AUG mutants were also analyzed **(Figure 3-2B)**. The relative gLuc activity was significantly affected with the abolishment of the 2nd AUG. Compared to the parental plasmid (100%), the Δ1 plasmid (121%), the Δ3 plasmid (85%), or the Δ4 plasmid (72%); the gLuc activity of the Gn/gLuc fusion proteins expressed from the Δ2 plasmid was significantly low (32%). The relative gLuc activity was also significantly reduced when other AUGs were abolished in combination with the 2nd AUG abolishment (1st, 2nd, and 3rd AUGs (Δ1+2+3) – 13%; 1st, 2nd, 3rd, and 4th AUGs (Δ1+2+3+4) - 15%) compared to the parental plasmid. When the 1st AUG was concomitantly abolished with the 2nd AUG (Δ1+2: 74%), the relative gLuc activity was not as low as Δ1+2+3 (13%). As the Δ1+2 mutant contains the 3rd AUG, a precursor-3 made from the 3rd AUGs can serve as a surrogate precursor protein for the production of Gn.

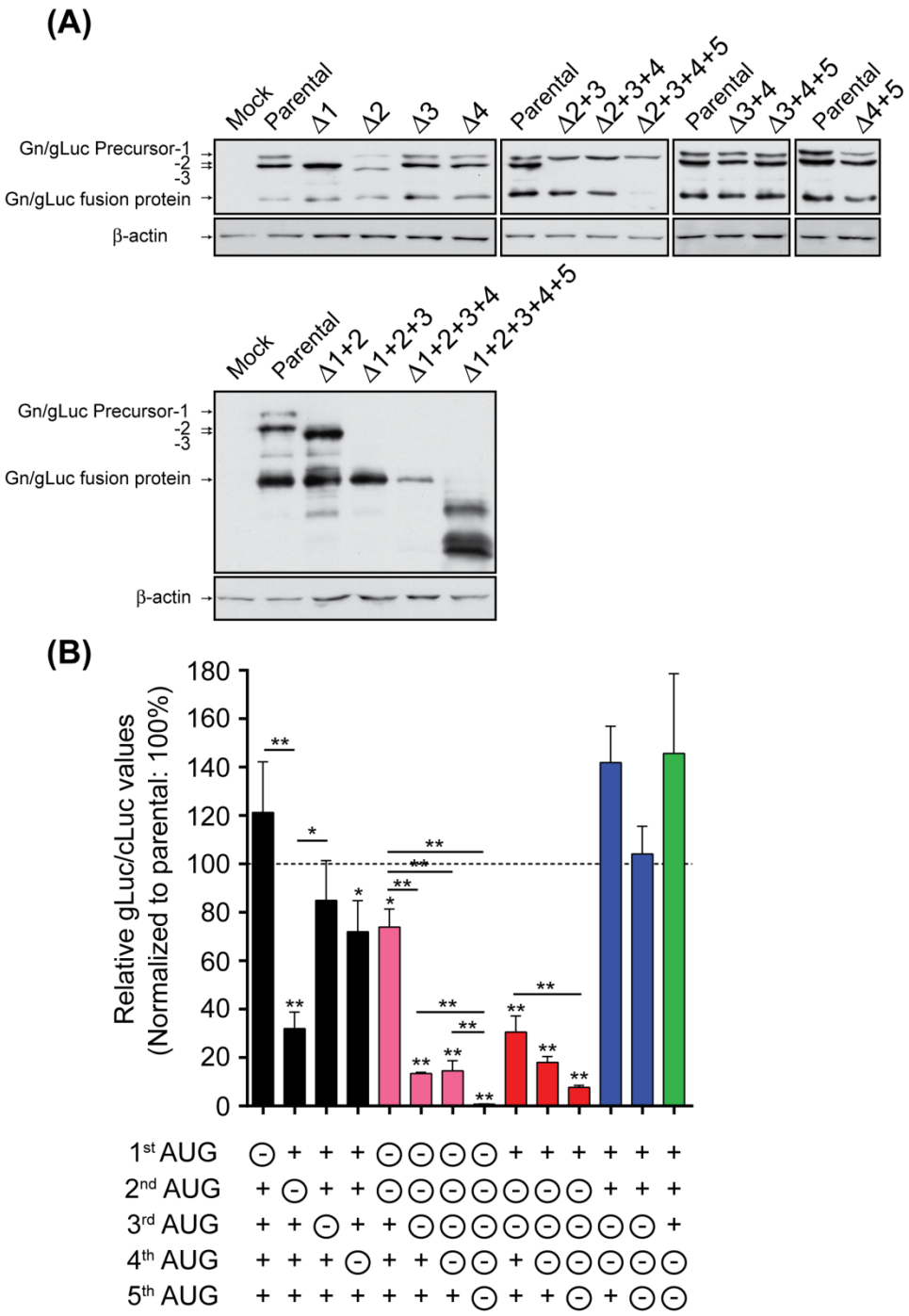

Figure 3-2: Relative Expression of Precursor Proteins and Cleaved Gn/gLuc Fusion Proteins after AUG Abolishment. (A) Western blot of cell lysates. 293 cells were co-transfected with pSV40-CLuc (transfection control), and pCAGGS-PreGn-gLuc-SF or the AUG mutant plasmids. At 36 hours post transfection, cell lysates were collected and analyzed by Western blot using anti-Flag antibody. (B) The extracellular Gn/gLuc fusion proteins were measured using the culture supernatant of transfected cells. The ratio of gLuc to cLuc (control plasmid) was normalized to that of parental pCAGGS-PreGn-gLuc-SF. The graph represents the mean + the standard error of three independent experiments. Asterisks represent statistically significant differences (One-way ANOVA, *p<0.05, **p<0.01, compared to the Δ4+5 mutant).

When the second AUG was concomitantly abolished with the third AUG, the gLuc activity was significantly lower than the parental plasmid (100%): Δ2+3 – 31%. Further abolishment of the 4th and the 5th AUGs lead to more significant reductions in gLuc activities: Δ2+3+4 – 18%; Δ2+3+4+5 – 8%. Comparison of the gLuc activities of mutants which still encode the 1st AUG [Δ2+3 (31%), Δ2+3+4 (18%)] with those lacking AUG 1 [Δ1+2+3 (13%); Δ1+2+3+4 (15%), respectively] indicate that precursor-1 does contribute, albeit slightly, to Gn/gLuc protein expression. However, when the downstream AUGs (3rd, 4th, and 5th,) were abolished, gLuc activity was not decreased, compared to the parental plasmid (100%): Δ3+4 (142%), Δ3+4+5 (104%), Δ4+5 (146%). These results indicate that precursor-3, -4, or -5 play little role in Gn/gLuc protein production when both the 1st and 2nd AUGs (precursor-1 and -2) are present.

The viral untranslated region sequence, upstream of the 4th or 5th AUG, affects efficient generation of Gn/gLuc fusion proteins.

A previous study indicated that slightly higher levels of Gn/Gc were produced from a DNA plasmid containing the ORF of the RVFV M-segment starting at the 4th AUG compared to a similar construct where the ORF started at the 2nd AUG (35). We hypothesized that the untranslated region (UTR) upstream of the Gn/gLuc precursor-4 and/or -5 (Δ1+2+3; Δ1+2+3+4) contributed to the decrease in gLuc activities of the Gn/gLuc fusion proteins expressed from those plasmids (13% and 15%, respectively). Therefore, we generated four plasmids, (AUG2-M, AUG3-M, AUG4-M, or AUG-5-M), that each encoded a truncated UTR sequence in the pCAGGS-PreGn-gLuc-SF **(Figure. 3-3A)**. These plasmids share a common UTR sequence [5'-ACACAAAGACGGUGCACGAGAUG (initiation codon is underlined)], and all of the downstream initiation codons (AUG) were also abolished to ensure that each plasmid produces a single Gn/gLuc precursor (AUG2-M: Precursor-2; AUG3-M: Precursor-3; AUG4-M: Precursor-4; AUG-5M: Precursor-5) **(Figure. 3-3C)**.

To determine the impact of UTR sequence upstream of the 2nd, the 3rd, the 4th, or the 5th AUG, we evaluated the relative gLuc activity found in the culture supernatant of cells transfected with each plasmid **(Figure. 3-3B)**. The gLuc activity of the AUG2-M was higher (282%) compared to the parental plasmid (100%), and significantly higher than the AUG3-M, AUG4-M, and AUG5-M plasmids. The gLuc activity of the AUG3-M, however, was significantly reduced (66%) compared to the AUG4-M (116%) and the AUG5-M mutants (92%). Precursor-4 (AUG4-M) and precursor-5 (AUG5-M) are more efficient at producing Gn/gLuc fusion proteins with precursor-4 (AUG4-M) being marginally increased significantly. Our results demonstrated that an in-frame deletion of the UTR upstream of the 2nd or the 4th AUG, but not that of the 3rd or 5th AUG, can increase the expression of Gn/gLuc fusion proteins.

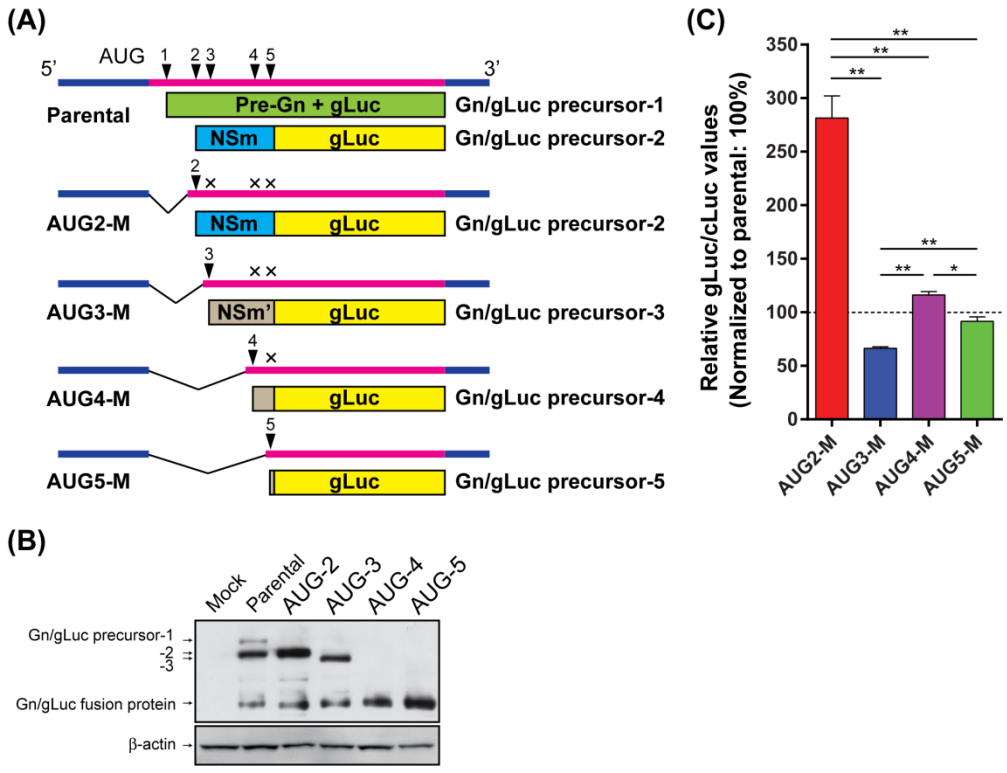

Figure 3-3: Relative Expression of Precursor Proteins and Cleaved Gn/gLuc after the Truncation of the Viral Sequence Upstream of the AUG. (A) Schematic representation of AUG2-M, AUG3-M, AUG4-M, or AUG5-M, which express a single precursor from the 2nd, 3rd, 4th, or the 5th AUG, respectively. AUG2-M lacks the 3rd, 4th, and 5th AUGs, AUG3-M lacks the 4th and 5th AUGs, and AUG4-M lacks the 5th AUG. The mutant plasmids encode a common 20 nt viral sequence upstream of the 1st AUG [5'-ACACAAAGACGGUGCACGAGAUG (initiation codon is underlined)]. (B) 293 cells were co-transfected

with pSV40-CLuc (transfection control), and pCAGGS-PreGn-gLuc-SF or the mutant plasmids. At 36 hours post transfection, culture supernatants were collected, and the gLuc and cLuc activities were measured. Then, the ratio of gLuc to cLuc was normalized to that of parental pCAGGS-PreGn-gLuc-SF plasmid. The graph represents the mean + the standard error of three independent experiments. Asterisks represent statistically significant differences (One-way ANOVA, *p<0.05, **p<0.01)

The rMP-12 encoding the AUG2-M mutation or the rMP-12 encoding the Δ2+3 mutation replicate less efficiently than parental rMP-12

We also determined the effects of M-segment modification on viral phenotypes. Two constructs were selected to analyze the impact of increased or decreased Gn expression due to mutagenesis in the preglycoprotein coding region: Δ2+3 (31%) and AUG2-M (282%). Recombinant MP-12 encoding either the Δ2+3 or AUG2-M mutations were rescued by reverse genetics. In addition, we also rescued rMP-12 encoding Δ1 (121%), Δ1+2 (74%), or Δ4+5 (146%), to compare replication kinetics. The AUG2-M, the Δ1, Δ1+2 mutants lacked expression of the 78 kDa protein. The Δ2+3 mutant also lacked expression of NSm and the AUG2-M encoded a mutated NSm (Met to Leu, at the 3rd, 4th, and 5th AUGs). The AUG2-M and Δ2+3 mutants lacked expression of NSm', while the Δ1+2 still encoded for NSm'. The Δ4+5 mutant was included because it encoded the 1st and 2nd AUG and is able to produce the precursors from those initiation codons.

Vero E6 cells were infected with the mutants at an MOI of 0.15. Though all of the mutants replicated in Vero cells, it was noted that both the AUG-2M, and Δ2+3 mutants replicated slower than the other mutants **(Figure 3-4A)**. The arithmetic means of the $\log_{10}$ titers of the AUG2-M mutant at 48 and 72 hpi were 7 and 2 times lower than those of the Δ4+5 mutant at 48 and 72 hpi, respectively ($p < 0.05$). The arithmetic means of the $\log_{10}$ titers of Δ2+3 mutant were 6 and 2 times lower than those of the Δ4 + 5 mutant at 48 and 72 hpi, respectively, but the differences were not statistically significant. The two mutants, AUG2-M and Δ2+3, were further analyzed at a higher MOI infection (1 MOI) **(Figure 3-4B)**. No significant differences were seen when compared to rMP-12 (data not shown). Western blot analysis confirmed that

the AUG2-M mutant did not produce the 78 kDa protein, and the Δ2+3 mutant did not produce NSm-Gn, whereas both proteins were produced by parental rMP-12 **(Figure 3-4B)**. An increase in all viral proteins at 6 hpi indicated that viral replication probably started around 5 to 6 hpi. In terms of plaque phenotype, the Δ2+3 mutant made smaller plaques (0.9 to 2.3mm in diameter) compared with parental rMP-12 (heterogeneous sizes: 2.6 to 5.7mm in diameter), while the AUG2-M mutant had intermediated-sized plaques (1.7 to 4.5mm in diameter) compared with the other two viruses. Thus, these results indicate that viral replication is affected in the AUG2-M and Δ2+3 mutants despite efficient expression of Gn by AUG2-M. In addition, the 78 kDa protein and/or NSm/NSm' may have a role(s) in expression of Gn at later stages in the viral life cycle.

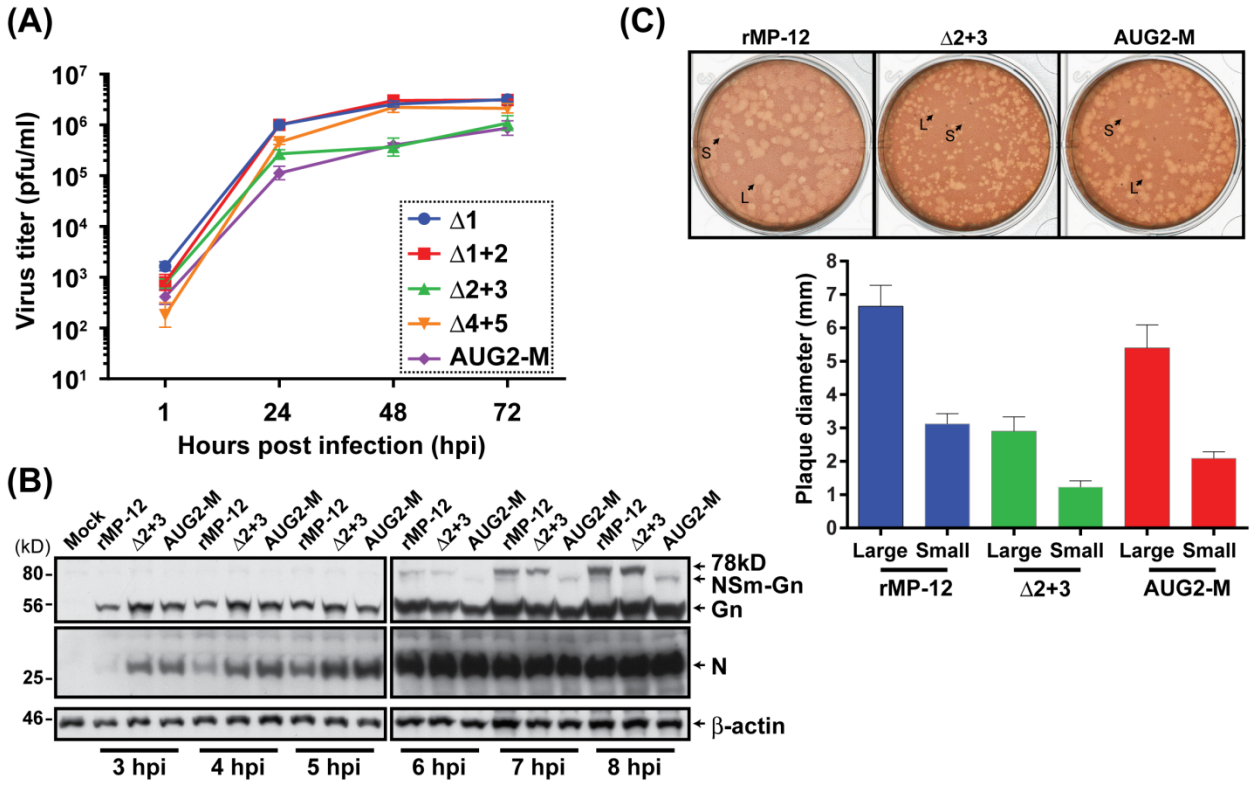

Figure 3-4: Characterization of Recombinant MP-12 encoding Mutations in the Pre-Gn region.
(A) Replication of rMP-12 mutants encoding the mutations either in the 1st AUG (Δ1), the 1st and 2nd AUG (Δ1+2), the 2nd and 3rd AUG (Δ2+3), the 4th and 5th AUG (Δ4+5), or the deletion of the UTR upstream of the 2nd AUG (AUG2-M: see Fig. 3A). Vero cells were infected with each virus at an MOI of 0.15. The graph represents the antilog of the arithmetic mean of the $\log_{10}$-transformed virus titers + the standard deviation of three independent experiments. (B) Western blot using Vero cells infected with either rMP-12, Δ2+3, or the AUG2-M mutants (an MOI of 1). The 78 kDa and Gn were detected by mouse anti-Gn

monoclonal antibody (4D4). The N proteins were detected using mouse anti-RVFV polyclonal antibody. b-actin is shown as sample loading controls. (C) Plaque phenotypes of rMP-12, Δ2+3, or the AUG2-M mutants in VeroE6 cells. Small (S) and large (L) plaques are shown with arrows. The diameters (mm) of small and large plaques were measured (n=10 per sample), and the average and standard errors are shown in the graph.

DISCUSSION

RVFV lacking accessory proteins, like the 78 kDa or NSm proteins, can be produced using reverse genetics, and RVFV lacking the first or second initiation codon can produce mutants lacking the 78 kDa or NSm proteins, respectively. This work confirmed that modification of the initiation codons within the pre-Gn region alters precursor protein production and affects the expression of Gn/gLuc proteins. However, an optimized pre-Gn region for abundant Gn expression did not lead to an increased viral replication (AUG2-M) in our experiments. Thus, a process downstream of viral protein translation may be involved in viral progeny release (e.g. viral assembly in the ER-Golgi intermediate compartment (ERGIC) or *cis*-Golgi). Both of the AUG2-M and Δ2+3 mutants, which replicate slowly in Vero cells, lack intact expression of both NSm and NSm'. The AUG2-M mutant lacks the 1st, 3rd, 4th, and 5th AUGs (Δ78 kDa and ΔNSm'), and also expresses a mutant NSm that encodes Met-to-Leu mutations at the 3rd, 4th, and 5th AUGs. The Δ2+3 mutant does not express NSm or NSm' proteins. Thus, NSm and/or NSm' might be involved with viral assembly or a further downstream step in virion release. A similar KO virus was produced by Kreher et al (2014), using the RVFV ZH548 strain backbone (92). RVFV ZH548 is the original virulent strain that was used to produce the attenuated MP-12 strain (131). Virulence of the RVFV ZH548 2+3 KO mutant was substantially reduced compared to the parental virus in C57BL/6 mice (92). Also, though no changes in viral kinetics were seen in murine fibroblast cells, the RVFV ZH548 2+3 KO did replicate to a lower titer than the wild-type strain in murine macrophages (92). Since the observations of our group and others are consistent, future studies should address the mechanism of NSm and NSm'-mediated viral progeny formation.

Precursor proteins produced from the 1st, 2nd, 3rd, 4th, or 5th initiation codons can be easily measured using our reporter assay, which encodes the RVFV preglycoprotein region followed by the N-terminal region of Gn fused to gLuc. However, RVFV Gn encodes a Golgi retention signal, whereas the Gn/gLuc proteins do not and are secreted from the transfected cells. Thus, precursor protein production and cleavage efficiency are determined by the gLuc activity in the culture supernatant. There was a detectable amount of gLuc activity in the supernatant of cells transfected with the Δ2+3+4+5 plasmid and accumulation of a detectable amount of Gn/gLuc proteins in the cell lysates analyzed by Western blot. In the natural RVFV infection, the 78 kDa protein is cleaved from the 78 kDa-Gc precursor produced from the 1st AUG, which encodes a signal sequence at its N-terminus (261). Folding of the 78 kDa protein in the ER lumen may hinder access of the second signal sequence, located between the NSm, and Gn coding regions, with signal peptidases. A lack of cleavage at this second signal sequence can prevent the accumulation of Gn from the 78 kDa-Gc precursor protein. This lack of Gn accumulation is most likely the reason that the rMP-12-Δ2+3+4+5 mutant could not be rescued. The Δ1, Δ3, or Δ4 plasmids efficiently produced Gn/gLuc fusion proteins, whereas the Δ2 plasmid did not. Also, when the downstream initiation codons were abolished, [e.g. Δ3+4+5 (AUG1 and AUG2 present)], gLuc activity was not affected. Thus, the expression of Gn/gLuc proteins is most efficient from AUG 2, which produces precursor-2. Also, precursor-3, produced from the 3rd initiation codon, can act as a surrogate of Gn/gLuc production in the absence of the 2nd initiation codon. The Δ1+2+3 plasmid displayed much less gLuc activity than the Δ1+2 plasmid. Taken together, expression of the Gn protein primarily occurs from the NSm-Gn-Gc precursor, while the NSm'-Gn-Gc precursor can act in a surrogate manner when the 2nd initiation is absent or skipped by the ribosome.

We also truncated the viral UTR upstream of each initiation codon to better determine the translation efficiency of Gn. The plasmids encoding the Δ1+2+3 and Δ1+2+3+4 mutations had low relative gLuc activities. Thus, reporter plasmids that lack the upstream viral UTR

sequence and encode a single initiation codon were generated: AUG2-M, AUG3-M, AUG4-M, and AUG5-M. The increased relative gLuc activity of the AUG4-M and the AUG5-M plasmids compared with the Δ1+2+3 and Δ1+2+3+4 plasmids indicated that removal of the UTR upstream of the 4th and 5th can increase Gn/gLuc expression. Thus, the expression of RVFV Gn/Gc from precursors produced by the 4th and 5th initiation codons can be enhanced by the deletion of the UTR sequence located upstream of these codons.

Though increase in translational efficiency of Gn/Gc did not result in an increase in viral production, the increase in Gn/Gc expression may be beneficial for a subunit vaccine (Gn only or Gn and Gc) or a virus-like particle vaccine (Gn, Gc, and N). Subunit vaccines and VLP vaccines do not require inactivation,

In the natural RVFV infection, Gn and Gc form heterodimers and accumulate in the Golgi via the Golgi retention signal within Gc (262-264). The viral nucleocapsid and the Gn-Gc heterodimers assemble in the ERGIC or the *cis*-Golgi, and then the viral particles egress from the cell. Because the Gn/gLuc fusion proteins produced by our reporter assay lack the Golgi retention signal, they are secreted from the cell without proceeding through the same viral assembly and budding processes as RVFV Gn/Gc. Thus, only the expression levels of Gn via translation of the mRNA and subsequent cleavage of precursor proteins can be predicted with this assay.

Not much is known of the roles that the 78 kDa, NSm, or NSm' may play in viral assembly. In this study, our rMP-12 encoding the AUG2-M mutant demonstrated increased Gn expression but still replicated more slowly than rMP-12. This mutant lacks the expression of the 78 kDa and NSm' proteins and encodes a mutant NSm Met-to-Leu substitutions at the 3rd, 4th, and 5th AUGs). Migration of the NSm protein has been demonstrated to decrease when a Met-to-Ala substitution is encoded by the 3rd initiation codon (92). Thus, RVFV NSm and/or NSm' may have roles in later stages of viral infection. In infection with Bunyamwera virus (genus *Orthobunyavirus*), the NSm protein facilitates viral assembly of the Gn/Gc heterodimers and the

viral ribonucleocapsid (RNP) via the formation of a “viral tube” (265). The NSm acts as a scaffolding protein, and viral production was reduced by 10-100-fold when NSm was not present. In another study, five serial passages of KO mutants that lacked the expression of the 78 kDa protein (Δ1, Δ1+2, and Δ1+2+3) in mammalian cells lead to an RVFV mutant encoding a new initiation codon upstream of the original AUG at nt. 21 (92). A new 78 kDa-Gc precursor protein could be generated from this initiation codon. It has been demonstrated that viral propagation in mammalian cells is affected by a lack of NSm or NSm’, while RVFV dissemination in mosquitoes is reduced in the absence of the 78 kDa protein (92). However, other studies have indicated that both the 78 kDa protein and NSm protein are not necessary for viral replication in cell culture (88). Thus, further studies are necessary to determine the true roles these viral proteins play in RVFV infection.

Mutant	Relative Gn/gLuc Expression (%)
Δ1	121
Δ1+2	74
Δ1+2+3	13
Δ1+2+3+4	15
Δ1+2+3+4+5	0.79
Δ2	32
Δ2+3	31
Δ2+3+4	18
Δ2+3+4+5	8
Δ3	85
Δ3+4	142
Δ3+4+5	104
Δ4	72
Δ4+5	146
Truncation up to AUG 2 (AUG2-M)	282
Truncation up to AUG 3 (AUG3-M)	66
Truncation up to AUG 4 (AUG4-M)	116
Truncation up to AUG 5 (AUG5-M)	92

Table 3-2: Relative Gn/gLuc Expression due to Abolishment of Initiation Codons or Truncation of Viral UTR. Summation of the data in Figures 3-2 and 3-4.

MP-12 is a live attenuated RVFV vaccine that is conditionally licensed in the U.S. for veterinary use, which has been demonstrated to be safe and effective (137-140, 257).

However, MP-12 lacks a DIVA marker, which is necessary to determine which animals have acquired a natural infection versus those which have been vaccinated. Previous studies involving the removal of the NSs protein, demonstrated reduced immunogenicity of the deletion mutants, (R566 strain or rMP12-ΔNSs16/198), compared to parental MP-12 (260). As the 78 kDa and NSm proteins have been demonstrated to be non-essential, introduction of a DIVA marker into MP-12 could be accomplished via the removal of these proteins. Indeed, studies using rMP-12 which lacks 78 kDa and NSm protein production (rMP12-ΔNSm21/384), demonstrated this mutant, which is similar to our AUG4-M mutant, displayed a similar efficacy and immunogenicity profile to that of parental MP-12 (136, 260).

Here we describe rMP-12 mutants with altered levels of Gn expression due to point mutations and truncation of the initiation codons. Alterations in the production of Gn lead to altered viral phenotypes compared to rMP-12. This works aids future studies that will focus on NSm or 78 kDa knockout mutants and subunit and VLP vaccine studies.

CHAPTER 4: Future Directions

The work presented in the first aim has laid the groundwork for future studies involving RVFV N-glycosylation and the viral interaction with DC-SIGN. Here, we have confirmed N-glycosylation of Gn at N438 and at three of the four sites within Gc, which we identified: N794, N1035, and N1077. We also noted the heterogeneous N-glycosylation of N1077, which results in the well-documented, Gc doublet. While we were also able to determine the presence of high mannose or hybrid N-glycans on Gn and Gc via Endo H digestion, this method is not rigorous enough to elucidate the actual N-glycans. Thus, future studies using Mass Spectrometry to analyze the glycoforms will characterize the specific N-glycans present at each site. Also, while our studies indicate that heterogeneous N-glycosylation of Gc N1077 occurs via post-translational N-glycosylation by the STT3B subunit of the OST, our studies would be further strengthened by STT3A and STT3B knockdown studies using siRNA (244).

We determined that the presence of Gn N438 or Gc N1077 is important for RVFV infectivity via DC-SIGN. DC-SIGN has specific ligand binding preferences (high mannose N-glycans and fucosylated N-glycans, such as Lewis antigens) and knowing the exact N-glycan present at each site within RVFV Gn/Gc will further elucidate which N-glycans are involved. DC-SIGN is involved in antigen-presenting to CD4+ T-cells through rapid degradation of internalized antigens (266-268). Further understanding of how viruses utilize DC-SIGN for their entry will lead to novel vaccine candidates targeting antigens to this lectin in an effort to increase antigen presentation rather than viral infection. Dodd et al. demonstrated that CD4+ responses are required for clearance of RVFV and prevention of neurological disease (269). Lastly, our *in vitro* results with Jurkat-DC-SIGN cells would further be enhanced by *in vivo* studies. Unfortunately, mice encode eight different orthologs of human DC-SIGN (216). However, recently, a transgenic mouse strain has been produced, in which the murine CD11c promoter controls human DC-SIGN (216, 270). In one study using these transgenic mice, strong antigen specific CD4+ and CD8+ T cell responses were produced and these responses lead to

protection from infection (270). Thus, hSIGN mice would be a valuable tool for the analyzing dendritic-cell based vaccine candidates.

The second aim of this study focuses on modification of the preglycoprotein region of the M-segment in an effort to alter Gn/Gc expression. Our initial hypothesis was that we could increase the translational efficiency of the M-segment by abolishing the initiation codons, individually or concomitantly, or via truncation of the preglycoprotein. This increase in translation efficiency would, then, lead to an increase in Gn expression, which would lead to an increase in the immune response. A previous study indicated that mice were protected from lethal RVFV challenge due to neutralizing antibodies to Gn and Gc induced by recombinant baculoviruses expressing the M-segment starting at the 2nd initiation codon (271). Indeed, our AUG-2M plasmid, truncated up to the 2nd AUG and expressing gLuc fused to the N-terminal region of Gn, demonstrated a significant increase in Gn/gLuc secretion compared to not only the parental plasmid, but all other combinations we investigated. However, this increase in Gn/gLuc secretion did not transfer over to the actual rescued virus. The rMP-12-AUG2-M displayed a lower titer compared to rMP-12. Also, our studies could be further enhanced by *in vivo* analyses to determine as previous studies have shown that 78 kDa/ NSm KO mutants can be protective against lethal RVFV challenge (136, 260).

Though our AUG2-M mutant plasmid displayed increased Gn expression, this did not result in a higher viral titer in the rMP-12-AUG2-M mutant virus. Thus, while this mutation may not be beneficial for a live attenuated vaccine, it may be beneficial in the production of a Gn/Gc subunit vaccine. Indeed, Faburay et al demonstrated that three doses of 50 µg of the Gn ectodomain in combination with adjuvant were sufficient to protect sheep from lethal RVFV challenge (154). In addition to the recombinant baculovirus system used by Faburay et al., Gn and Gc subunits have been produced using *Drosophila melanogaster* cells lines (152). The Stable Schneider 2 (S2) cell line was used because of its ability to secrete proteins into supernatant and ability to be cultured in serum-free medium (152). In addition to secretion of

proteins and serum-free media, this system has the added benefit of not requiring the removing of baculovirus proteins (152). Investigation of the potential of the ability of the AUG2-M mutant plasmid to be adapted to the S2 expression system and the subsequent studies on the efficacy of Gn/Gc proteins produced from this system will be invaluable to the development of a Gn/Gc subunit vaccine candidate.

We are also interested in whether the expression strategies of the preglycoprotein regions of other phleboviruses were similar to that of RVFV. To that end, we have generated pCAGGs plasmids that encode the preglycoprotein regions of Sandfly fever Sicilian virus (SFSV) and Toscana virus (TOSV), which are closely related to RVFV. A myc-tag has been inserted between the 1st and 2nd AUGs, and a V5-tag was inserted between the 2nd and 3rd AUGs for Western blot analysis. Similar to the pCAGGS-PreGn-gLuc-SF created for Aim 2 studies, the pCAGGS-SFS-PreGn-gLuc-SF and pCAGGS-TOS-PreGn-gLuc-SF plasmids have the N-terminal coding region of Gn that is fused to *Gaussia* luciferase (gLuc) for quantification of Gn/gLuc secretion by gLuc and cLuc assays. The C-terminus encodes Flag-SF tag for the detection of Gn/gLuc or precursor proteins.

For preliminary analyses, transIT-293 was used according to the manufacturer's instructions to co-transfect 293 cells (subconfluent, 1x10^6 cells) with the pCAGGS-SFS-PreGn-gLuc-SF or pCAGGS-TOS-PreGn-gLuc-SF plasmids (2.0 µg) along with pSV40-CLuc (0.1 µg; encodes *Cypridia* luciferase, cLuc, downstream of the SV40 promoter). Culture supernatants were harvested at 36 hpi, and we performed gLuc (BioLuc Gaussia Luciferase Assay Kit, New England BioLabs) and cLuc assays (BioLuc Cypridina Luciferase Assay Kit, New England BioLabs) following the manufacturer's instructions. Sample buffer (2X) was used to suspend the cells followed by boiling for 10 mins. Under reducing conditions, SDS-polyacrylamide gel electrophoresis (SDS-PAGE) was used to separate samples, followed by Western blot analysis (240) anti-Flag M2 antibody (Sigma-Aldrich), anti-cmyc (COMPANY), and anti-V5).

In the Western blot analysis of cell lystates, bands corresponding to the Precursor-1 generated from SFSV-M-gLuc and TOSV-M-gLuc were approximately 80 kD in size compared to Precursor-1 from RVFV-M-gLuc, which was 46 kD in size (data not shown). The precursors generated from the 2nd AUGs of SFSV and TOSV were 62 kD and 60 kD, respectively, compared to the 39 kD Precursor-2 of RVFV. Interestingly, despite encoding a myc-tag between the 1st and 2nd AUGs, no band of precursor-1 was detectable in TOSV-M-gLuc samples using an anti-myc antibody (data not shown). However, bands corresponding to the SVFV precursor-1 and NSm-1 were detected in SFSV-M-gLuc samples. A faint band was noted for the TOSV Precursor-1, with anti-V5 antibody (data not shown) indicating that an inserted myc-tag upstream of the 2nd AUG might be cleaved together with N-terminal signal peptide. Precursor-2 from both SFSV-M-gLuc and TOSV-M-gLuc was detected by the anti-V5 antibody along with NSm-2, which is generated from Precursor-2, from both plasmids. The results showed that both TOSV and SFSV M-segments make two glycoprotein precursors, like RVFV M-segment, and can be cleaved into NSm, Gn and Gc. In the western blot, multiple precursor bands were detected by anti-Flag antibody. Interestingly, TOSV and SFSV M-segment encodes 8 and 14 initiation codons in the preglycoprotein coding region, respectively. Multiple initiation codons in the preglycoprotein coding region is common in those phleboviruses, and may be a clue in understanding the roles of 78 kDa and NSm of RVFV in the viral life cycle, since neither SFSV or TOSV express the 78 kDa protein.

Analysis of gLuc activity indicated that secretion of Gn/gLuc fusion proteins was 3.5-fold higher for the pCAGGS-SFS-PreGn-gLuc-SF than the pCAGGS-PreGn-gLuc-SF control plasmid, whereas Gn/gLuc fusion protein secretion was also about 1.5 fold higher from the pCAGGS-TOS-PreGn-gLuc-SF plasmid. These results indicated that precursor proteins derived from TOSV, SFSV, and RVFV may have different co-translational cleavage efficiency of Gn/Gc. Taken together, these data indicate that there are differences in both protein expression and secretion between RVFV, SFSV, and TOSV, and our reporter system is a valuable

resource to further elucidate the mechanisms of protein expression and secretion from phlebovirus preglycoprotein regions. Further studies will be required to elucidate the exact mechanism of glycoprotein expression by SFSV and TOSV and if chimeric M-Segments that encode the preglycoprotein regions of SFSV and TOSV and the glycoproteins of RVFV are viable vaccine candidates.

References

1. **Daubney R, Hudson JR.** 1931. Enzootic hepatitis or Rift Valley fever: An undescribed virus disease of sheep cattle and man from east Africa. JPathBact **34:**545-579.
2. **Smithburn KC, Haddow AJ, Gillett JD.** 1948. Rift Valley fever; isolation of the virus from wild mosquitoes. Br J Exp Pathol **29:**107-121.
3. **Linthicum KJ, Davies FG, Kairo A, Bailey CL.** 1985. Rift Valley fever virus (family Bunyaviridae, genus Phlebovirus). Isolations from Diptera collected during an inter-epizootic period in Kenya. J Hyg (Lond) **95:**197-209.
4. **Swanepoel R, Coetzer JAW.** 2004. Rift Valley fever. *In* Coetzer J.A.W. and Tustin R.C. Infectious diseases of livestock with special reference to southern Africa. 2nd ed. Cape Town, South Africa. Oxford University Press, 2004. pp.1037-1070.
5. **Grobbelaar AA, Weyer J, Leman PA, Kemp A, Paweska JT, Swanepoel R.** 2011. Molecular epidemiology of Rift Valley fever virus. Emerg Infect Dis **17:**2270-2276.
6. **Bird BH, Bawiec DA, Ksiazek TG, Shoemaker TR, Nichol ST.** 2007. Highly sensitive and broadly reactive quantitative reverse transcription-PCR assay for high-throughput detection of Rift Valley fever virus. J Clin Microbiol **45:**3506-3513.
7. **Ikegami T.** 2012. Molecular biology and genetic diversity of Rift Valley fever virus. Antiviral Res **95:**293-310.
8. **Meegan JM.** 1979. The Rift Valley fever epizootic in Egypt 1977-78. 1. Description of the epizzotic and virological studies. Trans R Soc Trop Med Hyg **73:**618-623.
9. **Gad AM, Feinsod FM, Allam IH, Eisa M, Hassan AN, Soliman BA, el Said S, Saah AJ.** 1986. A possible route for the introduction of Rift Valley fever virus into Egypt during 1977. J Trop Med Hyg **89:**233-236.
10. **Sellers RF, Pedgley DE, Tucker MR.** 1982. Rift Valley fever, Egypt 1977: disease spread by windborne insect vectors? Vet Rec **110:**73-77.
11. **Ahmed Kamal S.** 2011. Observations on rift valley fever virus and vaccines in Egypt. Virol J **8:**532.
12. **Balkhy HH, Memish ZA.** 2003. Rift Valley fever: an uninvited zoonosis in the Arabian peninsula. Int J Antimicrob Agents **21:**153-157.
13. **Carroll SA, Reynes JM, Khristova ML, Andriamandimby SF, Rollin PE, Nichol ST.** 2011. Genetic evidence for Rift Valley fever outbreaks in Madagascar resulting from virus introductions from the East African mainland rather than enzootic maintenance. J Virol **85:**6162-6167.
14. **Botros B, Omar A, Elian K, Mohamed G, Soliman A, Salib A, Salman D, Saad M, Earhart K.** 2006. Adverse response of non-indigenous cattle of European breeds to live attenuated Smithburn Rift Valley fever vaccine. J Med Virol **78:**787-791.
15. **Lihoradova O, Ikegami T.** 2012. Modifying the NSs gene to improve live-attenuated vaccine for Rift Valley fever. Expert Rev Vaccines **11:**1283-1285.
16. **Kasari TR, Carr DA, Lynn TV, Weaver JT.** 2008. Evaluation of pathways for release of Rift Valley fever virus into domestic ruminant livestock, ruminant wildlife, and human populations in the continental United States. J Am Vet Med Assoc **232:**514-529.
17. **USDA.** 2005. Part II. 7 CFR Part 331 and 9 CFR Part 121 Agricultural Bioterrorism Protection Act of 2002; Possesion, use, and transfer of biological agents and toxins; final rule. Fed Register 2005; 70: 13241-13292.
18. **Dar O, McIntyre S, Hogarth S, Heymann D.** 2013. Rift Valley fever and a new paradigm of research and development for zoonotic disease control. Emerg Infect Dis **19:**189-193.
19. **cdc.gov.** 2016. Laboratory Biosafety Level Criteria. http://www.cdc.gov/biosafety/publications/bmbl5/BMBL5_sect_IV.pdf. Accessed 06/12/2016.

20. **Francis T, Magill TP.** 1935. Rift Valley Fever : A Report of Three Cases of Laboratory Infection and the Experimental Transmission of the Disease to Ferrets. J Exp Med **62:**433-448.
21. **Kitchen SF.** 1934. Laboratory infections with the virus of Rift Valley fever Am J Trop Med **14:**547-564.
22. **Sabin AB, Blumberg RW.** 1947. Human infection with Rift Valley fever virus and immunity twelve years after single attack. ProcSocExpBiolMed **64:**385-389.
23. **Schwentker FF, Rivers TM.** 1933. Report of a fatal laboratory infection complicated by thrombophlebitis. JExpMed **59:**305-313.
24. **Smithburn KC, Mahaffy AF, et al.** 1949. Rift Valley fever; accidental infections among laboratory workers. J Immunol **62:**213-227.
25. **Findlay GM.** 1931. Rift Valley fever on enzootic hepatitis. TransRoySocTropMedHyg **25:**229-262.
26. **Gear J, De Meillon B, Measroch V, Davis DH, Harwin H.** 1951. Rift valley fever in South Africa. 2. The occurrence of human cases in the Orange Free State, the North-Western Cape Province, the Western and Southern Transvaal. B. Field and laboratory investigation. S Afr Med J **25:**908-912.
27. **Joubert JD, Ferguson AL, Gear J.** 1951. Rift Valley fever in South Africa: 2. The occurrence of human cases in the Orange Free State, the north-western Cape province, the western and southern Transvaal. A Epidemiological and clinical findings. S Afr Med J **25:**890-891.
28. **Mundel B, Gear J.** 1951. Rift valley fever: The occurrence of human cases in Johannesburg. S Afr Med J **25:**797-800.
29. **Findlay GM, Daubney R.** 1931. The virus of Rift Valley fever or enzootic hepatitis. Lancet **221:**1350-1351.
30. **Abdel-Wahab KS, El Baz LM, El-Tayeb EM, Omar H, Ossman MA, Yasin W.** 1978. Rift Valley Fever virus infections in Egypt: Pathological and virological findings in man. Trans R Soc Trop Med Hyg **72:**392-396.
31. **Swanepoel R, Manning B, Watt JA.** 1979. Fatal Rift Valley fever of man in Rhodesia. Cent Afr J Med **25:**1-8.
32. **Yassin W.** 1978. Clinico-pathological picture in five human cases died with Rift Valley fever. J Egypt Public Health Assoc **53:**191-193.
33. **Al-Hazmi M, Ayoola EA, Abdurahman M, Banzal S, Ashraf J, El-Bushra A, Hazmi A, Abdullah M, Abbo H, Elamin A, Al-Sammani el T, Gadour M, Menon C, Hamza M, Rahim I, Hafez M, Jambavalikar M, Arishi H, Aqeel A.** 2003. Epidemic Rift Valley fever in Saudi Arabia: a clinical study of severe illness in humans. Clin Infect Dis **36:**245-252.
34. **Al-Khuwaitir TS, Al-Moghairi AM, Sherbeeni SM, Al-Ghamdi AS.** 2004. Rift Valley fever hepatitis complicated by disseminated intravascular coagulation and hepatorenal syndrome. Saudi Med J **25:**528-531.
35. **El Imam M, El Sabiq M, Omran M, Abdalkareem A, El Gaili Mohamed MA, Elbashir A, Khalafala O.** 2009. Acute renal failure associated with the rift valley fever: A single center study. Saudi J Kidney Dis Transpl **20:**1047-1052.
36. **Alrajhi AA, Al-Semari A, Al-Watban J.** 2004. Rift Valley fever encephalitis. Emerg Infect Dis **10:**554-555.
37. **van Velden DJ, Meyer JD, Olivier J, Gear JH, McIntosh B.** 1977. Rift Valley fever affecting humans in South Africa: a clinicopathological study. S Afr Med J **51:**867-871.
38. **Maar SA, Swanepoel R, Gelfand M.** 1979. Rift Valley fever encephalitis. A description of a case. Cent Afr J Med **25:**8-11.
39. **Laughlin LW, Girgis NI, Meegan JM, Strausbaugh LJ, Yassin MW, Watten RH.** 1978. Clinical studies on Rift Valley fever. Part 2: Ophthalmologic and central nervous system complications. J Egypt Public Health Assoc **53:**183-184.
40. **Deutman AF, Klomp HJ.** 1981. Rift Valley fever retinitis. Am J Ophthalmol **92:**38-42.

41. **Salib M, Sobhy MI.** 1978. Epidemic maculopathy. Bull Ophthalmol Soc Egypt **71:**103-106.
42. **Siam AL, Meegan JM.** 1980. Ocular disease resulting from infection with Rift Valley fever virus. Trans R Soc Trop Med Hyg **74:**539-541.
43. **Schrire L.** 1951. Macular changes in rift valley fever. S Afr Med J **25:**926-930.
44. **Al-Hazmi A, Al-Rajhi AA, Abboud EB, Ayoola EA, Al-Hazmi M, Saadi R, Ahmed N.** 2005. Ocular complications of Rift Valley fever outbreak in Saudi Arabia. Ophthalmology **112:**313-318.
45. **Ayoub M, Barhoma G, Zaghlol I.** 1978. Ocular manifestations of Rift Valley Fever. Bull Ophthalmol Soc Egypt **71:**125-133.
46. **Siam AL, Gharbawi KF, Meegan JM.** 1978. Ocular complications of Rift Valley fever. J Egypt Public Health Assoc **53:**185-186.
47. **Freed I.** 1951. Rift valley fever in man, complicated by retinal changes and loss of vision. S Afr Med J **25:**930-932.
48. **Olive MM, Goodman SM, Reynes JM.** 2012. The role of wild mammals in the maintenance of rift valley Fever virus. J Wildl Dis **48:**241-266.
49. **Pepin M, Bouloy M, Bird BH, Kemp A, Paweska J.** 2010. Rift Valley fever virus (Bunyaviridae: Phlebovirus): an update on pathogenesis, molecular epidemiology, vectors, diagnostics and prevention. Vet Res **41:**61.
50. **Bird BH, Ksiazek TG, Nichol ST, Maclachlan NJ.** 2009. Rift Valley fever virus. J Am Vet Med Assoc **234:**883-893.
51. **Linthicum KJ, Anyamba A, Tucker CJ, Kelley PW, Myers MF, Peters CJ.** 1999. Climate and satellite indicators to forecast Rift Valley fever epidemics in Kenya. Science **285:**397-400.
52. **Hoogstraal H, Meegan JM, Khalil GM, Adham FK.** 1979. The Rift Valley fever epizootic in Egypt 1977-78. 2. Ecological and entomological studies. Trans R Soc Trop Med Hyg **73:**624-629.
53. **Bird BH, Khristova ML, Rollin PE, Ksiazek TG, Nichol ST.** 2007. Complete genome analysis of 33 ecologically and biologically diverse Rift Valley fever virus strains reveals widespread virus movement and low genetic diversity due to recent common ancestry. J Virol **81:**2805-2816.
54. **Aradaib IE, Erickson BR, Elageb RM, Khristova ML, Carroll SA, Elkhidir IM, Karsany ME, Karrar AE, Elbashir MI, Nichol ST.** 2013. Rift Valley fever, Sudan, 2007 and 2010. Emerg Infect Dis **19:**246-253.
55. **LaBeaud AD, Cross PC, Getz WM, Glinka A, King CH.** 2011. Rift Valley fever virus infection in African buffalo (Syncerus caffer) herds in rural South Africa: evidence of interepidemic transmission. Am J Trop Med Hyg **84:**641-646.
56. **Chambers PG, Swanepoel R.** 1980. Rift valley fever in abattoir workers. Cent Afr J Med **26:**122-126.
57. **Arishi HM, Aqeel AY, Al Hazmi MM.** 2006. Vertical transmission of fatal Rift Valley fever in a newborn. Ann Trop Paediatr **26:**251-253.
58. **Abdel-Aziz AA, Meegan JM, Laughlin LW.** 1980. Rift Valley fever as a possible cause of human abortions. Trans R Soc Trop Med Hyg **74:**685-686.
59. **Psylvia Léger, Tetard M, Youness B, Nicole Cordes , Ronan Nicolas Rouxel, Marie Flamand, Lozach P-Y.** 2016. Differential use of the C-type lectins L-SIGN and DC-SIGN for phlebovirus endocytosis Traffic **17:**639-656.
60. **Lozach PY, Kuhbacher A, Meier R, Mancini R, Bitto D, Bouloy M, Helenius A.** 2011. DC-SIGN as a Receptor for Phleboviruses. Cell Host Microbe **10:**75-88.
61. **Dessau M, Modis Y.** 2013. Crystal structure of glycoprotein C from Rift Valley fever virus. Proc Natl Acad Sci U S A **110:**1696-1701.
62. **Freiberg AN, Sherman MB, Morais MC, Holbrook MR, Watowich SJ.** 2008. Three-dimensional organization of Rift Valley fever virus revealed by cryoelectron tomography. J Virol **82:**10341-10348.

63. **Terasaki K, Won S, Makino S.** 2013. The C-terminal region of Rift Valley fever virus NSm protein targets the protein to the mitochondrial outer membrane and exerts anti-apoptotic function. J Virol **87:**676-682.
64. **Won S, Ikegami T, Peters CJ, Makino S.** 2006. NSm and 78-kilodalton proteins of Rift Valley fever virus are nonessential for viral replication in cell culture. J Virol **80:**8274-8278.
65. **Gerrard SR, Bird BH, Albarino CG, Nichol ST.** 2007. The NSm proteins of Rift Valley fever virus are dispensable for maturation, replication and infection. Virology **359:**459-465.
66. **Kakach LT, Suzich JA, Collett MS.** 1989. Rift Valley fever virus M segment: phlebovirus expression strategy and protein glycosylation. Virology **170:**505-510.
67. **Patterson JL, Holloway B, Kolakofsky D.** 1984. La Crosse virions contain a primer-stimulated RNA polymerase and a methylated cap-dependent endonuclease. J Virol **52:**215-222.
68. **Bouloy M, Weber F.** 2010. Molecular biology of rift valley Fever virus. Open Virol J **4:**8-14.
69. **Iben S, Tschochner H, Bier M, Hoogstraten D, Hozák P, Egly J-M, I G.** 2002. TFIIH plays an essential role in RNA polymerase I transcription. Cell **41:**297–306.
70. **Lu H, Zawel L, Fisher L, Egly JM, Reinberg D.** 1992. Human general transcription factor IIH phosphorylates the C-terminal domain of RNA polymerase II. Nature **358:**641-645.
71. **Ikegami T, Narayanan K, Won S, Kamitani W, Peters CJ, Makino S.** 2009. Dual functions of Rift Valley fever virus NSs protein: inhibition of host mRNA transcription and post-transcriptional downregulation of protein kinase PKR. Ann N Y Acad Sci **1171 Suppl 1:**E75-85.
72. **Le May N, Mansuroglu Z, Leger P, Josse T, Blot G, Billecocq A, Flick R, Jacob Y, Bonnefoy E, Bouloy M.** 2008. A SAP30 complex inhibits IFN-beta expression in Rift Valley fever virus infected cells. PLoS Pathog **4:**e13.
73. **Compe E, Egly J-M.** 2012. TFIIH: when transcription met DNA repair. Nature Reviews: Molecular Cell Biology **13:**343-354.
74. **Le May N, Dubaele S, Proietti De Santis L, Billecocq A, Bouloy M, Egly JM.** 2004. TFIIH transcription factor, a target for the Rift Valley hemorrhagic fever virus. Cell **116:**541-550.
75. **Kalveram B, Lihoradova O, Ikegami T.** 2011. NSs Protein of Rift Valley Fever Virus Promotes Post-Translational Downregulation of the TFIIH Subunit p62. J Virol **85:**6234-6243.
76. **Kainulainen M, Lau S, Samuel CE, Hornung V, Weber F.** 2016. NSs virulence factor of Rift Valley fever virus engages the F-box proteins FBXW11 and ♌-TRCP1 to degrade the antiviral protein kinase PKR. Journal of Virology doi:doi:10.1128/JVI.00016-16.
77. **Ikegami T, Narayanan K, Won S, Kamitani W, Peters CJ, Makino S.** 2009. Rift Valley fever virus NSs protein promotes post-transcriptional downregulation of protein kinase PKR and inhibits eIF2alpha phosphorylation. PLoS Pathog **5:**e1000287.
78. **Habjan M, Pichlmair A, Elliott RM, Overby AK, Glatter T, Gstaiger M, Superti-Furga G, Unger H, Weber F.** 2009. NSs protein of rift valley fever virus induces the specific degradation of the double-stranded RNA-dependent protein kinase. J Virol **83:**4365-4375.
79. **Garcia MA, Meurs EF, Esteban M.** 2007. The dsRNA protein kinase PKR: virus and cell control. Biochimie **89:**799-811.
80. **Mudhasani R, Tran JP, Retterer C, Kota KP, Whitehouse CA, Bavari S.** 2016. Protein Kinase R Degradation Is Essential for Rift Valley Fever Virus Infection and Is Regulated by SKP1-CUL1-F-box (SCF)FBXW11-NSs E3 Ligase. PLoS Pathog **12:**e1005437.
81. **Billecocq A, Spiegel M, Vialat P, Kohl A, Weber F, Bouloy M, Haller O.** 2004. NSs protein of Rift Valley fever virus blocks interferon production by inhibiting host gene transcription. J Virol **78:**9798-9806.
82. **Yadani FZ, Kohl A, Prehaud C, Billecocq A, Bouloy M.** 1999. The carboxy-terminal acidic domain of Rift Valley Fever virus NSs protein is essential for the formation of filamentous structures but not for the nuclear localization of the protein. J Virol **73:**5018-5025.

83. **Swanepoel R, Blackburn NK.** 1977. Demonstration of nuclear immunofluorescence in Rift Valley fever infected cells. J Gen Virol **34:**557-561.
84. **Gray KK, Worthy MN, Juelich TL, Agar SL, Poussard A, Ragland D, Freiberg AN, Holbrook MR.** 2012. Chemotactic and inflammatory responses in the liver and brain are associated with pathogenesis of rift valley Fever virus infection in the mouse. PLoS Negl Trop Dis **6:**e1529.
85. **Head JA, Kalveram B, Ikegami T.** 2012. Functional analysis of Rift Valley fever virus NSs encoding a partial truncation. PLoS ONE **7:**e45730.
86. **Won S, Ikegami T, Peters CJ, Makino S.** 2007. NSm protein of Rift Valley fever virus suppresses virus-induced apoptosis. J Virol **81:**13335-13345.
87. **Narayanan A, Popova T, Turell M, Kidd J, Chertow J, Popov SG, Bailey C, Kashanchi F, Kehn-Hall K.** 2011. Alteration in superoxide dismutase 1 causes oxidative stress and p38 MAPK activation following RVFV infection. PLoS ONE **6:**e20354.
88. **Won S, Ikegami T, Peters CJ, Makino S.** 2006. NSm and 78-Kilodalton proteins of Rift Valley fever virus are nonessential for viral replication in cell culture. Journal of Virology **80:**8274-8278.
89. **Won S, Ikegami T, Peters CJ, Makino S.** 2007. NSm protein of Rift Valley fever virus suppresses virus-induced apoptosis. Journal of Virology **81:**13335-13345.
90. **Bird BH, Albarino CG, Nichol ST.** 2007. Rift Valley fever virus lacking NSm proteins retains high virulence in vivo and may provide a model of human delayed onset neurologic disease. Virology **362:**10-15.
91. **Nishiyama Shoko SO, Lokugamage N, Hill TE,Juelich TL, Zhang L, Smith JK, Perez D, Gong B, Freiberg AN, Ikegami T.** 2016. Attenuation of pathogenic Rift Valley fever virus strain through the chimeric S-segment encoding sandfly fever phlebovirus NSs or a dominant-negative PKR. Virulence **1**.
92. **Kreher F, Tamietti C, Gommet C, Guillemot L, Ermonval M, Failloux AB, Panthier JJ, Bouloy M, Flamand M.** 2014. The Rift Valley fever accessory proteins NSm and P78/NSm-Gn are determinants of virus propagation in vertebrate and invertebrate hosts. Emerg Microbe Infect **3:**e71.
93. **Crabtree MB, Kent Crockett RJ, Bird BH, Nichol ST, Erickson BR, Biggerstaff BJ, Horiuchi K, Miller BR.** 2012. Infection and transmission of Rift Valley fever viruses lacking the NSs and/or NSm genes in mosquitoes: potential role for NSm in mosquito infection. PLoS Negl Trop Dis **6:**e1639.
94. **Kading RC, Crabtree MB, Bird BH, Nichol ST, Erickson BR, Horiuchi K, Biggerstaff BJ, Miller BR.** 2014. Deletion of the NSm virulence gene of Rift Valley fever virus inhibits virus replication in and dissemination from the midgut of Aedes aegypti mosquitoes. PLoS Negl Trop Dis **8:**e2670.
95. **Thomas E, Ghany MG, Liang TJ.** 2012. The application and mechanism of action of ribavirin in therapy of hepatitis C. Antiviral Chemistry & Chemotherapy **23**.
96. **Bouloy M, Flick R.** 2009. Reverse genetics technology for Rift Valley fever virus: current and future applications for the development of therapeutics and vaccines. Antiviral Res **84:**101-118.
97. **Leyssen P, Balzarini J, De Clercq E, Neyts J.** 2005. The predominant mechanism by which ribavirin exerts its antiviral activity in vitro against flaviviruses and paramyxoviruses is mediated by inhibition of IMP dehydrogenase. J Virol **79:**1943-1947.
98. **Morrill JC, Jennings GB, Cosgriff TM, Gibbs PH, Peters CJ.** 1989. Prevention of Rift Valley fever in rhesus monkeys with interferon-alpha. Rev Infect Dis **11 Suppl 4:**S815-825.
99. **Kende M, Alving CR, Rill WL, Swartz GM, Jr., Canonico PG.** 1985. Enhanced efficacy of liposome-encapsulated ribavirin against Rift Valley fever virus infection in mice. Antimicrob Agents Chemother **27:**903-907.

100. **Kende M, Lupton HW, Rill WL, Levy HB, Canonico PG.** 1987. Enhanced therapeutic efficacy of poly(ICLC) and ribavirin combinations against Rift Valley fever virus infection in mice. Antimicrob Agents Chemother **31:**986-990.
101. **Manns MP, Wedemeyer H, Cornberg M.** 2006. Treating viral hepatitis C: efficacy, side effects, and complications. Gut **55:**1350-1359.
102. **Narayanan A, Kehn-Hall K, Senina S, Lundberg L, Van Duyne R, Guendel I, Das R, Baer A, Bethel L, Turell M, Hartman AL, Das B, Bailey C, Kashanchi F.** 2012. Curcumin inhibits rift valley Fever virus replication in human cells. J Biol Chem **287:**33198-33214.
103. **Aman MJ, Kinch MS, Warfield K, Warren T, Yunus A, Enterlein S, Stavale E, Wang P, Chang S, Tang Q, Porter K, Goldblatt M, Bavari S.** 2009. Development of a broad-spectrum antiviral with activity against Ebola virus. Antiviral Res **83:**245-251.
104. **Furuta Y TK, Kuno-Maekawa M, Sangawa H, Uehara S, Kozaki K, Nomura N, Egawa H, Shiraki K.** 2005. Mechanism of action of T-705 against influenza virus. Antimicrob Agents Chemother **49:**981–986.
105. **Jin Z SL, Rajwanshi VK, Kim B, Deval J.** 2013. The ambiguous base-pairing and high substrate efficiency of T-705 (Favipiravir) Ribofuranosyl 5'-triphosphate towards influenza A virus polymerase. PLoS One **8:**e68347.
106. **Sangawa H KT, Nishikawa H, Yoshida A, Takahashi K, Nomura N, Furuta Y.** 2013. Mechanism of Action of T-705 Ribosyl Triphosphate against Influenza Virus RNA Polymerase. Antimicrob Agents Chemother **57:**5202–5208.
107. **Scharton D, Bailey KW, Vesta Z, Westovera JB, Kumakia Y, Van Wetterea A, Furutae Y, Gowen BB.** 2014. Favipiravir (T-705) protects against peracute Rift Valley fever virus infection and reduces delayed-onset neurologic disease observed with ribavirin treatment. Antiviral Res **104:**84–92.
108. **Gowen BB, Wong MH, Jung KH, Sanders AB, Mendenhall M, Bailey KW, Furuta Y, Sidwell RW.** 2007. In vitro and in vivo activities of T-705 against arenavirus and bunyavirus infections. Antimicrob Agents Chemother **51:**3168-3176.
109. **Caroline AL PD, Bethel LM, Oury TD, Reed DS, Hartman AL.** 2014. Broad Spectrum Antiviral Activity of Favipiravir (T-705): Protection from Highly Lethal Inhalational Rift Valley Fever. PLoS Negl Trop Dis **8:**e2790.
110. **Gowen BB, Wong MH, Jung KH, Smee DF, Morrey JD, Furuta Y.** 2010. Efficacy of favipiravir (T-705) and T-1106 pyrazine derivatives in phlebovirus disease models. Antiviral Res **86:**121-127.
111. **Wolf MC, Freiberg AN, Zhang T, Akyol-Ataman Z, Grock A, Hong PW, Li J, Watson NF, Fang AQ, Aguilar HC, Porotto M, Honko AN, Damoiseaux R, Miller JP, Woodson SE, Chantasirivisal S, Fontanes V, Negrete OA, Krogstad P, Dasgupta A, Moscona A, Hensley LE, Whelan SP, Faull KF, Holbrook MR, Jung ME, Lee B.** 2010. A broad-spectrum antiviral targeting entry of enveloped viruses. Proc Natl Acad Sci U S A **107:**3157-3162.
112. **Koehler JW SJ, Ripoll DR, Spik KW, Taylor SL,Badger CV, Grant RJ, Ogg MM, Wallqvist A, Guttieri MC, Robert F. Garry3 CSS.** 2013. A Fusion-Inhibiting Peptide against Rift Valley Fever Virus Inhibits Multiple, Diverse Viruses. PLoS Negl Trop Dis **7:**e2430.
113. **Garry CE, Garry RF.** 2004. Proteomics computational analyses suggest that the carboxyl terminal glycoproteins of Bunyaviruses are class II viral fusion protein (beta-penetrenes). Theor Biol Med Model **1:**10.
114. **Niklasson BS, Meadors GF, Peters CJ.** 1984. Active and passive immunization against Rift Valley fever virus infection in Syrian hamsters. Acta Pathol Microbiol Immunol Scand [C] **92:**197-200.
115. **Smithburn KC.** 1949. Rift Valley fever; the neurotropic adaptation of the virus and the experimental use of this modified virus as a vaccine. Br J Exp Pathol **30:**1-16.

116. **WHO.** 1983. The use of veterinary vaccines for prevention and control of Rift Valley fever: memorandum from a WHO/FAO meeting. Bull World Health Organ **61:**261-268.
117. **Muller R, Saluzzo JF, Lopez N, Dreier T, Turell M, Smith J, Bouloy M.** 1995. Characterization of clone 13, a naturally attenuated avirulent isolate of Rift Valley fever virus, which is altered in the small segment. Am J Trop Med Hyg **53:**405-411.
118. **Bouloy M, Janzen C, Vialat P, Khun H, Pavlovic J, Huerre M, Haller O.** 2001. Genetic evidence for an interferon-antagonistic function of rift valley fever virus nonstructural protein NSs. J Virol **75:**1371-1377.
119. **Dungu B, Louw I, Lubisi A, Hunter P, von Teichman BF, Bouloy M.** 2010. Evaluation of the efficacy and safety of the Rift Valley Fever Clone 13 vaccine in sheep. Vaccine **28:**4581-4587.
120. **von Teichman B, Engelbrecht A, Zulu G, Dungu B, Pardini A, Bouloy M.** 2011. Safety and efficacy of Rift Valley fever Smithburn and Clone 13 vaccines in calves. Vaccine **29:**5771-5777.
121. **Fernandez JC, Billecocq A, Durand JP, Cetre-Sossah C, Cardinale E, Marianneau P, Pepin M, Tordo N, Bouloy M.** 2012. The Nonstructural Protein NSs Induces a Variable Antibody Response in Domestic Ruminants Naturally Infected with Rift Valley Fever Virus. Clin Vaccine Immunol **19:**5-10.
122. **FAO.** 2015. The last hurtles toward Rift Valley Fever control. Report on the Ad hoc workshop on the current state of Rift Valley fever vaccine and diagnostic development - Rome, 5-7 March 2014 **FAO Animal Production and Health:**Rome. Italy.
123. **Makoschey B vKE, Hubers WR, Vrijenhoek MP, Smit M, Wichgers Schreur PJ, Kortekaas J, Moulin V.** 2016. Rift Valley Fever Vaccine Virus Clone 13 Is Able to Cross the Ovine Placental Barrier Associated with Foetal Infections, Malformations, and Stillbirths. PLoS Negl Trop Dis **10:**e0004550.
124. **Ikegami T, Won S, Peters CJ, Makino S.** 2006. Rescue of infectious rift valley fever virus entirely from cDNA, analysis of virus lacking the NSs gene, and expression of a foreign gene. J Virol **80:**2933-2940.
125. **Habjan M, Penski N, Spiegel M, Weber F.** 2008. T7 RNA polymerase-dependent and -independent systems for cDNA-based rescue of Rift Valley fever virus. J Gen Virol **89:**2157-2166.
126. **Billecocq A, Gauliard N, Le May N, Elliott RM, Flick R, Bouloy M.** 2008. RNA polymerase I-mediated expression of viral RNA for the rescue of infectious virulent and avirulent Rift Valley fever viruses. Virology **378:**377-384.
127. **Bird BH, Albarino CG, Hartman AL, Erickson BR, Ksiazek TG, Nichol ST.** 2008. Rift valley fever virus lacking the NSs and NSm genes is highly attenuated, confers protective immunity from virulent virus challenge, and allows for differential identification of infected and vaccinated animals. J Virol **82:**2681-2691.
128. **Bird BH, Maartens LH, Campbell S, Erasmus BJ, Erickson BR, Dodd KA, Spiropoulou CF, Cannon D, Drew CP, Knust B, McElroy AK, Khristova ML, Albarino CG, Nichol ST.** 2011. Rift Valley Fever Virus Vaccine Lacking the NSs and NSm Genes Is Safe, Nonteratogenic, and Confers Protection from Viremia, Pyrexia, and Abortion following Challenge in Adult and Pregnant Sheep. J Virol **85:**12901-12909.
129. **McElroy AK, Albarino CG, Nichol ST.** 2009. Development of a RVFV ELISA that can distinguish infected from vaccinated animals. Virol J **6:**125.
130. **Dodd KA, McElroy AK, Jones TL, Zaki SR, Nichol ST, Spiropoulou CF.** 2014. Rift Valley fever virus Encephalitis is Associated with an Ineffective Systemic Immune Response and Activated T-cell Infiltration into the CNS in an Immunocompetent Mouse Model. PLoS Negl Trop Dis **8**.
131. **Caplen H, Peters CJ, Bishop DH.** 1985. Mutagen-directed attenuation of Rift Valley fever virus as a method for vaccine development. J Gen Virol **66 (Pt 10):**2271-2277.

132. **Takehara K, Min MK, Battles JK, Sugiyama K, Emery VC, Dalrymple JM, Bishop DH.** 1989. Identification of mutations in the M RNA of a candidate vaccine strain of Rift Valley fever virus. Virology **169:**452-457.
133. **Vialat P, Muller R, Vu TH, Prehaud C, Bouloy M.** 1997. Mapping of the mutations present in the genome of the Rift Valley fever virus attenuated MP12 strain and their putative role in attenuation. Virus Res **52:**43-50.
134. **Ikegami T, Hill TE, Smith JK, Zhang L, Juelich TL, Gong B, Slack OAL, Ly HJ, Lokugamage N, AN. F.** 2015. Rift Valley fever virus MP-12 vaccine is fully attenuated by a combination of partial attenuations in the S, M, and L segments. J Virol **89:**7262–7276.
135. **Hunter P, Erasmus BJ, Vorster JH.** 2002. Teratogenicity of a mutagenised Rift Valley fever virus (MVP 12) in sheep. Onderstepoort J Vet Res **69:**95-98.
136. **Morrill JC, Laughlin RC, Lokugamage N, Pugh R, Sbrana E, Weise WJ, Adams LG, Makino S, Peters CJ.** 2013. Safety and immunogenicity of recombinant Rift Valley fever MP-12 vaccine candidates in sheep. Vaccine **31:**559-565.
137. **Morrill JC, Carpenter L, Taylor D, Ramsburg HH, Quance J, Peters CJ.** 1991. Further evaluation of a mutagen-attenuated Rift Valley fever vaccine in sheep. Vaccine **9:**35-41.
138. **Morrill JC, Jennings GB, Caplen H, Turell MJ, Johnson AJ, Peters CJ.** 1987. Pathogenicity and immunogenicity of a mutagen-attenuated Rift Valley fever virus immunogen in pregnant ewes. Am J Vet Res **48:**1042-1047.
139. **Morrill JC, Mebus CA, Peters CJ.** 1997. Safety of a mutagen-attenuated Rift Valley fever virus vaccine in fetal and neonatal bovids. Am J Vet Res **58:**1110-1114.
140. **Morrill JC, Mebus CA, Peters CJ.** 1997. Safety and efficacy of a mutagen-attenuated Rift Valley fever virus vaccine in cattle. Am J Vet Res **58:**1104-1109.
141. **Lihoradova O, Kalveram B, Indran SV, Lokugamage N, Juelich TL, Hill TE, Tseng CT, Gong B, Fukushi S, Morikawa S, Freiberg AN, Ikegami T.** 2012. The dominant-negative inhibition of double-stranded RNA-dependent protein kinase PKR increases the efficacy of Rift Valley fever virus MP-12 vaccine. J Virol **86:**7650-7661.
142. **Ikegami T, Makino S.** 2009. Rift valley fever vaccines. Vaccine **27 Suppl 4:**D69-72.
143. **Brennan B, Welch SR, McLees A, Elliott RM.** 2011. Creation of a recombinant Rift Valley fever virus with a two-segmented genome. J Virol **85:**10310-10318.
144. **Randall R, Gibbs CJ, Jr., Aulisio CG, Binn LN, Harrison VR.** 1962. The development of a formalin-killed Rift Valley fever virus vaccine for use in man. J Immunol **89:**660-671.
145. **Eddy GA, Peters CJ, Meadors G, Cole Jr FE.** 1981. Rift Valley fever vaccine for humans. ContrEpidemBiostatist **3:**124-141.
146. **Niklasson B.** 1982. Rift Valley fever virus vaccine trial: study of side-effects in humans. Scand J Infect Dis **14:**105-109.
147. **Mansfield KL BA, McElhinney L, Johnson N, Horton DL, Hernández-Triana LM, Fooks AR.** 2015. Rift Valley fever virus: A review of diagnosis and vaccination, and implications for emergence in Europe. Vaccine **33:**5520-5531.
148. **Niklasson B, Eitrem R.** 1985. Sandfly fever among Swedish UN troops in Cyprus. Lancet **1:**1212.
149. **Pittman PR, Liu CT, Cannon TL, Makuch RS, Mangiafico JA, Gibbs PH, Peters CJ.** 2000. Immunogenicity of an inactivated Rift Valley fever vaccine in humans: a 12-year experience. Vaccine **18:**181-189.
150. **Kark JD, Aynor Y, Peters CJ.** 1985. A Rift Valley fever vaccine trial: 2. Serological response to booster doses with a comparison of intradermal versus subcutaneous injection. Vaccine **3:**117-122.
151. **Kamal SA.** 2009. Pathological studies on postvaccinal reactions of Rift Valley fever in goats. Virol J **6:**94.

152. **de Boer SM, Kortekaas J, Antonis AF, Kant J, van Oploo JL, Rottier PJ, Moormann RJ, Bosch BJ.** 2010. Rift Valley fever virus subunit vaccines confer complete protection against a lethal virus challenge. Vaccine **28:**2330-2339.
153. **Kortekaas J, Antonis AF, Kant J, Vloet RP, Vogel A, Oreshkova N, de Boer SM, Bosch BJ, Moormann RJ.** 2012. Efficacy of three candidate Rift Valley fever vaccines in sheep. Vaccine **30:**3423-3429.
154. **Faburay B LM, McVey DS, Wilson W, Morozov I, Young A, Richt JA.** 2014. A glycoprotein subunit vaccine elicits a strong Rift Valley fever virus neutralizing antibody response in sheep. Vector Borne Zoonotic Dis **14:**746-756.
155. **Roldao A, Mellado MC, Castilho LR, Carrondo MJ, Alves PM.** 2010. Virus-like particles in vaccine development. Expert Rev Vaccines **9:**1149-1176.
156. **Liu L, Celma CC, Roy P.** 2008. Rift Valley fever virus structural proteins: expression, characterization and assembly of recombinant proteins. Virol J **5:**82.
157. **Mandell RB, Koukuntla R, Mogler LJ, Carzoli AK, Holbrook MR, Martin BK, Vahanian N, Link CJ, Flick R.** 2010. Novel suspension cell-based vaccine production systems for Rift Valley fever virus-like particles. J Virol Methods **169:**259-268.
158. **Koukuntla R, Mandell RB, Flick R.** 2012. Virus-like particle-based countermeasures against Rift Valley fever virus. Zoonoses Public Health **59 Suppl 2:**142-150.
159. **Mandell RB, Koukuntla R, Mogler LJ, Carzoli AK, Freiberg AN, Holbrook MR, Martin BK, Staplin WR, Vahanian NN, Link CJ, Flick R.** 2009. A replication-incompetent Rift Valley fever vaccine: chimeric virus-like particles protect mice and rats against lethal challenge. Virology **397:**187-198.
160. **Naslund J, Lagerqvist N, Habjan M, Lundkvist A, Evander M, Ahlm C, Weber F, Bucht G.** 2009. Vaccination with virus-like particles protects mice from lethal infection of Rift Valley Fever Virus. Virology **385:**409-415.
161. **Habjan M, Penski N, Wagner V, Spiegel M, Overby AK, Kochs G, Huiskonen JT, Weber F.** 2009. Efficient production of Rift Valley fever virus-like particles: The antiviral protein MxA can inhibit primary transcription of bunyaviruses. Virology **385:**400-408.
162. **Pichlmair A, Habjan M, Unger H, Weber F.** 2010. Virus-like particles expressing the nucleocapsid gene as an efficient vaccine against Rift Valley fever virus. Vector Borne Zoonotic Dis **10:**701-703.
163. **Gorchakov R, Volkova E, Yun N, Petrakova O, Linde NS, Paessler S, Frolova E, Frolov I.** 2007. Comparative analysis of the alphavirus-based vectors expressing Rift Valley fever virus glycoproteins. Virology **366:**212-225.
164. **Heise MT, Whitmore A, Thompson J, Parsons M, Grobbelaar AA, Kemp A, Paweska JT, Madric K, White LJ, Swanepoel R, Burt FJ.** 2009. An alphavirus replicon-derived candidate vaccine against Rift Valley fever virus. Epidemiol Infect **137:**1309-1318.
165. **Holman DH, Penn-Nicholson A, Wang D, Woraratanadharm J, Harr MK, Luo M, Maher EM, Holbrook MR, Dong JY.** 2009. A complex adenovirus-vectored vaccine against Rift Valley fever virus protects mice against lethal infection in the presence of preexisting vector immunity. Clin Vaccine Immunol **16:**1624-1632.
166. **Wang D, Hevey M, Juompan LY, Trubey CM, Raja NU, Deitz SB, Woraratanadharm J, Luo M, Yu H, Swain BM, Moore KM, Dong JY.** 2006. Complex adenovirus-vectored vaccine protects guinea pigs from three strains of Marburg virus challenges. Virology **353:**324-332.
167. **Park MS, Garcia-Sastre A, Cros JF, Basler CF, Palese P.** 2003. Newcastle disease virus V protein is a determinant of host range restriction. J Virol **77:**9522-9532.
168. **Huang Z, Krishnamurthy S, Panda A, Samal SK.** 2001. High-level expression of a foreign gene from the most 3'-proximal locus of a recombinant Newcastle disease virus. J Gen Virol **82:**1729-1736.

169. **Peeters BP, de Leeuw OS, Koch G, Gielkens AL.** 1999. Rescue of Newcastle disease virus from cloned cDNA: evidence that cleavability of the fusion protein is a major determinant for virulence. J Virol **73:**5001-5009.
170. **Romer-Oberdorfer A, Mundt E, Mebatsion T, Buchholz UJ, Mettenleiter TC.** 1999. Generation of recombinant lentogenic Newcastle disease virus from cDNA. J Gen Virol **80 (Pt 11):**2987-2995.
171. **Kortekaas J, Dekker A, de Boer SM, Weerdmeester K, Vloet RP, de Wit AA, Peeters BP, Moormann RJ.** 2010. Intramuscular inoculation of calves with an experimental Newcastle disease virus-based vector vaccine elicits neutralizing antibodies against Rift Valley fever virus. Vaccine **28:**2271-2276.
172. **Spik K, Shurtleff A, McElroy AK, Guttieri MC, Hooper JW, SchmalJohn C.** 2006. Immunogenicity of combination DNA vaccines for Rift Valley fever virus, tick-borne encephalitis virus, Hantaan virus, and Crimean Congo hemorrhagic fever virus. Vaccine **24:**4657-4666.
173. **Lagerqvist N, Naslund J, Lundkvist A, Bouloy M, Ahlm C, Bucht G.** 2009. Characterisation of immune responses and protective efficacy in mice after immunisation with Rift Valley Fever virus cDNA constructs. Virol J **6:**6.
174. **Bhardwaj N, Heise MT, Ross TM.** 2010. Vaccination with DNA plasmids expressing Gn coupled to C3d or alphavirus replicons expressing gn protects mice against Rift Valley fever virus. PLoS Negl Trop Dis **4:**e725.
175. **Xu W, Watts DM, Costanzo MC, Tang X, Venegas LA, Jiao F, Sette A, Sidney J, Sewell AK, Wooldridge L, Makino S, Morrill JC, Peters CJ, Kan-Mitchell J.** 2013. The nucleocapsid protein of Rift Valley fever virus is a potent human CD8+ T cell antigen and elicits memory responses. PLoS ONE **8:**e59210.
176. **Jansen van Vuren P, Tiemessen CT, Paweska JT.** 2011. Anti-nucleocapsid protein immune responses counteract pathogenic effects of rift valley Fever virus infection in mice. PLoS ONE **6:**e25027.
177. **Boshra H, Lorenzo G, Rodriguez F, Brun A.** 2011. A DNA vaccine encoding ubiquitinated Rift Valley fever virus nucleoprotein provides consistent immunity and protects IFNAR(-/-) mice upon lethal virus challenge. Vaccine **15:**4469-4475.
178. **Dodd KA, Bird BH, Metcalfe MG, Nichol ST, Albarino CG.** 2012. Single-Dose Immunization with Virus Replicon Particles Confers Rapid Robust Protection against Rift Valley Fever Virus Challenge. J Virol **86:**4204-4212.
179. **Kortekaas J, Oreshkova N, Cobos-Jimenez V, Vloet RP, Potgieter CA, Moormann RJ.** 2011. Creation of a non-spreading Rift Valley fever virus. J Virol **85:**12622-12630.
180. **Gowen BB, Bailey KW, Scharton D, Vest Z, Westover JB, Skirpstunas R, Ikegami T.** 2013. Post-exposure vaccination with MP-12 lacking NSs protects mice against lethal Rift Valley fever virus challenge. Antiviral Res **98:**135-143.
181. **Stanley Pamela , Harry Schachter, Taniguchi N.** 2009. N-Glycans. *In* Varki A CR, Esko JD, et al. (ed), Essentials of Glycobiology, 2nd ed. Cold Spring Harbor Laboratory Press, Cold Spring Harbor, NY, USA.
182. **Kelleher DJ GR.** 2006. An evolving view of the eukaryotic oligosaccharyltransferase. Glycobiology **16:**47R-62R.
183. **Yan Q LW.** 2002. Studies on the function of oligosaccharyl transferase subunits. Stt3p is directly involved in the glycosylation process. J Biol Chem **277:**47692-47700.
184. **Shrimal S, Cherepanova NA, Gilmore R.** 2014. Cotranslational and posttranslocational N-glycosylation of proteins in the endoplasmic reticulum. Seminars in Cell & Developmental Biology doi:10.1016/j.semcbd.2014.11.005.

185. **Shibatani T DL, McCormack AL, Frueh K, Skach WR.** 2005. Proteomic analysis of mammalian oligosaccharyltransferase reveals multiple subcomplexes that contain Sec61, TRAP, and two potential new subunits. Biochemistry **44:**5982-5992.
186. **Kakach L, Wasmoen TL, Collett MS.** 1988. Rift Valley fever virus M segment: use of recombinant vaccinia viruses to study *Phlebovirus* gene expression. Journal of Virology **62:**826-833.
187. **Kakach L, Suzich JA, Collett MS.** 1989. Rift Valley fever virus M Segment: Phlebovirus expression strategy and protein glycosylation. Virology **170:**505-510.
188. **Collett MS, Purchio AF, Keegan K, Frazier S, Hays W, Anderson DK, Parker MD, Schmaljohn C, Schmidt J, Dalrymple JM.** 1985. Complete nucleotide sequence of the M RNA segment of Rift Valley fever virus. Virology **144:**228-245.
189. **Geijtenbeek TB, Torensma R, van Vliet SJ, van Duijnhoven GC, Adema GJ, van Kooyk Y, CG F.** 2000. Identification of DC-SIGN, a novel dendritic cell-specific ICAM-3 receptor that supports primary immune responses. Cell **100:**575-585.
190. **Figdor CG, van Kooyk Y, Adema GJ.** 2002. C-type lectin receptors on dendritic cells and Langerhans cells. Nat Rev Immunol **2:**77-84.
191. **Soilleux EJ, Barten R, Trowsdale J.** 2000. DC-SIGN; a related gene, DC-SIGNR; and CD23 form a cluster on 19p13. J Immunol **165:**2937–2942.
192. **Soilleux EJ, Morris LS, Leslie G, Chehimi J, Luo Q, Levroney E, Trowsdale J, Montaner LJ, Doms RW, Weissman D, Coleman N, Lee B.** 2002. Constitutive and induced expression of DC-SIGN on dendritic cell and macrophage subpopulations in situ and in vitro. Journal of Leukocyte Biology **71:**445-457.
193. **Soilleux EJ.** 2003. DC-SIGN (dendritic cell-specific ICAM-grabbing nonintegrin)and DC-SIGN-related (DC-SIGNR): friend or foe? Clin Sci (Lond) **104:**437–446.
194. **Van Kooyk Y, Geijtenbeek TB.** 2003. DC-SIGN: escape mechanism for pathogens. Nat Rev Immunol **3:**697–709.
195. **Schwartz AJ, Alvarez X, Lackner AA.** 2002. Distribution and immunophenotype of DC-SIGN-expressing cells in SIV-infected and uninfected macaques. AIDS Res Hum Retroviruses **18:**1021–1029.
196. **Guo Y, Feinberg H, Conroy E, et. a.** 2004. Structural basis for distinct ligandbinding and targeting properties of the receptors DC-SIGN and DC-SIGNR. NatStruct Mol Biol **11:**591–598.
197. **Van Liempt E, Imberty A, Bank CM, et. a.** 2004. Molecular basis of the differences in binding properties of the highly related C-type lectins DC-SIGN and L-SIGN to Lewis X trisaccharide and schistosoma mansoni egg antigens. J Biol Chem **279:**161-133.
198. **Lozach PY, Burleigh L, Staropoli I, . ae.** 2005. Dendritic cell-specific intercellular adhesion molecule 3-grabbing non-integrin (DC-SIGN)-mediated enhancement of Dengue virus infection is independent of DC-SIGN internalization signals. J Biol Chem **280:**698–623.
199. **Feinberg H, Guo Y, Mitchell DA, Drickamer K, Weis WI.** 2005. Extended neck regions stabilize tetramers of the receptors DC-SIGN and DCSIGNR. J Biol Chem **280:**1327–1335.
200. **Mitchell DA, Fadden AJ, Drickamer K.** 2001. A novel mechanism of carbohydrate recognition by the C-type lectins DC-SIGN and DC-SIGNR. Subunit organization and binding to multivalent ligands. J Biol Chem **276:**939–928.
201. **Engering A GT, van Vliet SJ, Wijers M, van Liempt E, Demaurex N, Lanzavecchia A, Fransen J, Figdor CG, Piguet V, van Kooyk Y.** 2002. The dendritic cell-specific adhesion receptor DC-SIGN internalizes antigen for presentation to T cells. J Immunol **168:**2118-2126.
202. **Appelmelk BJ vDI, van Vliet SJ, Vandenbroucke-Grauls CM, Geijtenbeek TB, van Kooyk Y.** 2003. Cutting edge: carbohydrate profiling identifies new pathogens that interact with dendritic cell-specific ICAM-3-grabbing nonintegrin on dendritic cells. J Immunol **170:**1635-1639.

203. **Arman A. Bashirova, Geijtenbeek Teunis B.H., C.F. vDG, van Vliet Sandra J. , Eilering Jeroen B.G., Martin Maureen P. , Wu Li , Thomas D. Martin, Nicola Viebig, Percy A. Knolle, Vineet N. KewalRamani, Yvette van Kooyk, Carrington M.** 2001. A Dendritic Cell–specific Intercellular Adhesion Molecule 3–grabbing Nonintegrin (DC-SIGN)–related Protein Is Highly Expressed on Human Liver Sinusoidal Endothelial Cells and Promotes HIV-1 Infection. Journal of Experimental Medicine **136:**671-678.
204. **Lin G SG, Pöhlmann S, Baribaud F, Ni H, Leslie GJ, Haggarty BS, Bates P, Weissman D, Hoxie JA, Doms RW.** 2003. Differential N-linked glycosylation of human immunodeficiency virus and Ebola virus envelope glycoproteins modulates interactions with DC-SIGN and DC-SIGNR. J Virol **77:**1337-1346.
205. **Klimstra WB, Nangle EM, Smith MS, Yurochko AD, Ryman KD.** 2003. DC-SIGN and L-SIGN can act as attachment receptors for alphaviruses and distinguish between mosquito cell- and mammalian cell-derived viruses. J Virol **77:**1022–1012.
206. **Goncalves AR MM, Pasquato A, Helenius A, Lozach PY, Kunz S.** 2013. Role of DC-SIGN in Lassa virus entry into human dendritic cells. J Virol **87:**11504-11515.
207. **Lozach PY, Lortat-Jacob H, de Lacroix de Lavalette, al. ae.** 2003. DC-SIGN and L-SIGN are high affinity binding receptors for hepatitis C virus glycoprotein E2. J Biol Chem **278**.
208. **Suda Y FS, Tani H, Murakami S, Saijo M, Horimoto T, Shimojima M.** 2016. Analysis of the entry mechanism of Crimean-Congo hemorrhagic fever virus, using a vesicular stomatitis virus pseudotyping system. Arch Virol **161:**1447-1454.
209. **Knolle PA, Limmer A.** 2003. Control of immune responses by savenger liver endothelial cells. Swiss Med Wkly **133:**501–506.
210. **Braet F, Wisse E.** 2002. Structural and functional aspects of liver sinusoidal endothelial cell fenestrae: a review. Comp Hepatol **1**.
211. **Feinberg H, Mitchell DA, Drickamer K, Weis WI.** 2001. Structural Basis for Selective Recognition of Oligosaccharides by DC-SIGN and DC-SIGNR. Science **294**.
212. **Hofmann H, Li X, Zhang X, Liu W, Kühl A, Kaup F, Soldan SS, González-Scarano F, Weber F, He Y, S. P.** 2013 Severe Fever with Thrombocytopenia Virus Glycoproteins Are Targeted by Neutralizing Antibodies and Can Use DC-SIGN as a Receptor for pH-Dependent Entry into Human and Animal Cell Lines. Journal of Virology **87:**4384–4394
213. **Powlesland AS, Ward EM, Sadhu SK, Guo Y, Taylor ME, Drickamer K.** 2006. Widely divergent biochemical properties of the complete set of mouse DC-SIGN-related proteins. The Journal of Biological Chemistry **281:**20440-20449.
214. **Cheong C MI, Choi JH, Dandamudi DB, Shrestha E, Longhi MP, Jeffrey KL, Anthony RM, Kluger C, Nchinda G, Koh H, Rodriguez A, Idoyaga J, Pack M, Velinzon K, Park CG, Steinman RM.** 2010. Microbial stimulation fully differentiates monocytes to DC-SIGN/CD209(+) dendritic cells for immune T cell areas. Cell **143:**416-429.
215. **Schaefer M RN, Fessler C, Stephani J, Taniuchi I, Hatam F, Yildirim AO, Fehrenbach H, Walter K, Ruland J, Wagner H, Ehlers S, Sparwasser T.** 2008. Decreased pathology and prolonged survival of human DC-SIGN transgenic mice during mycobacterial infection. J Immunol **180:**6836-6845.
216. **Garcia Vallejo JJ, Kooyk Yv.** 2013. The physiological role of DC-SIGN:A tale of mice and men. Trends in Immunology **34**.
217. **Swanepoel R, Coetzer JAW.** 2004. Rift Valley fever, p 1037-1070. *In* Coetzer JAW, Tustin RC (ed), Infectious Diseases of Livestock with special reference to southern Africa, 2nd ed. Oxford University Press, Cape Town, South Africa.
218. **Pepin M, Bouloy M, Bird BH, Kemp A, Paweska J.** 2010. Rift Valley fever virus (*Bunyaviridae: Phlebovirus*): an update on pathogenesis, molecular epidemiology, vectors, diagnostics, and prevention. Veterinary Research **41**.

219. **NICD.** 2011, May 20, 2011. " Rift Valley fever outbreak". http://www.nicd.ac.za/?page=rift_valley_fever_outbreak&id=94. Accessed
220. **WHO.** 2013. "Rift Valley fever in Mauritania". http://www.who.int/csr/don/2012_11_01/en/index.html. Accessed
221. **Turell MJ, Dohm DJ, Mores CN, Terracina L, Wallette Jr. DL, Hribar LJ, Pecor JE, Blow JA.** 2008. Potential for North American Mosquitoes to Transmit Rift Valley Fever virus. Journal of the American Mosquito Control Association **24:**502-507.
222. **Turell MJ, Wilson WC, Bennett KE.** 2010. Potential for North American Mosquitoes (Diptera: Culicidae) to transmit Rift Valley fever virus. Journal of Medical Entomology **47:**884-889.
223. **Meegan JM.** 1979. The Rift Valley fever epizootic in Egypt 1977-78 1: Description of the epizootic and virological studies. Transactions of The Royal Society of Tropical Medicine and Hygiene **73**.
224. **Lozach P-Y, Kuhbacher A, Meier R, Mancini R, Bitto D, Bouloy M.** 2011. DC-SIGN as a receptor for phleboviruses. Cell Host & Microbe **10:**75-88.
225. **Fehres CM, Garcia-Vallejo JJ, Unger WWJ, Kooyk YV.** 2013. Skin-resident antigen-presenting cells: instruction manual for vaccine development. Frontiers in Immunology **4**.
226. **Bird BH, Khristova ML, Rollin PE, Ksiazek TG, Nichol ST.** 2007. Complete genome analysis of 33 ecologically and biologically diverse Rift Valley fever virus strains reveals widespread virus movement and low genetic diversity due to recent common ancestry. Journal of Virology **81:**2805-2816.
227. **Suzich JA, Kakach L, Collett MS.** 1990. Expression strategy of a phlebovirus: biogenesis of proteins from the Rift Valley fever virus M segment. Journal of Virology **64:**1549-1555.
228. **Ikegami T, Makino S.** 2011. The Pathogenesis of Rift Valley Fever. Viruses **3:**493-519.
229. **Schmaljohn C, Nichol ST.** 2007. Bunyaviridae Knipe, DM, Howley, PM, Griffin, DE, Lamb, RA, Martin, MA, Roizman, B, Straus, SE eds In Fields Virology, 5th ed Lippincott, Williams & Wilkins Philadelphia, PA**:**pp.1741-1789.
230. **Suzich JA, Collett MS.** 1988. Rift Valley fever virus M segment: cell-free transcription and translation of virus-complementary RNA. Virology **164:**478-486.
231. **Weingartl HM, Zhang S, Marszal P, McGreevy A, Burton L, Wilson WC.** 2014. Rift Valley fever virus incorporates the 78 kDa glycoprotein into virions matured in mosquito C6/36 cells. PLoS ONE **9:**e87385.
232. **Kakach LT, Wasmoen TL, Collett MS.** 1988. Rift Valley fever virus M segment: use of recombinant vaccinia viruses to study Phlebovirus gene expression. J Virol **62:**826-833.
233. **Kielian M.** 2006. Class II virus membrane fusion proteins. Virology **344:**38-47.
234. **Soilleux EJ, Barten R, Trowsdale J.** 2000. DC-SIGN; a related gene, DC-SIGNR; and CD23 form a cluster on 19p13. J Immunol **165:**2937-2942.
235. **Hofmann H, Li X, Zhang X, Liu W, Kuhl A, Kaup F, Soldan SS, Gonzalez-Scarano F, Weber F, He Y, Pohlmann S.** Severe fever with thrombocytopenia virus glycoproteins are targeted by neutralizing antibodies and can use DC-SIGN as a receptor for pH-dependent entry into human and animal cell lines. J Virol **87:**4384-4394.
236. **Ito N, Takayama-Ito M, Yamada K, Hosokawa J, Sugiyama M, Minamoto N.** 2003. Improved recovery of rabies virus from cloned cDNA using a vaccinia virus-free reverse genetics system. Microbiol Immunol **47:**613-617.
237. **Alvarez CP, Lasala F, Carrillo J, Munez O, Corbi AL, Delgado R.** 2002. C-type lectins DC-SIGN and L-SIGN mediate cellular entry by Ebola virus in *cis* and *trans*. Journal of Virology **76:**6841-6844.
238. **Lokugamage N, Freiberg AN, Morrill JC, Ikegami T.** 2012. Genetic Subpopulations of Rift Valley Fever ZH548, MP-12 and Recombinant MP-12 Strains. J Virol **86:**13566-13575.

239. **Kalveram B, Lihoradova O, Indran SV, Ikegami T.** 2011. Using reverse genetics to manipulate the NSs gene of the Rift Valley fever virus MP-12 strain to improve vaccine safety and efficacy. J Vis Exp doi:3400 [pii]10.3791/3400**:**e3400.

240. **Kalveram B, Lihoradova O, Indran SV, Lokugamage N, Head JA, Ikegami T.** 2013. Rift Valley fever virus NSs inhibits host transcription independently of the degradation of dsRNA-dependent protein kinase PKR. Virology **435:**415-424.
241. **Atkinson PH, Lee JT.** 1984. Co-translational excision of alpha-glucose and alpha-mannose in nascent vesicular stomatitis virus G protein. J Cell Biol **98:**2245-2249.
242. **Kornfeld R, Kornfeld S.** 1985. Assembly of asparagine-linked oligosaccharides. Ann Rev Biochem **54:**631-664.
243. **Ben-Dor S, Esterman N, Rubin E, Sharon N.** 2004. Biases and complex patterns in the residues flanking protein N-glycosylation sites. Glycobiology **14:**95-101.
244. **Ruiz-Canada C, Kelleher DJ, Gilmore R.** 2009. Cotranslational and posttranslational N-glycosylation of polypeptides by distinct mammalian OST isoforms. Cell **136:**272-283.
245. **Bolt G, Kristensen C, Steenstrup TD.** 2005. Posttranslational N-glycosylation takes place during the normal processing of human coagulation factor VII. Glycobiology **15:**541-547.
246. **Ruiz-Canada C, Keller DJ, Gilmore R.** 2009. Cotranslation and Posttranslational N-Glycosylation of Polypeptides by Distinct Mammalian OST Isoforms. Cell **136:**272-283.
247. **de Boer SM, Kortekaas J, de Haan CA, Rottier PJ, Moormann RJ, Bosch BJ.** 2012. Heparan sulfate facilitates Rift Valley fever virus entry into the cell. J Virol **86:**13767-13771.
248. **Wojczyk BS, Takahashi N, Levy MT, Andrews DW, Abrams WR, Wunner WH, Spitalnik SL.** 2005. N-glycosylation at one rabies virus glycoprotein sequon influences N-glycan processing at a distant sequon on the same molecule. Glycobiology **15:**655-666.
249. **Pfeiffer G, Strube KH, Schmidt M, Geyer R.** 1994. Glycosylation of two recombinant human uterine tissue plasminogen activator variants carrying an additional N-glycosylation site in the epidermal-growth-factor-like domain. Eur J Biochem **219:**331-348.
250. **van Liempt E, Bank CM, Mehta P, Garcia-Vallejo JJ, Kawar ZS, Geyer R, Alvarez RA, Cummings RD, Kooyk Y, van Die I.** 2006. Specificity of DC-SIGN for mannose- and fucose-containing glycans. FEBS Lett **580:**6123-6131.
251. **Davis CW, Nguyen HY, Hanna SL, Sanchez MD, Doms RW, Pierson TC.** 2006. West Nile virus discriminates between DC-SIGN and DC-SIGNR for cellular attachment and infection. J Virol **80:**1290-1301.
252. **Guo Y, Feinberg H, Conroy E, Mitchell DA, Alvarez R, Blixt O, Taylor ME, Weis WI, Drickamer K.** 2004. Structural basis for distinct ligand-binding and targeting properties of the receptors DC-SIGN and DC-SIGNR. Nat Struct Mol Biol **11:**591-598.
253. **Shi X, Brauburger K, Elliott RM.** 2005. Role of N-linked glycans on bunyamwera virus glycoproteins in intracellular trafficking, protein folding, and virus infectivity. J Virol **79:**13725-13734.
254. **Shi X, Elliott RM.** 2004. Analysis of N-linked glycosylation of hantaan virus glycoproteins and the role of oligosaccharide side chains in protein folding and intracellular trafficking. J Virol **78:**5414-5422.
255. **Suzich JA, Kakach LT, Collett MS.** 1990. Expression strategy of a phlebovirus: biogenesis of proteins from the Rift Valley fever virus M segment. J Virol **64:**1549-1555.
256. **Kozak M.** 1991. An analysis of vertebrate mRNA sequences: intimations of translational control. J Cell Biol **115:**887-903.

257. **Ikegami T, Hill TE, Smith JK, Zhang L, Juelich TL, Gong B, Slack OA, Ly HJ, Lokugamage N, Freiberg AN.** 2015. Rift Valley Fever Virus MP-12 Vaccine Is Fully Attenuated by a Combination of Partial Attenuations in the S, M, and L Segments. J Virol **89:**7262-7276.
258. **Nishiyama S, Lokugamage N, Ikegami T.** 2016. The L-, M- and S-segments of Rift Valley fever virus MP-12 vaccine independently contribute to a temperature-sensitive phenotype. J Virol doi:10.1128/JVI.02241-15.
259. **Miller MM, Bennett KE, Drolet BS, Lindsay R, Mecham JO, Reeves WK, Weingartl HM, Wilson WC.** 2015. Evaluation of the efficacy, potential for vector transmission, and duration of immunity of MP-12, an attenuated Rift Valley fever virus vaccine candidate, in sheep. Clin Vaccine Immunol **22:**930-937.
260. **Morrill JC, Laughlin RC, Lokugamage, N, Wu J, Pugh R, Kanani P, Adams LG, Makino S, Peters CJ** 2013. Immunogenicity of a recombinant Rift Valley fever MP-12-NSm deletion vaccine candidate in calves. Vaccine **31:**4988-4994.
261. **Gerrard SR, Nichol ST.** 2007. Synthesis, proteolytic processing and complex formation of N-terminally nested precursor proteins of the Rift Valley fever virus glycoproteins. Virology **357:**124-133.
262. **Gerrard SR, Nichol ST.** 2002. Characterization of the Golgi retention motif of Rift Valley fever virus G(N) glycoprotein. J Virol **76:**12200-12210.
263. **Huiskonen JT, Overby AK, Weber F, Grunewald K.** 2009. Electron cryo-microscopy and single-particle averaging of Rift Valley fever virus: evidence for GN-GC glycoprotein heterodimers. J Virol **83:**3762-3769.
264. **Rusu M, Bonneau R, Holbrook MR, Watowich SJ, Birmanns S, Wriggers W, Freiberg AN.** An assembly model of rift valley Fever virus. Front Microbiol **3:**254.
265. **Fontana J, Lopez-Montero N, Elliott RM, Fernandez JJ, Risco C.** 2008. The unique architecture of Bunyamwera virus factories around the Golgi complex. Cell Microbiol **10:**2012-2028.
266. **Banchereau J PS, Blanco P, Bennett L, Pascual V, Fay J, Palucka AK.** 2003. Dendritic cells: controllers of the immune system and a new promise for immunotherapy. Ann N Y Acad Sci **987:**180–187.
267. **Kaiserlian D DB.** 2001. Dendritic cells and viral immunity: friends or foes? Semin Immunol **13:**303–310.
268. **Zhou LJ TT.** 1996. CD14+ blood monocytes can differentiate into functionally mature CD83+ dendritic cells. Proc Natl Acad Sci U S A **93:**2588–2592.
269. **Dodd KA, McElroy AK, Jones ME, Nichol ST, Spiropoulou CF.** 2013. Rift Valley Fever Virus Clearance and Protection from Neurologic Disease Are Dependent on CD4+ T Cell and Virus-Specific Antibody Responses. J Virol **87:**6161-6171.
270. **Hesse C, Ginter W, Forg T, Mayer CT, Baru AM, Arnold-Schrauf C, Unger WWJ, Kalay H, Kooyk Yv, Berod L, Sparwasser T.** 2013. In vivo targeting of human DC-SIGN drastically enhances CD8+ T-cell-mediated protective immunity. European Journal of Immunology doi:10.1002/eji.201343429.
271. **Schmaljohn C, Parker MD, Ennis WH, Dalrymple JM, Collett MS, Suzich JA, Schmaljohn AL.** 1989. Baculovirus expression of the M genome segment of Rift Valley fever virus and examination of antigenic and immunogenic properties of the expressed proteins. Virology **170:**184-192.

Date: 07-01-2016

CURRICULUM VITAE

NAME: Inaia Rochelle Phoenix, Ph.D.

PRESENT POSITION AND ADDRESS:

Present position: Graduate Student, Experimental Pathology Program, Department of Pathology, The University of Texas Medical Branch at Galveston
Address: Mary Moody Northen Pavilion 3.212, 301 University Blvd. Galveston TX 77555-0438
E-mail: inphoeni@utmb.edu

BIOGRAPHICAL:

Citizenship: US citizen
Business Address: Mary Moody Northen Pavilion 3.212, 301 University Blvd. Galveston TX77555-0438
Business phone: 409-747-8158
Home Address: 1719 Market St. Galveston TX 77550
Home phone: 409-770-3139

EDUCATION:

8/2003-5/2007 **B.S., Biology/Zoology,** Southern Oklahoma University, Durant, OK.

8/2010-Present **Ph.D. (ABD), Pathology**, Experimental Pathology Program, Department of Pathology. The University of Texas Medical Branch at Galveston, TX.

PROFESSIONAL AND TEACHING EXPERIENCE:

Academic:

05/2005- 08 /2005 **Public Outreach Intern**, US Fish & Wildlife Service, Errol, NH.
05/2006- 01 /2007 **Research Intern**, USDA Agricultural Research Facility, Lane, OK.
08/2010-Present **Graduate Assistant**, Department of Pathology. The University of Texas Medical Branch at Galveston, TX.

Teaching experience:

2004-2005 **Genetic Laboratory/Teacher's Assistant**, Southern Oklahoma State University, Durant, OK.
2005-2006 **Biology Laboratory Assistant**, Southern Oklahoma State University, Durant, OK.
2007 **Chemistry Laboratory Assistant**, Southern Oklahoma State University, Durant, OK.
2008-2009 **Science Education Instructor**, All Saints Camp & Conference Center, Pottsboro, TX.
2013, 2014 **Poster Judge**, Summer Undergrad Research Program (SURP), Galveston, TX

Non-academic:

10/2008- 08 /2009	**Veterinary Technician**, Animal Hospital HWY 6, Sugarland, TX.
08/2009- 08 /2010	**Veterinary Technician**, Tanner Lakes Animal Clinic, Houston, TX.

RESEARCH ACTIVITIES:

Research experience:

10/2004-5/2007	**Laboratory Assistant**, Departments of Biology and Chemistry, Southeastern Oklahoma University. (Advisors: Dr. Michael Turnage; Ms. Josie Mendenall, Dr. Douglas Wood, and Dr. Nancy Paiva)
8/2011-Present	**Graduate Assistant**, Department of Pathology, The University of Texas Medical Branch at Galveston. (Advisor: Dr. Tetsuro Ikegami) Title of dissertation in progress: Manipulation of the Rift Valley fever virus M-segment for vaccine development

Area of Research:
Overall the aim of my Ph.D. study is to rationally design an improved RVFV MP-12 vaccine encoding a further attenuated M-segment. The first aim of my dissertation focused on N-glycosylation profile of the RVFV glycoproteins and the role of N-glycans in DC-SIGN-mediated viral infection. As a second project, I characterized the mechanism of RVFV Gn and Gc expression via the ribosomal leaking scanning of the five initiation codons within the preglycoprotein region.

My long-term interests include emerging/re-emerging zoonotic diseases. I hope to become a leader in the scientific community, which would afford me the opportunity to encourage, empower, and inspire young women and minorities to pursue careers in science. Ultimately, I see myself working for a research institution where my passion for vaccine development, zoonotic diseases, and global public health and welfare will be put to the best use.

PROFESSIONAL AFFILIATIONS:

2010-	**Associate member**, American Association for the Advancement of Science (AAAS)
2011-	**Associate member**, Institute for Human Infections & Immunity
2011-	**Associate member**, American Society for Virology (ASV)
2013-	**Associate member**, American Society of Tropical Medicine & Hygiene (ASTMH)
2013-	**Associate member**, American Society for Microbiology (ASM)

HONORS AND AWARDS:

2007	Honors Program Graduate
2007	Graduated Cum Laude
2013-2015	Recipient, James W. McLaughlin Endowment: Predoctoral fellowship
2013	Recipient, Travel award: 32nd Annual Meeting for American Society for Virology meeting, 2013
2015	Recipient, Poster award, McLaughlin Colloquium, UTMB, 2014
2015	Recipient, Travel award: 34th Annual Meeting for American Society for

Virology meeting, 2015

2016 Intramural NIAID Research Opportunities (INRO)

PROFESSIONAL SKILLS:

- Research manuscript writing
- Scholarship/Fellowship grant writing
- Proof-reading/Editing of research grants and scientific papers (including those written by non-native English speakers)
- Presenting research projects at local, national, and international conferences
- Cooperation and organization skills in research projects
- Professional recording and inventory

TECHNICAL SKILLS:

- Northern Blot
- Western Blot, Lectin blotting, glycosidase digestion analysis
- Immunoprecipation, Ultracentrifugation
- Fluorescent labeling of proteins and cellular receptors
- ELISA: Indirect, Direct, Antigen-capture
- PCR, digital droplet PCR, molecular cloning and mutagenesis (restriction enzyme digestion, Gibson assembly), transfection
- Protein purification
- Virus isolation and titration
- Flow cytometry, Fluorescence-activated cell sorting
- Mammalian and Insect cell culture (Sf9, High Five, *Drosophila* S2, C6/36 cells).

COMPLETED TRAINING:

- Biosafety Level 2 and Animal Biosafety Level 2 training
- Radiation safety training
- Field epidemiology course; Peru 2015
- Good Laboratory Practice (GLP)
- ASM Science Teaching Fellows Program, 2016
- ASM Scientific Writing and Publishing Institute Online, 2016

BIBIOLOGRAPHY:

Ph.D Thesis: Manipulation of the Rift Valley fever virus M-Segment for Vaccine Development

Articles in Peer-Reviewed Journals:

1. Indran SV, Lihoradova OA, **Phoenix I**, Lokugamage N, Kalveram B, Head JA, Tigabu B, Smith JK, Zhang L, Juelich TL, Gong B, Freiberg AN, Ikegami T. **2013**. Rift Valley fever virus MP-12 vaccine encoding Toscana virus NSs retains the neuroinvasiveness in mice. ***J.Gen.Virol****.* 94: 1441-50.
2. **Phoenix I**, Nishiyama S, Lokugamage N, Hill TE, Huante M, Slack O, Carpio V, Freiberg AN, Ikegami T. **2016**. N-glycans on the Rift Valley fever virus Envelope Glycoproteins Gn and Gc Redundantly Support Viral Infection via DC-SIGN. ***Viruses*****.** 8, 149. doi: 10.3390/v8050149.
3. **Phoenix I**, Lokugamage N, Nishiyama S, Ikegami T. **2016.** Mutational Analysis fo the Rift Valley fever virus Glycoprotein Precursor Proteins for Gn Protein Expression. ***Viruses*****.** 8,

151. doi: 10.3390/v8060151.

Book Chapters:

1. **Phoenix I**, Ikegami T. Pathogenesis of Rift Valley fever in humans. **2015**. Pathogenesis of Rift Valley fever virus in Humans. In Singh, S.K. (Ed), *Emerging and Re-emerging Human Infections* (pp. 73-92). John Wiley & Sons/Wiley Blackwell Press.

Published Abstracts:

2012

1. Indran SV, Lihoradova O, **Phoenix I**, Lokugamage N, Juelich TL, Freiberg AN, Ikegami T. Characterization of MP-12 vaccine strain encoding Toscana virus NSs or its mutants. (Poster presentation) ***15th annual conference on vaccine research***, 5/7-9/2012, Baltimore, MA.
2. Indran SV, Lihoradova O, **Phoenix I**, Lokugamage N, Juelich TL, Freiberg AN and Ikegami T. Characterization of RVFV MP-12 Vaccine Encoding Toscana virus NSs or its Mutants.(oral presentation) ***31st Annual Meeting of American Society for Virology***, July 21-25, 2012, Madison, WI.

2013

1. **Phoenix I**, Hill TE, Lihoradova O, Indran SV, Freiberg AN, Ikegami T. Characterization of recombinant RVFV MP-12 with abolished N-glycosylation sites. (oral presentation) ***32nd Annual Meeting of American Society for Virology***, July 20-24, 2013, University Park, PA. **(Phoenix I was funded for travel by ASV)**
2. **Phoenix I**, Hill TE, Lihoradova O, Indran SV, Kalveram B, Freiberg AN, Ikegami T**.** Role of N-glycosylation of Rift Valley fever virus glycosylations in infectivity via DC-SIGN. (Poster presentation) ***San Antonio Vaccine Development Center 2md Annual Vaccine Symposium***, Nov 15, 2013, UT San Antonio, TX.

2014

1. **Phoenix I**, Hill TE, Lihoradova O, Indran SV, Freiberg AN, Ikegami T. Abolishment of Individual N-glycan Sites within Rift Valley fever virus Gn/Gc alters infectivity via DC-SIGN. (poster presentation) ***McLaughlin Colloquium***, April 11, 2014, UTMB, Galveston, TX. **(Phoenix I was selected for poster award)**
2. **Phoenix I**, Hill TE, Lihoradova O, Indran SV, Freiberg AN, Ikegami T. Abolishment of Individual N-glycan Sites within Rift Valley fever virus Gn/Gc alters infectivity via DC-SIGN. (poster presentation) ***63rd Annual Meeting of The American Society of Tropical Medicine and Hygiene***, Nov 2-6, 2014, New Orleans, LA.

2015

1. **Phoenix I**, Hill TE, Carpio V, Lokugamage N, Indran SV, Freiberg AN, Ikegami T. Abolishment of Individual N-glycan Sites within Rift Valley fever virus Gn/Gc alters infectivity via DC-SIGN. (Poster presentation) ***McLaughlin Colloquium***, March 27, 2015, UTMB, Galveston, TX.
2. **Phoenix I**, Hill TE, Carpio V, Lokugamage N, Indran SV, Freiberg AN, Ikegami T. Abolishment of Individual N-glycan Sites within Rift Valley fever virus Gn/Gc alters infectivity via DC-SIGN. (oral presentation) ***34th Annual Meeting for American Society for Virology meeting***, Bunyavirus session. July 11-15, 2015, Western Ontario University, London, ON, Canada. **(Phoenix I was funded for travel by ASV).**

2016

1. **Phoenix I,** Lokugamage N, Nishiyama S, Ikegami T. Analysis of Rift Valley fever virus Glycoprotein Precursors for Gn Expression (Poster presentation). ***McLaughlin Colloquium,*** April 1st, 2016. UTMB, Galveston, TX.
2. **Phoenix I,** Lokugamage N, Nishiyama S, Ikegami T. Analysis of Rift Valley fever virus Glycoprotein Precursors for Gn Expression (Poster presentation). ***Experimental Pathology Trainee Day,*** May 19th, 2016. UTMB, Galveston, TX.
3. **Phoenix I,** Lokugamage N, Nishiyama S, Ikegami T. Analysis of Rift Valley fever virus Glycoprotein Precursors for Gn Expression (oral presentation) ***35th Annual Meeting for American Society for Virology meeting***, Bunyavirus session. June 18-22, 2016, Virginia Tech, Blacksburg, VA, USA.